NASA/TP-1998-208439

Flight Evaluation of Center-TRACON Automation System Trajectory Prediction Process

David H. Williams
Langley Research Center, Hampton, Virginia

Steven M. Green
Ames Research Center, Moffett Field, California

July 1998

Contents

iv

Abbreviations and Symbols

ADS	automatic dependent surveillance
ARTCC, Center	Air Route Traffic Control Center
ATC	Air Traffic Control
accel	acceleration
BOD	bottom-of-descent
BODG	bottom-of-descent gate
C_D	drag coefficient, $\dfrac{\text{Drag}}{qS_{\text{ref}}}$
$C_{D,m}$	performance model drag coefficient
CAS	calibrated airspeed
CDI	course deviation indicator
CDU	control and display unit
CRT	cathode ray tube
CTAS	Center-TRACON Automation System
D	airplane drag, lb
DA	Descent Advisor
DME	distance measuring equipment
decel	deceleration
EPR	engine pressure ratio
FAA	Federal Aviation Administration
FAST	Final Approach Spacing Tool
FFD	forward flight deck
FL	flight level
FMS	Flight Management System
GPS	Global Positioning System
g	acceleration of gravity, 32.17 ft/sec^2
HA	high altitude
h	true altitude, ft
h_p	pressure altitude, ft
IC	initial condition
IP	initial position for a test run
J	jet route
KCAS	knots calibrated airspeed
LA	low altitude
LNAV	lateral navigation
M	Mach number
MAG	magnetic
MAPS	Mesoscale Analysis and Prediction System
MCP	mode control panel

MF	metering fix
N_{mag}	magnetic north
NASA	National Aeronautics and Space Administration
ND	navigation display
NOAA	National Oceanographic and Atmospheric Administration
PD	pilot discretion
PFD	primary flight display
PGA4D	profile generation algorithm, 4D
PGUI	planview graphical user interface
q	free-stream dynamic pressure, lb/ft^2
RFD	research flight deck
RTA	required time of arrival
rms	root-mean-square
S_{ref}	reference wing area, ft^2
std. dev.	standard deviation
T	airplane net thrust, lb
T_k	atmospheric temperature, K
$T_{k,s}$	standard day atmospheric temperature, K
TAS	true airspeed
TMA	Traffic Management Advisor
TMD	airplane net thrust minus drag, $T - D$, lb
TMU	Traffic Management Unit
TOC	top of climb
TOD	top of descent
TODG	top-of-descent gate
TRACON	Terminal Radar Approach Control
TRK	track
TSRV	Transport Systems Research Vehicle
UTC	universal time coordinated
V_a	true airspeed, ft/sec
V_w	wind speed, ft/sec
VCSS	velocity control stick steering
VNAV	vertical navigation
VOR	very high frequency omnidirectional radio range
W	weight, lb
δ_{am}	atmospheric ambient pressure ratio
γ	air-mass flight path angle, rad
4D	four dimensional, time being the fourth dimension

A dot over a symbol denotes derivative with respect to time.

1. Summary

The Center-TRACON Automation System (CTAS), under development at the Ames Research Center, is designed to assist controllers with the management and control of air traffic in the extended terminal area. The Langley Research Center is participating in a joint program with Ames to investigate the issues of and develop systems and procedures for the integration of CTAS and airborne automation systems. A central issue in this research is the accuracy of the CTAS trajectory prediction process and compatibility with airborne Flight Management Systems for the scheduling and control of arrival traffic.

Two flight experiments were conducted (Phase I in October 1992 and Phase II in September 1994) at Denver to evaluate the accuracy of the CTAS trajectory prediction process during the en route arrival phase of flight. The Transport Systems Research Vehicle (TSRV) Boeing 737 airplane based at the Langley Research Center flew a combined total of 57 arrival trajectories from cruise altitude to a terminal-area metering fix while following CTAS descent clearance advisories. Actual trajectories of the airplane were compared with the trajectories predicted by the CTAS trajectory synthesis algorithms and airplane Flight Management System. Trajectory prediction accuracy was evaluated over several levels of cockpit automation, which ranged from a conventional cockpit to a performance-based vertical navigation (VNAV) Flight Management System. Error sources and their magnitudes were identified and measured from the flight data.

The CTAS descent advisor was found to provide a reasonable prediction of metering fix arrival time performance during these tests. Overall arrival time errors (Mean + Standard deviation) were measured to be approximately 24 sec during Phase I and 15 sec during Phase II. The major source of error during these tests was found to be the predicted winds aloft used by CTAS. Position and velocity estimates of the airplane provided to CTAS by the Air Traffic Control (ATC) Host radar tracker were found to be a relatively insignificant error source. Airplane performance modeling errors within CTAS were found to not significantly affect arrival time errors when the constrained descent procedures were used. The most significant effect related to the flight guidance was observed to be the cross-track and turn-overshoot errors associated with conventional VOR (very high frequency omnidirectional radio range) guidance. Lateral navigation (LNAV) guidance significantly reduced both the cross-track and turn-overshoot errors. Pilot procedures and VNAV guidance were found to significantly reduce the vertical profile errors associated with atmospheric and airplane performance model errors.

2. Introduction

Since 1989, a joint program has been underway between the Ames Research Center and the Langley Research Center to investigate the issues of and develop systems for the integration of Air Traffic Control (ATC) and airborne automation systems. Ames has developed the Center-TRACON Automation System (CTAS), a ground-based ATC automation system designed to assist controllers in the efficient handling of traffic of all types and capabilities (ref. 1). This system has the ability to accurately predict airplane trajectories and determine effective advisories to assist the controller in managing traffic. Langley has been conducting and sponsoring research on flight operations and Flight Management Systems (FMSs) of advanced transport airplanes for a number of years.

During the course of this joint research, operational issues have been a primary concern; these include the practical integration of Flight Management System concepts to permit fuel efficient operations in a time-based ATC environment. The primary focus has been on the transition from en route cruise to the arrival phase of flight because of the significant impact of terminal area constraints on the en route trajectory. Concepts for airplane-ATC automation integration were evaluated in two real-time piloted-cockpit ATC simulations described in references 2 through 5. Early studies focused on the development and evaluation of automation functions and procedures for integrating CTAS, FMS, and data-link systems in the extended terminal area. The emphasis was on time-based traffic management, long lead-time (approximately 20 min) conflict prediction, and efficient conflict resolution in the en route and arrival phases of flight.

A central issue to integration of FMS and ATC automation is the accuracy of the trajectory prediction process used by each system. CTAS uses trajectory

predictions of each airplane to schedule arrivals, ensure conflict-free trajectories, and provide suggested speed, altitude, and routing clearances to maximize throughput with minimum deviation from user preferences. Airborne FMS trajectory predictions are used to provide economical flight profiles which satisfy airplane performance restrictions while adhering to operational constraints.

Early piloted-simulation testing of CTAS trajectories with airline flight crews demonstrated favorable results in terms of arrival time accuracy at a terminal-area metering fix (refs. 6 and 7). These tests, however, evaluated CTAS trajectory predictions based on ideal knowledge of airplane state, airplane performance, and atmospheric characteristics (winds and temperatures aloft). The next step was to evaluate CTAS trajectory prediction accuracy under realistic field conditions including the errors associated with radar tracking, airplane performance modeling, and atmospheric modeling.

The establishment of CTAS field sites at several FAA ATC facilities provided an opportunity to exercise CTAS under actual traffic and weather conditions. However, accurate airplane and atmospheric state information was not available for trajectory prediction validation. Following the initial fielding of CTAS at the Denver Air Route Traffic Control Center (ARTCC or Center), it was recognized that the Transport Systems Research Vehicle (TSRV) Boeing 737 airplane based at Langley Research Center could be used for actual flight test verification of the CTAS trajectory prediction process. Use of the TSRV airplane provided several advantages including the opportunity to exercise CTAS clearance advisories (with minimum impact on the airspace users), a platform for the accurate measurement of actual airplane and atmospheric state, and the ability to evaluate new cockpit procedures in a flight environment.

Ames began conducting field tests of the descent advisor (DA) portion of CTAS in 1992. Designed for Center airspace, DA provides clearance advisories for traffic management restrictions (e.g., metering) while assisting the controller with the detection and resolution of conflicts between airplanes in all phases of flight (ascent, cruise, and descent). The primary goal of these tests was to evaluate the accuracy of the CTAS trajectory prediction process for the en route arrival phase of flight. Two TSRV flight experiments

were conducted: Phase I in October 1992 and Phase II in September 1994.

This report describes both phases and presents results in terms of the trajectory prediction accuracy and the sources and magnitudes of trajectory prediction errors. Although the combined flight test data set is not large enough to be statistically significant, the data do provide insight into the size and impact of errors associated with trajectory prediction under real-world operating conditions. These data can be used as input and validation for trajectory sensitivity studies to determine the statistical representation of errors (refs. 8, 9, and 10). The results of such studies can be used to guide improvements to prediction algorithms and data sources (e.g., prediction of atmospheric characteristics and airplane tracking), determine the appropriate buffers for conflict prediction, and develop trajectory prediction error models for real-time analysis of conflict probability.

3. Background

Capacity and efficiency improvements in the national airspace system are needed to cope with increased traffic demand and ensure the economic viability of the air transportation industry. Airborne flight management systems have been developed to provide cost-efficient flight guidance for individual airplane operations. Air traffic control automation tools (decision support tools) are currently being designed to assist controllers in achieving greater efficiency with current ATC procedures as well as enable the introduction of new, more efficient procedures. Such tools include conflict prediction and resolution tools, for allowing more user-preferred flight paths, and time-based traffic management tools for minimizing delay. Both the FMS and ATC automation systems share the common need for accurate prediction of airplane flight trajectories in order to achieve their respective performance goals. The focus of this publication is on the CTAS trajectory prediction process, with reference and comparison with airborne FMS as deemed appropriate.

3.1. Center-TRACON Automation System

CTAS is an integrated system comprised of three tools that provide computer-generated advisories for both en route (Center) and terminal (TRACON) controllers (ref. 1). The three tools include the Traffic Management Advisor (TMA), the Descent Advisor

(DA), and the Final Approach Spacing Tool (FAST). These tools are designed to assist controllers in achieving greater efficiency in the management and control of arrival traffic in the extended terminal area as well as assist in the conflict prediction and resolution of traffic along airway and user-preferred trajectories. As flights approach their destination (e.g., within 200 n.mi.), DA predicts the trajectories of airplanes in Center airspace. The TMA then generates sequences and schedules for arriving flights including those that originate from nearby feeder airports. DA iterates on speed profile, in addition to path and altitude, to provide the Center controller with clearance advisories that meet the TMA schedule with fuel-efficient cruise and descent profiles. DA conflict prediction and resolution tools assist the controller in separating traffic in all en route phases of flight (climb, cruise, and descent) while minimizing clearance changes. As airplanes enter the terminal area, FAST updates the sequences and schedules and provides TRACON controllers with advisories for runway assignment, sequence, headings, and speeds to optimize the delivery of airplanes to the runways.

3.2. CTAS Trajectory Prediction Process

The trajectory prediction process is the foundation of CTAS. Because it has been developed from an airborne FMS concept, the CTAS trajectory prediction process is similar in many ways to that employed for an FMS. Whereas an FMS application tends to focus on trajectory optimization for a single airplane, the ATC application must also consider the interrelationships of trajectories of multiple flights. The ATC application goes beyond the single focus of required time of arrival (RTA) for time-based traffic management and must consider separation between neighboring flights along entire trajectories not just at procedurally controlled focal points such as a metering fix. The task of reliable conflict prediction along random 4D trajectories is critical to achieving the benefits associated with the "free-flight" concept (ref. 11). The effectiveness and efficiency of conflict resolution actions depend on the accuracy of the trajectory predictions used for conflict detection.

CTAS trajectory synthesis begins with the trajectory initial condition and a series of flight path constraints. The initial condition (position, altitude, and velocity) is based on airplane track (radar or airplane reported) or flight plan data. The set of flight path constraints is based on a series of waypoints and segments which define the bounds of a horizontal path to the runway or trajectory end-point. The horizontal path prediction is based on the current state of the airplane, flight plan, airspace procedures, and heuristics which relate the current state of the airplane to the flight plan and local ATC procedures. For exceptional cases where the CTAS heuristics do not match controller intent, the controller may update the CTAS path prediction with quick keyboard and graphical inputs that are separate from the formal Host flight plan amendments. The waypoint constraints, generated to comply with ATC procedures as defined in a CTAS navigation database, may include altitude, airspeed, course, and/or time.

CTAS trajectories are synthesized in two steps. First, a horizontal ground track is generated by curve fitting the waypoints with a series of straight-line and circular-turn segments. The waypoints are designated as either "fly-by," or "fly-over" based on the CTAS navigational database adapted for a particular airspace. The turn segments are based on a parameterized bank angle and an estimated ground speed. This ground speed is computed from an airspeed profile and a wind estimate along a simple kinematic altitude profile. The airspeed profile is either inferred from a combination of flight plan, controller input, and the CTAS database or selected for time-control iteration. Second, the altitude and time profiles are computed by integrating a set of simplified point-mass equations of motion along the established ground track. Within Center airspace, a detailed set of airplane performance models is used to determine thrust, drag, and speed envelope as a function of airplane type. The atmosphere is modeled with a three-dimensional grid of wind, temperature, and pressure (ref. 12). A detailed description of the CTAS trajectory synthesis process is presented in references 13 and 14.

3.3. Error Sources

Trajectory prediction accuracy is the key for creating effective and efficient ATC advisories. Errors refer to the difference between the predicted and actual airplane state along a flight path. Error sources include the estimation of an airplane state (position and velocity) for initializing a trajectory prediction, trajectory modeling, and clearance conformance. Trajectory

modeling includes airplane performance (e.g., thrust, drag, weight), flight procedures, atmospheric characteristics (e.g., wind and temperature aloft), and trajectory generation algorithms.

Although both CTAS and FMS are subject to errors, differences between the two systems depend on the environment and application. If the basic trajectory generation algorithms are assumed similar, the differences between FMS and CTAS predictions are primarily due to differences in the sensors and modeling databases used by either system. Whereas the most accurate sensors for determining airplane position and velocity are available to the FMS, ATC systems are currently dependent on less-accurate radar tracking. As for winds and temperature, FMS-equipped airplanes typically have the most accurate data at the current position of the airplane whereas ATC systems have access to the latest prediction over the future flight path, particularly the descent profile. Most FMS systems allow the flight crew to enter forecast winds and temperatures at each waypoint along a flight plan, as well as at several altitudes spanning the descent profile. A few newer airplanes support automatic uplink of these winds and temperatures; however, such data are rarely updated in flight and may be 3 to 6 hr old upon entry. Regarding airplane performance modeling, most FMS systems have extensive performance data which may be "tuned" to the airframe and engine. In comparison, ATC systems must rely on engineering data when available or synthesized data when they are not. Given the current FAA flight plan procedures, ATC systems must estimate weight (usually known to the FMS) and must categorize airplanes within FAA designated types. Many of the differences between CTAS and a particular FMS may be mitigated through the use of data exchange to provide increased precision between the air and ground computations as well as an overall increase in trajectory prediction accuracy (ref. 15).

4. Experiment Design

4.1. Objective

The primary objective of the flight tests was the evaluation of CTAS trajectory prediction accuracy for the en route arrival phase of flight, including identification and measurement of significant potential error sources. Secondary objectives included investigation of flight procedures as well as the application of cock-

pit automation tools for improving flight precision in descent.

4.1.1. Phase I

Phase I, October 1992, focused on straight-path descents with an emphasis on the analysis of modeling errors. In addition, the basic descent procedures tested in simulation would be used for the first time in a flight environment. Flight-idle descent procedures were used to isolate modeling errors, and "constrained" descents were flown to investigate flight procedures for efficient vertical profile control to a required altitude and speed at a fix. Constrained-descent procedures were evaluated with and without cockpit automation for visualizing the bottom-of-descent crossing restriction. A limited FMS capability, consisting of lateral navigation (LNAV) and guidance along the straight path and navigation map display of range to intercept of a selected altitude, was used for the cockpit automation in Phase I.

4.1.2. Phase II

The primary objective of Phase II, September 1994, was to evaluate CTAS trajectory prediction accuracy along a more complex arrival route with expanded flight procedures and a wider range of FMS capability for LNAV and performance-based vertical navigation (VNAV). The arrival route was chosen to provide a large turn during the middle of the descent. Previous simulation testing at Ames (ref. 6) had shown that pilots without LNAV exhibit a tendency to overshoot the turn and subsequently fly a longer than predicted path. Imprecision in the pilot overshoot presents an additional challenge in accurately predicting the lateral path of a conventionally equipped airplane. The intent was to determine whether the lateral errors observed in the earlier simulation tests and the vertical errors observed in Phase I could be reduced by improved piloting procedures and what additional improvement could be gained by utilizing FMS LNAV and VNAV capability. A secondary objective of Phase II was to sample actual atmospheric conditions for comparison with the CTAS model along the arrival test route as well as at additional locations in the test airport vicinity.

4.2. Approach

The test was designed to expose DA to realistic modeling errors under field conditions with minimum

4

impact on the ATC facility and commercial flight operations. During both test phases, the TSRV was operated on an arrival flight plan tailored to replicate a typical commercial airline arrival at Denver. Each test flight consisted of several test runs conducted by using a closed-circuit routing designed to maximize the amount of data collected on a given flight. The TSRV was flown from both the forward flight deck, representing a conventionally equipped airplane (e.g., Boeing 737-200, Boeing 727-200, McDonnell Douglas DC-9/MD-80), and the research flight deck, representing an FMS-equipped airplane (e.g., Boeing 737-400, Boeing 757/767).

Test runs were conducted during low traffic periods to minimize the impact on commercial flight operations and to allow the TSRV to conduct uninterrupted descents. Although interruptions commonly occur as a part of normal ATC operations, isolating the TSRV was desirable to enable identification and measurement of trajectory prediction error sources. CTAS was operated by a test engineer due to the absence, at that time, of an FAA-approved CTAS interface for the radar controllers. The approach was for the TSRV pilot and controller to coordinate pilot discretion (PD) descents while the CTAS operator relayed the DA advisories to the TSRV over a dedicated (non-ATC) frequency.

CTAS was operated with data sources that represent the quality of data available to a current operational system. Airplane track and flight plan data were obtained by CTAS through established operational interfaces to the ATC Host computer. For the TSRV airplane, CTAS used manufacturer's performance data. The performance data included drag, thrust, and fuel consumption as a function of airplane and atmospheric state. Atmospheric data (winds and temperature aloft) were obtained from the National Oceanographic and Atmospheric Administration (NOAA) Mesoscale Analysis and Prediction System (MAPS) (ref. 16). MAPS is the research prototype version of the Rapid Update Cycle (ref. 17) operated by the National Center for Environmental Prediction (NCEP), formerly the National Meteorological Center (NMC).

For Phase II, the TSRV FMS used data from different sources than CTAS, which were also the most accurate sources of data available. Airplane state data

were taken directly from airplane measurements, atmospheric data were entered into the FMS by hand based on the measurements of previous runs, and the performance data were based on data from earlier flight tests. These differences in input data between CTAS and the TSRV FMS were used to ensure differences in the respective trajectory predictions. This approach provided two advantages:

1. It would highlight the potential differences between CTAS and FMS trajectories under operational conditions

2. It would provide insight into the sensitivity of trajectory prediction accuracy to the accuracy of these data sources

Airplane state and observed atmospheric data were recorded onboard the TSRV airplane for post-flight comparison with the real-time CTAS trajectory predictions, airplane track, and MAPS data. Throughout this report, the term "actual" refers to the measurements made onboard the TSRV airplane with the Global Positioning System (GPS) navigation system.

4.3. Flight Test Area

4.3.1. Phase I

The area of test operations for Phase I, including the nominal flight path of the airplane, is shown in figure 1. The test was confined to one area (group of sectors) within Denver Center and primarily involved two radar sectors. The high altitude sector 9 (HA9) sets the sequence of arrivals from the northeast and controls the airspace including flight level (FL) 240 and above. Arriving flights are typically handed off to the low altitude sector 15 (LA15) for metering into the Denver TRACON via the KEANN metering fix.

A flight plan was developed, with the assistance of the Denver Center and TRACON controllers, to allow for a closed-circuit routing using jet route 10 (J10) for the test runs and the airspace southeast of J10 for climb out and prerun maneuvering. The nominal plan was to depart from Denver Stapleton International Airport, proceed direct to AKO (Akron VOR station), direct to LEWEL, direct to PONNY, direct to Denver Airport. The test run was conducted between the initial point (IP) at PONNY and the TRACON boundary

5

at KEANN. The actual flight path between AKO and PONNY varied from run to run, depending on the climb performance of the TSRV and traffic conditions, to enable the TSRV to be stabilized in cruise at the IP. Descents were initiated from FL350 with a metering fix crossing condition at KEANN of FL170 at or below 250 KCAS. Pressure altitude was used throughout the descent to remove the step change in altitude effect from the data analysis for this test phase. After crossing KEANN, the airplane would either climb eastbound for another run or return to Denver for landing.

4.3.2. Phase II

Figure 2 illustrates the Phase II area of test operations along with the nominal flight path. This test was conducted primarily in the northwest area. The high altitude sector HA14 sets the sequence of arrivals from the northwest and controls the airspace including FL240 and above. Arriving flights are typically handed off to the low altitude sector LA13 for metering into the Denver TRACON via the DRAKO metering fix.

In Phase II, the primary test runs were flown along J56 with the airspace to the south used for climb out and prerun maneuvering. The descents were initiated from FL330 with a metering fix crossing condition at DRAKO of 17000 feet at or below 250 KCAS. During Phase II, the proper altimeter setting was used to determine metering fix crossing altitude. The initial point for the primary test runs was at CHE (Hayden) VOR. A second route, beginning at IP2, joined the arrival traffic inbound to the KEANN metering fix. This second route was used to obtain additional atmospheric data with the TSRV from a different quadrant. Runs conducted along this secondary route were not used to complete the primary test matrix of descent trajectory cases.

4.4. Research System

The primary equipment used for these tests consisted of the TSRV airplane operating in the Denver terminal area and the CTAS field system on the ground at Denver Center. In addition to standard two-way voice communication between the pilots and ATC, a dedicated frequency was used to support two-

way voice communication between the TSRV airplane and the CTAS ground station.

4.4.1. TSRV Airplane

The airplane used in these tests was the TSRV airplane, a modified Boeing 737-100 (fig. 3). The TSRV is a flying laboratory equipped with a research flight deck (RFD) located in the cabin behind the conventional forward flight deck (FFD), as shown in the cutaway model of the airplane in figure 4. The interior of the RFD is a full-size flight deck that features eight 8-by 8-in. flight-quality, color CRT displays and sidestick flight controllers (fig. 5). Experimental systems used in the RFD consist of an electronic flight display system, a digital fly-by-wire flight control and flight guidance system, and an advanced area navigation system with GPS sensor inputs. The airplane may be flown from either the RFD or FFD.

The TSRV airplane was equipped with a fully capable four-dimensional (4D) navigation and guidance system developed during the mid 1970's in support of the Terminal Configured Vehicle Program (ref. 18). This baseline system, however, did not incorporate performance management features necessary for computation of vertical trajectories. Ground speeds and altitudes were required inputs to each waypoint in the guidance buffer of the flight management computer. The system also lacked the flexibility of flight plan generation and modification found in current commercial flight management systems.

The system was upgraded in the late 1980's to incorporate modern control display units, as illustrated in figure 6. At the same time, expanded lateral flight plan generation capability was added which closely approximated the functionality of commercial flight management systems. In addition to the lateral navigation features, the navigation display included a range-altitude arc for displaying the predicted intercept of a desired altitude. This capability was used during Phase I.

For Phase II, the capability was added to compute vertical trajectories and provide vertical guidance similar to the commercial Boeing 737-300 commercial systems. This was accomplished with the NASA-developed profile generation algorithm (PGA4D) described in references 2 and 4. The time-control (4D)

6

mode was not implemented for this test. In addition, the range-altitude arc was augmented with the capability to display the projected altitude intercept along a curved path, as shown in figure 7.

Selection of flight guidance and control modes in the RFD are made through the mode control panel (MCP) located in the center of the glare shield (fig. 8). A description of the MCP and baseline guidance modes available in the RFD may be found in reference 19.

4.4.2. CTAS System

Figure 9 illustrates the test setup within the Denver Center. The CTAS station, located adjacent to the Traffic Management Unit (TMU) on the control room floor, was comprised of a distributed network of Sun Microsystems Sparc-10 workstations. Real-time updates of radar track and flight plan data for arrivals were received from the FAA Host computer via a one-way (Host-to-CTAS) interface. Radar track data (position, mode-C altitude, and velocity) were nominally updated by the Host computer on a 12-sec cycle. MAPS forecasts of winds and temperatures aloft were received from NOAA on a 3-hr update cycle. These forecast updates were received (and used) by CTAS approximately 30 min prior to the forecast period. Host track data were displayed on a CTAS plan view graphical user interface (PGUI) with DA advisory data superimposed on the display in both tabular and color graphical form (ref. 20).

For the purposes of these flight tests, the descent speed profiles for the TSRV airplane were selected from a test matrix to provide a controlled set of speed profile conditions to support the analysis of trajectory prediction accuracy. The test matrix speed profiles were input to DA for each run and used to compute a top-of-descent (TOD) clearance advisory. Additional DA functionality, including advisories for cruise speed, cruise altitude, direct headings, delay vectors, and conflict detection and resolution, was not evaluated in these tests.

Prior to both Phases, the CTAS/DA trajectory calculations were validated against the FMS/PGA4D calculations. The validation was based on running a series of trajectory predictions, over a range of speed profiles, for a common set of input data (atmospheric conditions and performance data). The comparison

trajectories were based on a nominal flight distance of 100 n.mi. with descents that were on par with those to be explored in the flight tests. Results indicated that the two systems produced comparable trajectories with no more difference than 1 n.mi. in top of descent and 2 sec in arrival time.

4.5. Test Procedures

The test procedures used during both Phases were essentially the same. TSRV flights were coordinated with Denver traffic management to allow multiple descent runs during low traffic periods. A list of desired test conditions (including speed profile and cockpit procedure) was prepared prior to each flight. The desired test condition for each run was chosen during the climb phase of the run. Selection of this test condition was a function of the traffic situation, performance capability of the airplane, fuel status, and test matrix completion. During Phase I, the DA conflict probe was used by the test engineer to shadow the arrival traffic and determine which test conditions would allow for an uninterrupted descent. The high altitude controller would then issue radar vectors to the TSRV, prior to the IP, to allow a pilot discretion descent without traffic conflicts. A traffic management controller coordinated test activities between the CTAS station and each participating radar sector.

The CTAS test engineer monitored the progress of the TSRV airplane on the DA PGUI. After the airplane crossed the IP, the TSRV test engineer would report the CAS, ground speed, and measured wind for comparison with the test condition and CTAS estimates of the same variables. When the airplane was stable at the desired cruise speed, the CTAS engineer would relay the approximate TOD to the TSRV engineer and high altitude controller. When the airplane was nominally within 20 to 50 n.mi. of the TOD, the CTAS trajectory was recorded and final TOD location transmitted to the TSRV engineer. With the PD descent clearance issued, the TSRV engineer would relay the TOD to the flight crew to simulate the controller's issuance of a DA-based descent clearance. Airborne measurements of actual airplane and atmospheric state were recorded automatically on the TSRV.

The flight crew onboard the TSRV airplane consisted of two pilots in the FFD and a single pilot in the

7

left seat of the RFD. The right seat of the RFD was occupied by the TSRV test engineer. All normal ATC communications were handled by the FFD pilots. Communication with the CTAS workstation was handled by the TSRV test engineer. Voice communications to both ATC and CTAS could be monitored by all pilots.

Each test condition specified whether the run would be flown from the FFD or the RFD. Prior to reaching the IP waypoint, the flight crew in the appropriate cockpit would assume control of the airplane. All FFD test runs were flown manually by the pilots without the use of autopilot or autothrottle. The RFD pilot used manual control during Phase I and autopilot during Phase II.

The pilot began each run by establishing the airplane in level cruise at the appropriate altitude and speed for the test condition. Prior to top of descent, the pilot was advised by the TSRV engineer of the desired TOD in terms of DME distance from the Denver VOR. The pilot would monitor DME distance and initiate descent upon reaching the specified range to Denver. The pilot conducted the descent by using the profile descent tracking procedures specified by the test condition (defined later). The test run ended when the airplane reached the final altitude and speed and crossed the MF waypoint (KEANN or DRAKO).

4.6. Data Recording

Two primary sets of data parameters were collected during these tests:

1. Measured conditions, such as airplane state and atmospheric data

2. Predicted conditions, such as trajectory predictions from CTAS DA and the airplane FMS as well as predicted atmospheric conditions

Data recording onboard the airplane and at the CTAS workstations was tagged to Universal Time (UTC) for postflight correlation.

4.6.1. Measured Data

The TSRV sensors provided airplane state data, such as position (latitude and longitude), airspeed,

ground speed, altitude, body angles, and accelerations. Wind speed and wind direction were computed in real time based on airspeed, ground speed, and body angles. Atmospheric temperature measurement was also provided by the TSRV air data system. Most parameters were updated and recorded at a rate of 20 Hz but were averaged over 1 sec in postprocessing. Airplane tracking data, including position (x,y coordinates in the Denver Center reference frame), mode-C altitude, track angle, and ground speed, were obtained from the Denver Center Host computer with an approximate update rate of one track report every 12 sec (ref. 21). Radar track position data were provided to CTAS in the Denver Center reference frame, a stereographic coordinate system with the origin approximately 700 n.mi. southwest of the Denver airport. For the purposes of comparison, TSRV position data were converted to the Denver Center reference frame.

4.6.2. Predicted Data

Trajectory predictions were computed and recorded by the CTAS DA for all test runs during both Phases. In addition, the TSRV FMS computed and recorded predicted trajectories for Phase II (FMS predictions were not available in Phase I). Both sources of trajectory predictions provided point-to-point four-dimensional trajectories for each descent from the initial position of the airplane up to and including the metering fix location. CTAS received and recorded the 3-hr MAPS forecast on a 3-hr update cycle. This forecast was received approximately 30 min prior to the forecast period and was based on an analysis of the atmosphere during the preceding period. CTAS obtained the predicted winds and temperature along a flight path by interpolating within the MAPS data grid.

5. Test Conditions

The test conditions employed in both tests were designed to provide a reasonable representation of commercial airline jet transport descents as anticipated in a CTAS Descent Advisor operational environment. Cockpit automation and the corresponding pilot procedures were studied to investigate their impact on the descent trajectory. The NASA test pilots were instructed to fly the descents as precisely as possible in order to minimize pilot-induced variations in the

8

descent profiles. The goal was to emphasize the differences between the systems (and associated procedures).

5.1. Phase I

Two specific types of descent procedures were used in Phase I: (1) idle descents, in which idle thrust was used from TOD to BOD altitude and metering fix crossing speed and (2) constrained descents in which the pilot employed thrust and/or speed brake during the descent in order to achieve BOD altitude and airspeed as closely as possible to the metering fix location. The purpose of the idle descent procedure was to provide a direct measurement of the trajectory prediction accuracy of CTAS, which utilized an idle descent model in the trajectory predictions for this test. Operational versions of CTAS are anticipated to use a near-idle thrust model for descent trajectory predictions to match the procedures related to individual airplane performance types and operating conditions. The constrained descent procedure represented a more realistic procedure in which the pilot adjusts the altitude profile in descent to achieve the desired crossing conditions (speed and altitude) at a waypoint assigned by ATC. This procedure has the added benefit of mitigating the impact of trajectory prediction errors by closing the loop on the vertical profile. The idle and constrained descents were flown from both the FFD and RFD. All descents were flown manually since the TSRV was not equipped with autopilot functions which held airspeed by using pitch control. The specific procedures used are detailed in the following paragraphs.

5.1.1. Idle Descent

The pilot procedures for idle descents were essentially the same for both the FFD and RFD. The pilot would begin the idle descent procedure when the airplane reached the CTAS-specified TOD point. This point was identified as a DME distance from the Denver VOR. Following TOD, the pilot flew one of three vertical profile types, depending on speed (fig. 10). If the descent CAS was less than or equal to the cruise CAS, the pilot flew a slow descent profile (fig. 10(a)). At TOD, the pilot would immediately retard the throttle to idle and decelerate in level flight. Once the descent speed was achieved, the pilot initiated a descent while using pitch control to maintain airspeed. If the descent Mach was equal to the cruise Mach, the pilot flew a nominal descent profile (fig. 10(b)). At

TOD, the pilot would immediately retard the throttle to idle and initiate a descent while using pitch control to maintain the Mach/CAS speed schedule. If the descent Mach was greater than the cruise Mach, the pilot flew a fast descent profile (fig. 10(c)). At TOD, the pilot would immediately initiate a descent (nominally 3000 ft/min) while maintaining cruise thrust to accelerate to the descent Mach. Once the descent Mach was achieved, the pilot would retard the throttle to idle while using pitch control to maintain the Mach/CAS speed schedule.

As the airplane approached the metering fix crossing altitude, the pilot would initiate a level-off deceleration segment, depending on the descent speed and metering fix crossing speed. If the speeds required a deceleration, the pilot maintained idle throttle until the airplane approached the metering fix speed and then increased throttle as necessary to maintain speed until crossing the metering fix. If no deceleration was necessary, the pilot increased throttle as necessary to level off and maintain the descent speed until crossing the metering fix.

5.1.2. Constrained Descent

The pilot procedures for the constrained descents were the same as for the idle descents up to the constant CAS segment of the descent. Once the constant CAS segment was established, the pilot would adjust the descent angle to achieve a BOD point which was just prior to the metering fix. The BOD location was chosen by a rule of thumb, to allow 1 n.mi. of deceleration distance for each 10 knots of speed reduction required to achieve the assigned crossing speed at the metering fix.

The RFD pilot used the range-altitude arc on the navigation display to target the desired BOD point (fig. 7). This arc showed the range at which the airplane would reach the altitude selected on the mode control panel at the current inertial flight path angle of the airplane. The pilot would then adjust throttle and/or speed brake to hold the descent CAS while targeting the desired BOD location.

The FFD pilot procedures for constrained descents were somewhat more complex than the RFD procedures since the FFD pilots had no direct indication of the range at which they would reach the BOD altitude. Commercial crews typically use the 3:1 rule of thumb

to plan 3 n.mi. of descent path for every 1000 ft of descent. This rule works well in terms of workload and fuel efficiency for a small range of descent speeds which vary as a function of airplane type, weight, and atmosphere. However, for the CTAS application, it is desirable for ATC to specify descent speed to allow for safe and efficient merging of arrivals. Under these conditions, it is desirable to allow the flight path (e.g., TOD) to vary as a function of descent speed, type, and atmosphere, much like an FMS would. For fuel-efficient descents, the TOD and flight path angle may vary as much as 30 to 40 percent over the speed envelope of typical jet transport types. The challenge is for the pilot to maintain a situational awareness of vertical profile progress.

Paper charts and a custom-programmed hand calculator were provided to the FFD pilots to assist in the constrained descents. The charts provided tables of DME distance, altitude, and corresponding flight path angles for each of the descent speed conditions in the test. The pilots would determine the required flight path angle to achieve BOD altitude by noting their altitude and DME distance when the airplane reached the target descent CAS. With this flight path angle as a reference, the pilots could then determine the proper altitude at a given DME distance or conversely the proper DME distance at a given altitude needed to maintain the correct decent angle. The descent rate could then be adjusted with throttle or speed brake, depending on whether the airplane was below or above the desired altitude. The programmed hand calculator provided the same information. Both the charts and calculator were developed during local flight testing of the descent procedures as aids for the NASA test pilots. They were not intended to represent operational techniques for airline pilots to use for CTAS descent advisories. Such operational procedures would require careful development and testing with actual airline crews.

5.1.3. Test Matrix

The test matrix for Phase I, given in table 1, was defined to evaluate CTAS trajectory prediction accuracy over two primary test variables: speed profile and pilot procedure. Seven speed profiles were selected to exercise the nominal speed envelope of the TSRV while generating a representative set of constant-speed and variable-speed trajectory segments. This approach

was used to generate a balanced set of trajectory cases for analysis of prediction accuracy as well as a broad data set for evaluating the TSRV performance characteristics. Each of the seven speed profiles was flown by using the idle-thrust descent procedure. The first three speed profile cases were repeated with the constrained descent procedures from both the FFD and RFD. The goal was to complete two runs for each of the 13 conditions combining speed profile and pilot procedures.

5.2. Phase II

Test conditions for Phase II were designed to expand on Phase I with an emphasis on evaluating how to best utilize current FMS capabilities for constrained descents within a CTAS environment. Descents with turns were of particular interest due to the increased complexity of lateral and vertical profile tracking. Three different levels of FMS automation were chosen to represent a cross section of FMS automation capabilities available within the current commercial fleet. These levels represent

1. Conventional airplanes (without FMS)

2. FMS-equipped airplanes with VNAV capability

3. FMS-equipped airplanes with range-altitude arc capability

These levels of FMS automation were simulated by restricting the usage of the FMS on the TSRV at the defined levels.

Four sets of pilot procedures were developed for the TSRV to take advantage of these levels of FMS automation. These procedures included

1. Conventional non-FMS

2. Conventional FMS (using FMS TOD)

3. FMS with CTAS TOD

4. Range-altitude arc

The TSRV pilot procedures were not intended as exact prototypes for operational use because of the

significant differences in the TSRV FMS, pilot interface devices (mode control panel, CDUs, and side-stick flight controllers), and flight control mode (velocity control stick steering) compared with typical commercial equipment. Instead, the procedures were designed to mimic as closely as possible the techniques proposed for use by airline flight crews following CTAS descent advisories. A focused investigation of operational procedures and flight crew human factors was beyond the scope of this test. However, an evaluation of pilot procedures involving commercial airline flights was conducted in parallel with this test phase (ref. 22).

The test conditions flown in the RFD required significant preparation and pilot training. The RFD mode control panel was designed many years before the development of the performance-based VNAV systems which are common on modern commercial flight decks. The TSRV system is highly flexible, however, and techniques were devised to closely approximate the commercial FMS modes. Flight cards were developed for each test condition with an event sequence of TSRV-specific procedures to be followed in order to mimic the desired commercial FMS functionality. The exact procedures and flight cards used in the test are described in the following sections.

5.2.1. Conventional non-FMS

These conventional non-FMS procedures were designed to represent airplanes which are not equipped with flight management systems. They were flown by the pilots in the FFD. One pilot was designated as the flying pilot and manually flew the airplane from the IP to the metering fix. The other pilot in the FFD handled the nonflying duties, including communication with ATC and the TSRV and CTAS test engineers. A TSRV test engineer (or observer) was located in the jump seat behind the FFD to observe and assist in communication.

The flying pilot established the airplane on the inbound leg of the flight plan at the desired cruise altitude and speed prior to crossing the IP. Conventional VOR guidance was used for lateral tracking of the flight plan route. The pilot maintained altitude and speed up to the CTAS TOD.

The CTAS TOD was identified as a DME distance to a reference VOR station (DEN). The nonflying pilot

tuned a navigation radio to the appropriate station and monitored the DME distance. The flying pilot was instructed to begin the descent procedure within 0.1 n.mi. of the CTAS-specified DME range.

At the top of descent, the flying pilot would initiate the descent by retarding the throttle smoothly to idle. If the descent speed was less than cruise speed, the pilot would decelerate in level flight to achieve the desired descent speed. The flying pilot flew the remainder of the descent by using pitch to hold the Mach/CAS speed schedule. Prior to crossing 18 000 ft, the altimeter setting was changed to the local altimeter setting. The pilots were instructed to target their BOD to be just prior to crossing the metering fix. Throttle and/or speed brake were used to adjust the descent rate in order to reach BOD with just enough distance to decelerate from the descent CAS to the crossing speed of 250 knots at the metering fix.

5.2.2. Conventional FMS

These conventional FMS descent procedures were designed to utilize the VNAV capability of FMS-equipped airplanes to generate and fly a VNAV profile, including TOD, based on the CTAS-assigned descent speed profile. They were flown from the RFD by a NASA test pilot with the assistance of the TSRV test engineer acting as the nonflying pilot. All RFD test runs were flown by using autopilot for lateral tracking of the FMS flight plan in order to provide consistent performance for comparison with CTAS horizontal path predictions.

The appropriate flight plan (company route) and prestored approach were entered into the CDU prior to reaching the IP for the test scenario. Measured wind speed, wind direction, and static air temperature were hand recorded at intervals of 4000-ft altitude from 17 000 to 33 000 ft during the initial climb and on each subsequent descent. The latest data were manually entered into the descent wind page of the CDU for use in the FMS trajectory prediction. (This approach enabled using the FMS prediction to represent the ideal case of minimum modeling error for trajectory prediction, airborne or ground based.) Cruise speed (Mach = 0.72 or 0.76, depending on test condition) was entered as the selected speed on the CRUISE CDU page, and the EXECUTE button pressed to

11

activate the flight plan. The airplane was stabilized at cruise altitude and speed prior to crossing the IP.

After crossing the IP, the appropriate test card shown in figure 11 was used to specify the sequence of activities in the RFD. As shown on the card, there were six key events which required specific actions by the pilot and test engineer. The test engineer would monitor the events and call out the activities. The pilot would cross-check and confirm the activities. Typically the test engineer would perform the activities which required CDU entries and the pilot would handle mode control panel, throttle, and flight controller inputs. The test engineer would also handle some mode control panel entries at the request of the pilot.

The first event was after the IP and prior to receiving the CTAS descent advisory clearance. The crew verified that the airplane was level at the correct cruise altitude and speed and on path. The mode control panel was set to indicate AUTO, ALT, HOR PATH, and CAS ENG selected. This indicated autopilot engaged with pitch control holding altitude, roll control following the programmed flight plan horizontal path, and throttle holding airspeed.

After receiving the CTAS descent advisor clearance from the CTAS test engineer, the TSRV test engineer would select the LEGS page on the CDU to verify the proper crossing restrictions at DRAKO, enter the appropriate descent speed on the DESCENT page, and press EXECUTE to generate an updated trajectory. The CTAS TOD DME distance was entered on the CDU FIX page to display a circle with that radius around the reference VOR. The TSRV test engineer noted the discrepancy, if any, between the CTAS TOD and that computed by the FMS. The MCP altitude was then set to 17000 ft, the crossing restriction at the metering fix. At approximately 10 mi from the FMS TOD point, the autothrottle was disengaged and the DESCENT page was selected on the CDU in preparation for the descent.

Upon reaching the FMS TOD, the pilot would bring the throttle to idle and set the MCP CAS to the test condition descent CAS. The autopilot would pitch the airplane to follow the programmed descent path. During the descent, the pilot would use throttle to hold airspeed to within 5 to 10 knots of the desired descent speed schedule. If the airplane speed increased to

more than 5 knots above the desired speed, the RFD pilot would request the FFD pilot to deploy speed brakes to slow the airplane. This was necessary since the TSRV RFD did not have direct speed brake controls.

The final event occurred near the bottom of descent. Altimeter setting was changed to the local pressure prior to crossing 19000 ft, MCP CAS was set to the metering fix crossing speed (if necessary), and autopilot disengaged prior to 18000 ft. The pilot would then manually level the airplane at 17000 ft and adjust throttle to cross at the desired airspeed.

5.2.3. FMS With CTAS TOD

The FMS with CTAS TOD procedures were an extension of the FMS VNAV procedures with the airplane now restricted to initiate descent at the CTAS-specified point rather than the FMS-computed point. The primary advantage of the CTAS TOD procedure is that it establishes a predictable TOD for the controller to plan for separation with minimum workload. Four flight cards were prepared to account for the possible situations which could be encountered in the test. These situations were

1. Descent prior to FMS TOD with no deceleration required

2. Descent after FMS TOD with no deceleration

3. Descent prior to FMS TOD with deceleration

4. Descent after FMS TOD with deceleration

Figure 12 shows the flight card for each situation.

The procedures used for all four situations were the same as the conventional FMS procedures up to the point where the CTAS TOD DME distance was entered into the CDU FIX page. At 10 mi from the CTAS TOD (event 3 on the test card), the pilot would select FPA mode (flight path angle hold) for the autopilot. This selection prevented the autopilot from descending at the FMS TOD and allowed a manually selected descent at the CTAS TOD. Upon reaching the CTAS TOD, the pilot would execute the following descent procedures:

CTAS TOD prior to FMS TOD: If a deceleration was required, the throttle would be set to idle and cruise altitude maintained until the descent speed was achieved. A descent angle of $-1.5°$ (adjusted to provide a descent rate approximately 1000 to 1500 ft/min) was set in the MCP to initiate descent and capture the FMS VNAV path from below. Throttle was then used to maintain the descent speed schedule. Once the FMS-computed TOD was crossed, vertical path guidance was selected by pressing VERT PATH on the MCP. The desired FPA was reset to the appropriate value to continue a descent rate of 1500 ft/min until the vertical path was captured. The rest of the descent was flown the same as described for the conventional FMS case.

CTAS TOD after FMS TOD: Throttles were retarded to idle and descent initiated by using the MCP FPA mode. Deceleration to descent speed, if necessary, was done in level flight. Initial target descent angles of between $-3°$ and $-6°$ were selected, based on the descent speed, to capture the FMS VNAV path from above. VERT PATH was then selected to arm vertical path guidance. Descent angle was adjusted as necessary to maintain a reasonable closure on the programmed vertical path. Speed brakes were deployed as necessary to maintain descent speed. Upon capture of the FMS descent path, the speed brakes were retracted and the remainder of the descent was flown the same as described for the conventional FMS.

5.2.4. Range-Altitude Arc

The range-altitude arc conditions were designed to represent descents which do not require FMS VNAV to achieve the proper BOD. Instead, the so-called range-altitude arc would be used to target BOD, with CTAS providing the TOD. The goal was to explore the feasibility of a simple alternative to VNAV for improving the precision of vertical profile conformance. Figure 13 shows the flight cards used for these procedures.

These procedures were similar to the constrained descents flown from the RFD during the Phase I flights. During this test, however, the range-altitude arc was modified to show the projected range along the FMS lateral path at which the airplane would reach the MCP altitude (fig. 7) in addition to the straight-line distance. This modification allowed the pilot to more

accurately target the proper BOD location during the early stages of the descent. Also for this test, the RFD pilot had the FMS-computed TOD to assist in determining the possible throttle and/or speed brake control activity needed during the descent. An early descent would generally require throttle, whereas a late descent would need some speed brake. As seen in the flight cards, the procedures for early and late descents were identical, with only the wording in step 5 modified to indicate the expected primary speed control device.

5.2.5. Test Matrix

The Phase II test matrix, as in Phase I, was based on two primary test variables: speed profile and pilot procedure. Table 2 presents the 12 conditions defined by the combination of 3 speed profiles and 4 procedures. The goal was to complete two runs of each of the 12 conditions combining speed profile and pilot procedures. In addition, as time permitted, several flights into the northeastern arrival gate (KEANN) at Denver were conducted to collect atmospheric data away from the Rocky Mountains.

6. Results and Discussion

The TSRV Boeing 737 airplane was deployed on two separate occasions to Denver Stapleton International Airport for these tests. During each deployment, the airplane conducted multiple descents from cruise altitude into the Denver terminal area while the CTAS field system at Denver ARTCC provided real-time descent advisories.

Phase I included 23 descent runs conducted during 7 flights over a period of 1 week in October 1992. Nine runs were conducted during two night flights, and the rest were day flights. Three additional runs were excluded from the analysis due to experimental system errors encountered while conducting the runs. Table 3 provides a summary of the test conditions completed for Phase I.

Weather conditions during Phase I were generally good, with no adverse conditions encountered which delayed or canceled a planned flight. The most significant weather events encountered were strong jet stream winds during the two night flights (R679 and R680), with pronounced wind gradients during

13

descent. The impact of these winds is discussed in section 6.1.3.

Phase II included 25 descents conducted during 9 daylight flights over a period of 1 week in September 1994. Four additional runs were conducted to collect atmospheric and radar tracking data in another area and one additional run was conducted to investigate a mid-descent correction in speed profile. An additional six descent runs were initiated but aborted because of experimental system errors and ATC interruptions encountered in conducting the runs. Table 4 provides a summary of the test conditions completed for Phase II.

A variety of weather conditions were encountered during Phase II. Light winds and stable atmospheric conditions prevailed for the first 2 days (flight R728 and R729). Convective buildups and slightly stronger winds were encountered during flight R730, with storm cells and light rain near the turn at ESTUS during descent. On flight R732, a frontal passage, associated with a brief snow storm in the Colorado area, provided strong and variable winds aloft and forced early termination of the flight. The following day (flight R733) was clear with strong, steady northerly winds at all altitudes. High pressure dominated the area throughout the test period with altimeter setting above standard each day.

The analysis of the results from these flight tests is divided into four major sections. First, the trajectory prediction error sources encountered during the test are examined. Second, the actual flight trajectories are compared with the CTAS predictions to determine the overall accuracy. Third, a sensitivity analysis of the modeling error sources is performed to identify their contributions to both metering fix arrival time and vertical trajectory errors. The sensitivity analysis involved recomputing the idle descent trajectories of Phase I by using combinations of updated performance and atmospheric models using both the CTAS trajectory synthesis program and the TSRV flight management profile generation algorithms. Finally, the error sources and their impact on trajectory prediction accuracy are summarized.

6.1. Error Sources

There were four basic trajectory prediction error sources encountered during these tests:

Radar tracking errors

Airplane performance model errors

Atmospheric modeling errors

Pilot conformance

An additional source of error, in section 6.1.5, also affected test results. Unlike the four basic error sources, these errors were due to problems uniquely attributable to the experimental nature of the CTAS field system used for these tests.

6.1.1. Radar Tracking Errors

Until more accurate track data become available (via airplane data link reports or improved radar tracking algorithms), CTAS will depend on FAA Host radar track data to initialize trajectory predictions. The track data provide the airplane position, altitude (mode-C), and inertial velocity (ground speed and track angle). Errors in the current radar tracking system translate directly into initial condition errors for CTAS. Determination of the nature and magnitude of the radar tracking errors is therefore of significant importance to the CTAS project as well as other ground-based trajectory prediction tools.

Actual airplane state conditions, as measured by the TSRV during these flight tests, were compared with the ATC radar track data provided to CTAS from the ATC Host computer. During Phase I, TSRV data were only recorded during the actual test runs; this limited the data to nonturning conditions in which the airplane was heading directly toward Denver. During Phase II, TSRV data were recorded continuously throughout each flight; this allowed a more comprehensive analysis of radar tracking errors under conditions that included climbing, descending, turning, and accelerating segments of flight.

Errors in radar track to TSRV flight data are presented in three tables. Errors are expressed as airplane measurements minus radar track. Table 5 presents the summary of radar tracking errors for both Phases at the initial and final conditions used for the CTAS trajectory predictions. These differences represent the sole contribution of radar tracking errors to the CTAS predictions evaluated in these tests. Tables 6 and 7 present similar data for position and velocity, respectively, based on the entire set of flight data collected

14

during Phase II. These data represent the potential errors that affect trajectory prediction and conformance monitoring in en route airspace.

Table 5 presents both the velocity and position errors at the initial and final conditions associated with the CTAS predictions in these tests. The initial condition errors (Mean + Standard deviation) for both Phases were less than 10 knots in ground speed and 8° in track angle. Although these errors are small for the Host track data (typical of level unaccelerated flight at cruise), the ground speed error provides a direct contribution to CTAS accuracy. An error of 10 knots for a typical jet airplane operating at a ground speed of 450 knots translates into an error of 18 sec for every 100 n.mi. of cruise. The final condition (metering fix) velocity errors listed in table 5(b) do not affect the accuracy of CTAS but are indicative of the tracker accuracy during level-flight deceleration segments. Particularly notable are the ground speed errors which were due to the transients in velocity associated with the descent and level-off deceleration to the metering fix. The position error shown in table 5 was the absolute range difference from the GPS-measured location of the airplane to the radar tracked position of the airplane. The along-track error is the projection of the position error along the instantaneous track angle of the airplane. The cross-track error is the component of the position error normal to the airplane track angle. As seen in the table, nearly all the position error was contained in the along-track error component. An "equivalent" time error was computed by dividing the along-track error component by the airplane ground speed at that position. Essentially, the radar-tracked position of the airplane was lagging the actual airplane position by this equivalent time error. The position errors in table 5(a) add a direct contribution to CTAS trajectory prediction error, whereas the errors in table 5(b) represent the errors that would be included if the Host tracker was used to measure the end-point accuracy of the trajectory prediction. From a controller's point of view, the mean along-track errors would essentially cancel themselves while the variation will most likely introduce some error. From an air-ground integration (trajectory exchange) point of view, both the mean and variation in along-track error will affect trajectory prediction accuracy if not accounted for.

Some of the equivalent along-track time error is attributed to the lack of a time stamp on the track data

received from the Host computer. CTAS processing must assign its own time stamp based on the time of receipt. Since the Host transmits track data to CTAS in batches, the CTAS time stamp estimate may be off by as much as one update period (approximately 12 sec).

The data in table 5 were generated based on the initial and final conditions of the test runs listed in tables 3 and 4. A summary of all radar-track position errors from the Phase II flights is given in table 6.

As seen in table 6, the track position errors were extremely consistent throughout all the flights. The average along-track error of about 0.7 n.mi. was slightly less than recorded at the CTAS initial condition point because it includes flight at all altitudes and speeds. The CTAS initial conditions were recorded at cruise altitude with the highest ground speeds resulting in larger along-track errors. The along-track error of 6 to 7 sec was consistent for all conditions. The cross-track error was also consistent for all conditions and was relatively insignificant.

Table 7 presents the ground speed and track angle errors associated with level flight, altitude change, and turning segments for all data collected in Phase II. The turning segments are further divided into turn and postturn segments. Turn segments are defined as a segment where the actual airplane turn rate exceeds 0.5 deg/sec. Postturn segments are defined as segments which immediately follow a turn segment and continue until the radar tracking ground speed error falls below a value of 10 knots. The altitude change segments are defined by segments involving ascent and descent rates greater than 100 ft/min and not in a turning segment. Level flight segments are defined as everything else (constant altitude and not in a turning segment).

For level flight segments, for which the CTAS initial conditions were a subset, the mean ground speed error was approximately 2 knots with a standard deviation of about 12 knots. These segments included level, unaccelerated flight, as well as level acceleration and deceleration segments. The differences between these level flight data and the ground speed errors in table 5 were caused by several factors. Table 5 included a very small subset of the data in table 7 (less than 4 percent). Table 5(a) represents

unaccelerated flight, whereas table 5(b) represents level deceleration segments at the peak of the deceleration transient in radar track ground speed. Comparatively, the ground speed errors during altitude change segments were nearly the same as the errors for level flight segments. For turning segments, ground speed errors were substantially greater, with the tracker ground speed less than actual ground speed. The mean error was 37 knots during the actual turn with a standard deviation of 59 knots. During the postturn segments, the error was observed to be significantly greater in mean with about the same variation. The larger postturn mean error was caused in part by the segment definition as well as the characteristics of the tracker. By definition, the postturn segment included ground-speed errors of at least 10 knots (the 10-knot criterion was considered reasonable in order to separate the relatively large turn-induced errors from the normal variation experienced in level flight). Regarding tracker characteristics, the initial error growth lags the actual start of the turn and the maximum error tends to occur just after the actual turn is completed. Both these lags tend to reduce the mean error measured during the turn compared with the mean error in the postturn. The length of the postturn segment was observed to be quite variable and dependent on the size of the turn, magnitude of the ground speed error, and acceleration rate of the airplane following the turn. For the data shown in table 7, there were 45 turns analyzed, with turn angles ranging from 3° to 305°. Mean turn angle was 68° with the average length of the postturn segment being 93 sec.

In comparison with the position errors, velocity errors may have a greater impact on trajectory prediction accuracy, particularly for cruise flight where the track velocity is used to infer the velocity for that segment of the trajectory. For example, each 15 knots of error results in an along-track prediction error growth rate of 0.25 n.mi./min (5 n.mi. for a 20-min prediction). Controllers, who accept these velocity anomalies as a part of their job, have learned to anticipate and filter out the errors from their decision making and/or provide larger separation buffers to protect against anomalies. To the extent that these anomalies may be reduced or filtered, automation may be able to lead to a reduction in excess separation buffers.

With regard to track angle errors for both level flight and altitude change segments, the track angle errors exhibited a negligible mean with a standard deviation of about 5°. For turning segments, the angle

error was substantially greater as was seen for the ground speed error. During both turn and postturn segments, the mean error was observed to be approximately 5° with a standard deviation of 28° and 13°, respectively. The difference in variations is explained by the observation that the track angle error tended to die off before the ground speed error did. Because the postturn segments were defined based on ground speed error, the track angle computation included a considerable number of data points with relatively little error.

6.1.2. Airplane Performance Model Errors

The CTAS trajectory synthesis algorithms use detailed models of airplane drag and idle thrust to compute descent trajectories. Drag is represented by high-speed drag polars providing drag coefficient as a function of lift coefficient and Mach number. Thrust is modeled as a function of engine setting, Mach number, altitude, and temperature. For this test and airplane type, the CTAS descent prediction was nominally based on an idle-thrust engine setting.

Langley has developed performance models for the Boeing 737-100 airplane suitable for use in trajectory generation programs for airborne flight management systems. These models are based on manufacturer's performance data for the generic Boeing 737-100 airplane. These models were used to generate data tables of drag coefficient and thrust for use by the CTAS trajectory synthesis program.

The performance of the TSRV airplane was known to differ from that expected from the generic data. The airplane was the original prototype for the Boeing 737-100 series of jet transports and was well over 20 years old at the time of these tests. In addition, this airplane has numerous external antennas and exposed rivets on the fuselage which were not present during the original performance testing by the manufacturer. Langley had previously developed adjustments to the baseline Boeing 737-100 performance for use in the airborne flight management system to account for the degraded performance of the airplane. These adjustments were not included in the data used by CTAS during the flight test experiment. These adjustments were excluded from CTAS in order to introduce performance-model error into the test. Operational airplanes, of the same type, are expected to

vary in actual performance due to age as well as equipment variation (e.g., power plants, antennas, and airframe modifications).

The stabilized cruise and descent conditions flown in Phase I were used to refine the performance model of the airplane to reflect the actual performance measured during the test. Data tables were then generated by this revised performance model for use in the sensitivity studies described later in this report. The appendix describes the methods used in updating the airplane performance model and presents the resulting modifications made to the thrust and drag models. The actual TSRV drag differed from the manufacturer's performance data by approximately 11 percent (greater). The idle thrust also differed with a variation over altitude. The combined effect on the descent performance of the airplane was, on the average, a 5-percent lower value of net TMD, which resulted in a 5-percent increase in descent rate. These updated performance data were the basis for the FMS computations in Phase II.

In addition to thrust and drag, CTAS estimates the airplane weight to evaluate the point mass equations of motion for the vertical profile calculations. CTAS is capable of estimating the weight of individual flights as a function of time based on knowledge of a reference weight (e.g., takeoff gross weight) and fuel-burn estimation. It is anticipated that the reference in-flight weight could be made available to CTAS via a new field in the files flight plan or by data link. Until the FAA infrastructure is in place to supply a reference weight, CTAS relies on an estimated weight as a function of airplane type and phase of flight. For descents, a typical descent weight is used for descent calculations. For the flight tests, a typical descent weight of 85000 lb was used for all runs. For the Phase I idle runs, the average weight of the TSRV was 83560 lb with a standard deviation of 4380 lb.

6.1.3. Atmospheric Modeling Errors

CTAS trajectory prediction accuracy depends, in large part, on the accuracy of the atmospheric model data it receives from external sources such as MAPS. Atmospheric characteristics (winds and temperature), as a function of position and altitude, affect CTAS trajectories in several ways. Winds aloft form the basis of predicting the ground speed profile, as a function of

airspeed and path, as well as estimating airspeed from radar-based ground speed. Wind gradient, with respect to altitude, can also have a significant influence on rate of ascent and descent. Temperature profiles and altimeter setting are used to determine geometric altitude, as a function of pressure altitude and position, to provide an inertial basis for integrating the point mass equations of motion over ascent and descent segments. Temperature is also used to correct performance data for nonstandard temperatures and convert between TAS and Mach/CAS.

Atmospheric modeling errors were determined by comparing the airplane measurements of winds and temperature with the CTAS interpolated model values at specific altitudes along the predicted descent trajectory. Figure 14 summarizes the altitude profile of air temperature with measurements and corresponding model errors for all flights in both Phases. These data are presented in pressure altitude intervals of 2000 ft in terms of the mean value and standard deviation for each Phase. The temperature profiles were similar for both Phases. Compared with the standard atmosphere, the profiles tended to be warmer with a greater gradient (lapse rate) in temperature with altitude. The mean temperatures ranged from 8° to 9°C above standard at the lower altitudes (17000 ft) to approximately 2°C above standard at cruise altitude. The mean errors tended to be within 3°C for Phase I, with greater accuracy at the lower altitudes, whereas the errors in Phase II were within 1°C. These temperature errors, although only representative of a small sample of realistic atmospheres, were considered to have a negligible effect on the trajectory prediction accuracy results.

Figures 15 and 16 present a summary of measured winds (resolved into components in the true north and east directions) for each flight within Phases I and II. The data are presented in terms of the mean and standard deviation of the wind, at common altitudes, over each descent run of a particular flight. The cruise altitude data are presented slightly differently for each Phase. For Phase I, a single data point (mean and standard deviation) is presented at cruise altitude based on the mean wind over the cruise segment of each run. The average length of the Phase I cruise segments was 9.8 n.mi. with a standard deviation of 6.5 n.mi. For Phase II, the cruise winds are presented at three positions corresponding to the analysis gates introduced in section 6.2. These data points include

17

the initial condition, TOD, and a position in the middle of cruise. The average length of the Phase II cruise segments was 21.3 n.mi. with a standard deviation of 7.0 n.mi. The variation in measurement (between and within the Phase II cruise data points) may be due to several factors that include variation in wind with position, variation in wind with time (at a position), and measurement error. Airborne measurements of wind tend to be more accurate in the along-track component and during steady-state (nonturning) flight.

Figures 17 and 18 present the differences between measured winds and the CTAS model winds for Phases I and II. These data include the along-track component of the wind error to better illustrate the wind contribution to trajectory prediction errors. In some flights (figs. 17(c), 17(e), and 18(e)), the along-track wind-error component was relatively small compared with the total wind error. In particular, flight 732 (fig. 18(e)) experienced a total wind error greater than 60 knots at the higher altitudes with negligible along-track wind errors. The unusually large variation in along-track error at cruise altitude in flight 729 is due to the CTAS interpolation error described in section 6.1.5.

A composite of all wind errors for Phases I and II is shown in figure 19. Although the mean errors tend to indicate that CTAS/MAPS does a better job of predicting the winds along the descent at lower altitude than at cruise, the variations are relatively large. These variations, coupled with a relatively small data set representing a few atmospheric conditions, make it difficult to interpret atmospheric prediction performance. Several of the Phase II runs were analyzed further to determine what errors, if any, were contributed by the CTAS processing of MAPS data (ref. 23). Results indicated that although CTAS processing of MAPS data contributed a measurable amount of error, the errors in the MAPS data (compared with the TSRV measurements) were substantially greater. For example, analysis of flights 729, 730, and 732 indicate that the CTAS-processed winds had a combined root-mean-square (rms) wind error of 21 knots compared with 18 knots for the actual MAPS data.

Figure 20 shows the differences between measured winds and those entered into the FMS during Phase II. These data are used to support the analysis of the TSRV FMS-based trajectory predictions in section 6.2.

6.1.4. Pilot Conformance

The pilot conformance errors are related to the accuracy of the pilot's tracking (manually or automatically) of the clearance speed, TOD, and course. The TSRV airplane was flown by NASA pilots who were instructed to fly as accurately as possible in order to minimize piloting errors and isolate the effect of the other error sources. Table 8 presents the overall pilot-induced speed errors for both Phases I and II. The data represent the mean and standard deviation of speed error sampled at a rate of once per second throughout the cruise, constant Mach descent, and constant CAS descent segments for the FFD and RFD runs. As seen in the table, the pilots were able to follow the CTAS speed schedule with a high degree of accuracy and effectively eliminate speed conformance error from the flight data analysis. Extension of the results in this paper to commercial flight operations should consider the variation with which line pilots would maintain speed.

With regard to TOD, the pilots were careful to initiate the descent procedure no sooner than and within 1 n.mi. of the CTAS TOD advisory. The measurement of actual TOD errors is presented in section 6.2.3.

Lateral-path errors (cross track and along track) were not a factor for the straight-path descents in Phase I. For Phase II however, the runs involving conventional VOR radial tracking experienced lateral-path deviations which made a significant contribution to the trajectory prediction error. During these runs, the pilots tracked the radials as precisely as possible and were generally within one needle width of the outbound radial from CHE. Lateral-path deviations of greater than a mile occurred during and after the turn inbound to DEN even though the pilots were using the flight director and course deviation indicator (CDI) to their best advantage. Although no data were recorded on CDI deflection, cross-track error was recorded and is examined in section 6.2.1 as part of the trajectory prediction error analysis.

6.1.5. Experimental System Errors

The experimental system errors were introduced during the tests but are not representative of operational errors faced by CTAS. Where possible, corrections for these errors were introduced into the analysis. These errors, and the associated corrections

applied to the data, are described in the following paragraphs.

During Phase I, three CTAS trajectory predictions were not recorded and had to be regenerated based on the recorded track of the airplane. The recomputed trajectories produced TOD advisories which were within 0.5 n.mi. of the original descent advisory given to the airplane. This difference was considered to have a negligible effect on the Phase I results. The absolute time profile, however, could not be reproduced for the regenerated trajectory data because of limitations in the regeneration technique which was used. In order to properly account for initialization errors, the recomputed trajectories were combined with the actual radar tracking data to determine the initial condition which would have produced the resultant descent advisory. This determination was done by computing the distance to the Denver VOR for each radar tracking point during a test run. The trajectory range from the CTAS-predicted trajectory was then used to interpolate on the radar track data to determine the time at which the airplane was at this range according to the radar data. This time was then used as the initial condition for the CTAS prediction.

A second problem, affecting all Phase I runs, involved the computation of wind gradient and its effect on the descent rate prediction. A new atmospheric data interpolation scheme was introduced into CTAS just prior to Phase I and the wind gradient computation was inadvertently switched off. This problem, detected in posttest analysis, was corrected prior to Phase II. The impact of this problem was analyzed by using a stand-alone version of the CTAS trajectory generator. A series of descent trajectories were generated with and without the wind gradient computation for a Boeing 737 airplane model. This series of trajectories included along-track wind gradients ranging from 0 to 4 knots/1000 ft. In general, each 1 knot/1000 ft of wind gradient (along track) contributes approximately 3.5 percent to the descent rate.

During Phase II a different problem was encountered. Following completion of the flight testing, it was discovered that a change to the Denver radar coordinate system had been implemented in the ATC radar tracking data which had not been added to the CTAS software used during the test. The result was a systematic error of approximately 1.5 n.mi. to the initial conditions used by CTAS. In order to compensate for this error, the TSRV flight data were converted to both the

CTAS and Denver ATC radar coordinate systems during data analysis. Radar tracking and lateral-path errors were calculated with the Denver ATC radar coordinates. Comparison with CTAS vertical trajectory prediction was done with the CTAS coordinate system.

CTAS initial condition errors for Phase II could not be precisely determined due to the error introduced by the coordinate system difference between CTAS and the ATC radar tracker. Correcting the TSRV flight data to the CTAS coordinates resulted in a lateral offset at the beginning of the trajectory. This offset was an artifact of the coordinate system error and not indicative of the CTAS prediction process under normal conditions. In order to compare CTAS and flight vertical trajectories, the small offset in lateral path was ignored, and vertical trajectory parameters were compared solely based on distance to go along their respective paths. The initial condition errors were assumed to be zero for the trajectory comparisons. An approximation of initial condition errors for Phase II was determined from the comparison of flight and radar tracking data, as described in section 6.2.

An error in the initial conditions for a few of the runs in Phase II was introduced by a CTAS software error in the interpolation of the atmospheric model data. This error resulted in an incorrect initial ground speed calculation. The initial cruise airspeed was determined correctly from radar tracking ground speed and atmospheric data models. The cruise trajectory is generated based on either holding the initial cruise airspeed constant or accelerating to an "advisory" airspeed to be held constant. By holding the cruise airspeed constant, CTAS correctly predicts the variations in ground speed caused by variations in wind and course. During cruise trajectory integration, however, the interpolation error resulted in a predicted ground speed that differed from the radar track value at the initial condition. Only the first three runs during flight 729 were affected by this error.

An additional systematic error, related to the definition of the metering fix crossing altitude, was introduced into Phase II runs. Although the descents are initiated at flight level altitudes, the bottom of descent is defined by an indicated altitude based on the local altimeter setting correction. For the purposes of this test, the altimeter correction was applied manually. (CTAS software and interface for automatic collection and processing of the local altimeter setting were not

available in time for this test.) The correction was applied in the opposite sense throughout the test and the error was not discovered until after the test was completed.

6.2. CTAS Trajectory Prediction Accuracy

The trajectory accuracy analysis is based on a comparison between the CTAS-predicted trajectories and TSRV-measured flight trajectories. The analysis is facilitated by the decomposition of the 4D trajectory into five component 2D profiles that are

Cross-track profile

Along-track profile

Altitude profile

Speed profile

Time profile

Comparisons are accomplished by correlating the profile parameters (e.g., distance flown, speed, altitude, and time) to a common reference path defined by the predicted trajectory. The profile decomposition facilitates the identification of the primary error sources affecting each profile parameter and provides insight into the influence of errors in one profile parameter on another.

Analysis of the Phase II runs includes a similar comparison between the onboard TSRV FMS predictions and the measured trajectories flown. The TSRV FMS predictions, based on an updated performance model and atmospheric observations, represent the case of minimal modeling error. Because both TSRV and CTAS predictions result in nearly the same trajectories given the same model data, this approach provides insight into the sources of errors affecting the CTAS trajectories and the potential differences between airborne and ground-based predictions.

The comparison of flight and trajectory prediction data (CTAS and FMS) involved a multistep process. First, the flight and FMS prediction data were converted from latitude and longitude to the Denver Center radar-track reference frame used by CTAS. Next, radar tracking errors, which introduced initialization errors to the CTAS prediction process, were quantified (table 5). The actual trajectories were then adjusted to common initialization conditions (position

and time) to isolate the errors introduced by other elements of the trajectory prediction process. Finally, the trajectory comparisons were accomplished by referencing the trajectory parameters to a common along-track range based on the predicted trajectory. Phase I trajectories were flown direct to the metering fix (KEANN) along a straight-line route. The distance to go to KEANN was therefore used as the common reference for trajectory comparison. The Phase II route involved a more complex path with a turn during the middle of the descent. The FMS- and CTAS-computed lateral paths were nearly the same, with only a small discrepancy at the initial condition (IC) caused by the coordinate system transformation problem described in section 6.1.5. This error, along with the turn radius differences between CTAS and the FMS lateral paths, was found to contribute no more than 0.1 n.m. difference in the calculated distance along the path. The respective range along the reference CTAS and FMS lateral paths was therefore used as the common reference for comparing trajectory parameters for the Phase II data.

Differences between the actual and predicted trajectories were computed at specific locations (gates) along the flight path. The analysis gates were defined as reference positions along the predicted path (CTAS or FMS) which vary with the geometry of each trajectory altitude profile. The gates were defined at fixed geographic locations, vertical profile transitions, and at even increments of pressure altitude. Figure 21 illustrates the analysis gates for both Phases I and II. During Phase I, the airplane was stabilized (constant altitude, heading, and speed) in cruise at the PONNY intersection. The initial condition gate (IC in fig. 21(a)) was the point at which the final CTAS-predicted trajectory was computed. This point varied from run to run. The top-of-descent gate (TODG) was defined as the final point at cruise altitude of the predicted trajectory. TODG represents the same point as TOD except when the airplane must decelerate to its descent speed (the difference being equivalent to the deceleration distance). TODG was chosen for analysis to provide a consistent comparison between runs. The bottom-of-descent gate (BODG) was defined as the point where the predicted trajectory reached the altitude constraint for crossing the metering fix. The trajectory ended at the metering fix (KEANN in fig. 21(a)). For Phase II, the airplane was stabilized inbound at the Hayden VOR (CHE in fig. 21(b)). The IC was chosen to be the location of either the final

CTAS or FMS prediction, whichever was later. An additional analysis gate at the GOULL intersection during the cruise portion of the run was included for Phase II. The TODG and altitude gates were defined the same as Phase I for the CTAS comparisons but were referenced to the FMS predicted trajectory for the FMS comparisons. There was no BODG for Phase II, since analysis of errors at BOD was not significantly different than at the metering fix. The Phase II trajectories ended at the DRAKO metering fix. The ground tracks are presented in terms of the Denver Center x,y coordinate system which corresponds to true east and north, respectively. The TSRV flight data, CTAS predictions, and FMS predictions (Phase II only) were interpolated to provide data corresponding to the gate locations.

The following sections summarize the results of the trajectory analysis in terms of the cross-track, along-track, altitude, speed, and time profiles. The cross-track and along-track analyses presented herein focus on Phase II. The straight path utilized in Phase I essentially negated the influence of cross-track errors on the CTAS trajectory prediction accuracy. The turn within the descent of the Phase II path was designed to emphasize the potential influence of cross-track and along-track path errors on trajectory prediction accuracy.

6.2.1. Cross-Track Profile

Figure 22 shows a summary of lateral cross-track error for Phase II at each trajectory analysis gate as a function of FMS automation level. The three levels for which LNAV was used for lateral guidance (FMS TOD, CTAS TOD, and ND arc) exhibited essentially no cross-track error, as might be expected. The non-FMS runs, however, showed an average offset of approximately 5000 ft left of desired course during the run prior to the turn that increased to an average 13000 ft left of desired course following the turn (which was to the right). Figure 23 illustrates the ground track of the non-FMS runs conducted during flight 729. The left offset during the preturn segment was well within the expected navigational accuracy of VOR-based airways. Pilot comments indicated that the predominant tailwind changing to a crosswind following the turn encountered along this route contributed to the inbound course overshoot. The largest error occurred during run 3 of flight 729 (fig. 23) when the

pilot followed flight director commands throughout the turn (by keeping the lateral flight director command bar centered) and did not attempt to adjust for the indicated overshoot on the CDI. Pilot comments indicated that most pilots would wait for the flight director cue to initiate the turn; however, they tended to apply additional correction back to the desired course once the overshoot occurred.

6.2.2. Along-Track Profile

The effect of the VOR-radial offset and turn overshoot on the distance flown is shown in figure 24. The actual distance flown by the airplane was compared with the predicted distance flown at each analysis gate. The distance flown during the non-FMS runs was, on average, 1.3 n.mi. greater than predicted, with a standard deviation of 1.1 n.mi. This increased range occurs at the turn, which typically happened between the FL250 and FL210 analysis gates. Anticipation of the overshoot and initiating the turn earlier than indicated by the flight director could reduce this error. The CTAS path generation could be modified to remove the mean contribution of the overshoot phenomenon by modeling the overshoot as a function of turn angle. However, trajectory prediction errors due to variations in pilot navigation error can only be reduced by improving the precision with which pilots navigate.

6.2.3. Altitude Profile

Figure 25 presents the altitude error, for Phase I, between the idle and constrained descent procedures flown from the RFD. The constrained procedures result in a significant reduction in altitude error (both mean and variation) over the idle procedure. Both procedures behave similarly in the initial stages of the descent, by first exhibiting a slight positive altitude error followed by an increasingly negative (below path) error. The initial error is due to the unmodeled (within CTAS) segment at the TOD related to the pilot response and throttle reduction as well as the rounding off to the nearest nautical mile of the CTAS TOD advisory from the reference fix. The airplane then descends at a higher than predicted rate (about 15 percent), primarily due to two factors: performance modeling and wind gradient effects.

The performance modeling errors described previously account for a descent rate error of approximately

5 percent. The along-track wind gradient, which averaged approximately 2 knots/1000 ft over the Phase I idle runs, accounts for a descent rate error of about 7 percent. The sensitivity of descent rate error to unmodeled wind gradient was determined through a series of fast-time trajectory simulations. CTAS was used to generate a set of descent trajectories for a Boeing 737 airplane with a standard atmosphere, nominal weight (85000 lb), and a descent from FL350 to 10000 ft at 0.72 Mach/280 KCAS. Trajectories were generated with an along-track headwind gradient which varied between 0 and 4 knots/1000 ft in 1-knot increments. Weight errors contributed little, if any, effect on the altitude profile accuracy in descent for the airplane and conditions tested (weight would have a significant effect on climb profile accuracy). The mean descent rate error due to weight was slightly less than 1 percent (actual steeper than predicted).

After the Mach/CAS transition point, the altitude error continues to increase for the idle descent conditions until the pilot begins to level off at the crossing altitude. The largest errors occur as the airplane levels off with a mean altitude error of just over 1500 ft plus a standard deviation of 900 ft. For the constrained conditions, however, the growth in altitude error is arrested midway in the descent as the pilot initiated corrections during the constant CAS portion of the descent. The constrained procedures reduced the maximum mean error in altitude by nearly 800 ft and the standard deviation by 400 ft. Although modeling errors reduce the efficiency of the planned descent profile, the pilot procedure serves as a useful tool to minimize the associated trajectory prediction errors.

The altitude error results from Phase II were more complex, as shown in figure 26 for the CTAS predictions. The ND arc runs, which were nearly the same procedures as the constrained descent runs of Phase I, exhibited the same characteristics of increasingly negative altitude errors (below the predicted path) correcting back toward zero error midway through the descent. The non-FMS runs, however, showed a strong increase in negative altitude error near the bottom of descent. This result was caused by the longer distance flown during the non-FMS runs which masked the altitude error until after the turn (at approximately FL210). Each nautical mile of extra distance flown contributes approximately 300 ft of altitude error (below path). The FMS runs, using both CTAS TOD and FMS TOD, had a more positive altitude error due to the general tendency of the FMS path to be steeper than the CTAS path (resulting in a later TOD). In comparing the CTAS and FMS TOD runs, relatively large errors are associated with the CTAS TOD runs. These larger errors were not caused by the CTAS TOD procedures per se but were because of the small number of runs flown. In fact, the CTAS TOD procedure reduces the altitude error at the top by initiating the descent at the CTAS TOD. After capturing the FMS path within the first 1000 ft of descent, the remainder of the descent was an exact duplicate of the FMS procedure at all gates from FL310 to DRAKO. The larger errors associated with using the CTAS TOD was a random phenomenon attributable to variations in the atmospheric prediction errors. All Phase II runs show a small negative (below predicted path) altitude error at the metering fix. This anomaly, due to the altimeter setting error described earlier, actually introduced a bias in each descent trajectory equivalent to the final error.

The most significant influence of altitude profile error is the impact on the top of descent point. Table 9 presents the along-track error of the TOD event for Phase II. These data present the differences between the measured airplane TOD and the CTAS prediction. A positive error indicates the airplane descended later than the prediction. This convention was used to facilitate comparison between results from these flight tests and from later field trials involving commercial flights.

As seen in table 9, those procedures which actively used the CTAS TOD for descent guidance exhibited a mean error of about 1 n.mi. with a standard deviation of another mile. Most of this error was due to time required for the reduction of throttle (not modeled within CTAS) and rounding off in the TOD advisory issued to the pilot. By comparison, the FMS TOD procedure had a mean error of 2.5 n.mi. with a standard deviation of 2.8 n.mi. This larger error reflects the differences in TOD computed by the FMS compared with that computed by CTAS. A comparison of the difference between FMS and CTAS TOD predictions for all Phase II runs revealed a mean error of 3.8 n.mi. with a standard deviation of 3.4 n.mi. The largest differences in FMS versus CTAS TOD actually occurred during the ND arc and CTAS TOD procedure cases. These results are consistent with the altitude errors shown in figure 26.

Altitude errors from the FMS-predicted vertical profile were also computed for the Phase II test (fig. 27). The ND arc and non-FMS runs were excluded from this analysis because those procedures did not follow the FMS path. As expected, the FMS TOD and CTAS TOD runs exhibited very little error as the procedures called for the pilot to fly the FMS-generated altitude profile. The slight negative error of about 300 ft at FL190 and DRAKO for all runs was caused by the lack of an altimeter setting correction within the FMS path generation. The flight crew entered the altimeter setting prior to reaching FL190 and flew the airplane to a barometric altitude of 17000 ft as required. The only substantial difference between the two procedures was the difference in TOD which was caused by differences in model data (atmosphere and performance).

6.2.4. Speed Profile

Errors in the CTAS prediction of a ground speed profile depend on (1) piloting conformance to speed schedule, (2) errors in the altitude profile which result in true airspeed errors at the correct Mach/CAS speeds, (3) errors in the predicted wind and temperature aloft which result in ground speed errors at the correct Mach/CAS and altitude, and (4) ATC radar tracking errors which result in incorrect initial condition ground speed.

For this test, pilot conformance errors with the speed schedule were negligible as described in section 6.1.4. The effects of altitude profile errors, atmospheric modeling errors, and ATC radar tracking errors on the speed profile can be observed by determining speed errors along the predicted path at common range locations. The Phase I test results exhibit altitude error effects induced by the idle versus constrained descents as discussed previously. Phase II attempted to minimize altitude errors by using various vertical guidance techniques. Radar tracking and atmospheric modeling errors were encountered to differing degrees in both tests.

Figure 28 presents the ground speed, true airspeed, and calibrated airspeed errors at the trajectory analysis gates for the Phase I flight test. The IC errors from the radar tracker were on the order of about 7 knots standard deviation with negligible mean error throughout cruise (IC to TODG). This result is consistent with the raw radar ground speed in table 5. In

comparison, a true airspeed error of about 12 knots mean with about 12 knots standard deviation is seen at the IC. Since CTAS estimates true (and calibrated) airspeed at the IC based on radar-tracked ground speed and atmospheric wind and temperature models, the additional true airspeed error is induced by errors in the atmospheric model. CTAS uses this estimated cruise true airspeed in conjunction with the atmosphere model to predict the ground speed for the rest of the cruise segment. For the descent prediction, CTAS uses the scheduled descent Mach/CAS (with an appropriate acceleration or deceleration from the computed cruise speed) to predict true airspeed. At the first trajectory gate past TOD (FL330 in fig. 21(a)), the initial true and calibrated airspeed errors are shifted toward zero with the ground speed error exhibiting a comparable shift in mean error to approximately −10 knots. Altitude variations during the constant Mach descent segments (FL330 through FL250) produced true airspeed (and calibrated airspeed) errors even though the airplane flew the Mach schedule precisely. The calibrated airspeed error at the FL230 and FL210 gates, where all runs were at the scheduled descent CAS, is reduced to the level of piloting accuracy presented in table 8. The true airspeed error is shifted by 5 to 10 knots slower than predicted primarily because of the mean altitude error of 500 to 1500 ft below the predicted altitude as shown in figure 25 (true airspeed changes by approximately 6 knots for each 1000 ft of altitude change at the same calibrated airspeed for these test conditions). The idle descent procedures required the pilot to slow to the metering fix crossing speed before bringing the throttles up to hold speed and altitude. As a result, the true airspeed error at predicted BOD was seen to be an average of nearly 30 knots slow for the idle descents, even though the altitude error was insignificant at that point. In contrast, the constrained descent procedures resulted in a significant reduction in the airspeed errors at the BODG. Overall, the ground speed error essentially tracked the true airspeed error due to the negligible mean wind error during descent as illustrated in figure 19(a).

The speed error results from Phase II for the CTAS trajectory predictions are presented in figure 29. In comparison with the constrained descents of Phase I, the ground speed errors appeared greater in Phase II. The mean ground speed errors during cruise (IC through TODG) were significantly greater than Phase I, with mean errors between 10 and 30 knots at

TODG. Five knots of this error is due to the initial condition ground speed error from radar tracking (table 5), and some of the error growth in the cruise segment is attributed to a variation in the wind modeling error along the cruise path. However, a significant portion of the mean error (and variation) in cruise was due to the three non-FMS runs within flight 729 which experienced the wind interpolation error discussed in section 6.1.5. For the descent segment, all of which were constrained in Phase II, a much more uniform calibrated airspeed error distribution is observed throughout the descent (figs. 29(b) and (c)). The true airspeed errors followed the calibrated errors closely with only slight difference in mean error (5 knots in some cases at lower altitude) caused primarily by small errors in the altitude profile (fig. 26). The somewhat larger variation in true airspeed error was further attributed to small errors (typically less than 3 knots) that were induced by variations in the atmospheric pressure and geometric altitude tables used by CTAS. The value of atmospheric pressure determined from these tables at a given geometric altitude was used by CTAS for the calculation of true airspeed for a given calibrated airspeed. These tables were constructed based on MAPS weather models for each test run and at times did not accurately represent the correlation of atmospheric pressure to pressure altitude. This minor problem has subsequently been corrected in the CTAS airspeed conversion routines. The relatively larger ground speed errors (both mean and variation) were directly attributable to the wind error as illustrated in figure 19(b). The differences in ground speed errors between procedures (e.g., non-FMS versus FMS TOD) were not due to the procedures themselves but to the large variation in wind errors from flight to flight as shown in figure 18.

Speed errors for the FMS-predicted paths of Phase II are presented in figure 30. The ND arc and non-FMS runs were excluded from this analysis because those procedures did not follow the FMS path. As expected, the ground speed errors in cruise were significantly better than for the CTAS predictions. The relatively large increase in variation at the FL250 and FL230 gates was attributed to a ground speed interpolation anomaly during the turn.

6.2.5. Time Profile

The ultimate output of the CTAS trajectory prediction process is the time profile along the predicted path. CTAS sequences and schedules airplanes based on the predicted time of arrival at traffic merge points (e.g., common metering fix, approach segment, or runway). Furthermore, the time profile forms the basis of conflict probing along the trajectory. Knowledge of trajectory prediction accuracy may be used to scale separation buffers and determine conflict probability. Smaller time errors can allow smaller separation buffers and permit higher terminal arrival capacity or more efficiency at the same capacity.

The analysis of the time errors from these flight tests focuses on the basic trajectory prediction results based on the comparison of CTAS predictions with TSRV-measured position. ATC radar position errors, as well as the coordinate system errors, are explicitly removed from the analysis. Final application of these time error results, such as the sizing of separation buffers or calculation of conflict probability, must account for ATC radar position errors.

A key output of the CTAS Descent Advisor trajectory prediction is the time of arrival at the metering fix. Table 10 summarizes the time-of-arrival accuracy results from the Phase I flight test for the idle and constrained descent runs.

The arrival time error (Mean + Standard deviation) for all runs (idle and constrained procedures) was less than 25 sec. However, a significant difference in results existed between the procedures. The constrained procedures were expected to be more accurate because the procedure would reduce speed profile errors by mitigating the effect of modeling errors on the vertical profile as evidenced by figure 28. The RFD constrained cases did result in a 40-percent reduction in mean error (and a 33-percent reduction in std. dev.) compared with idle. However, the FFD constrained cases resulted in similar mean error with a 50-percent increase in standard deviation.

This anomaly in the FFD constrained cases is attributed to two factors. First the number of FFD constrained runs was significantly smaller, and second, it was difficult for the research pilots to interpret vertical profile progress with the conventional instrumentation of the FFD cockpit. The lessons learned in Phase I led to improvements in the Phase II pilot procedures and training which supported a more comprehensive study of conventional cockpit (non-FMS) cases within Phase II.

24

Figure 31 illustrates the trends in time profile error that lead to the differences in results between the idle and constrained procedures. In comparing the error growth between procedures, the time error is nearly the same up to the FL190 gate. Below the FL190 gate, the growth of time error for the idle cases increases dramatically as the airplane reaches its clearance altitude early and initiates deceleration. These characteristics are clearly illustrated in the altitude profile errors of figure 25 and the airspeed profiles of figure 28. Comparatively, the constrained procedures reduce the altitude error leading to early deceleration. This "additional" time error associated with the idle descent procedure could be largely eliminated by procedures which require the pilot to maintain descent speed until it is necessary to decelerate for a crossing restriction. The most efficient method to accomplish such a procedure is for the pilot to adjust the vertical profile to target an appropriate bottom of descent. Cockpit automation such as VNAV guidance and/or range-altitude arcs provides valuable assistance to visualize and control the vertical profile, particularly for off-airway navigation.

The trajectory prediction results for Phase II included comparisons of actual time profiles with both CTAS-predicted and FMS-predicted trajectories. The CTAS predictions provide a measure of trajectory prediction accuracy using CTAS (atmospheric and performance) models and radar ground speed, whereas the FMS predictions provide a similar measure using the actual airplane performance, measured atmospheric conditions, and actual ground speed. Caution is advised when comparing these CTAS and FMS results because of the influence of the pilot procedures on the actual trajectories flown. In all but the FMS TOD cases, the pilots used the CTAS TOD location for descent, whereas the FMS trajectories are all based on the FMS TOD. In addition, the extremely small number of test cases (no more than 6 for each condition) precludes any statistically significant analysis.

Table 11 summarizes the error results at the metering fix arrival time using the CTAS trajectory predictions for Phase II. An interesting comparison may be made between the CTAS arrival time results of Phases I and II. A comparison of tables 10 and 11 shows a general shift in the mean arrival time error. In general, the airplane arrived later than predicted in Phase I compared with Phase II where the airplane arrived earlier than predicted. This general shift is

attributed to the effect of wind modeling errors and flight path orientation. Although the winds were generally out of the west and stronger than predicted for both Phases, the mean along-track wind error differed between the two Phases (fig. 19) because of the nearly opposite course orientation. The Phase I course was generally into the wind and resulted in the airplane flying a slower ground speed than predicted, whereas the Phase II course was with the wind and resulted in the airplane flying faster than predicted. This comparison underscores the influence of the wind-error field on conflict prediction accuracy, namely that two crossing trajectories may share the same wind field, but the net effect of the wind error on each trajectory varies with its orientation.

For the Phase II data alone, the comparison between the non-FMS and FMS-related runs was unexpected. In particular, the non-FMS runs were expected to result in a greater time error (mean and standard deviation) than FMS-related runs due to the advantages of FMS guidance. Further analysis of the time errors, in terms of their growth along the path (fig. 32), revealed several interesting characteristics that were a direct result of the small and unique sample of data taken. For the non-FMS runs, the mean time error had built up to about −15 sec at FL250 due to the large ground speed errors seen in figure 29(a). Following the turn, however, the time error reversed and ended with a mean error of +2 sec. The wind errors in the CTAS prediction were therefore compensated by the longer distance flown in the non-FMS runs to end with a coincidentally small time error at the metering fix.

To quantify the effect of the longer distance flown by the non-FMS runs, the arrival times were adjusted to remove the time associated with the longer distance flown. This adjustment provides for a more consistent comparison with the other runs which used FMS guidance to fly the lateral path. The adjustment was computed for each run based on the excess distance flown and the ground speed of the airplane at FL190. The result was a mean arrival time error of −11.0 sec with a standard deviation of 15.5 sec. These adjusted time errors clearly show the overriding effect of wind error on the arrival time performance during this test. Conversely, had the wind errors been less (or more consistent), the CTAS TOD and FMS TOD conditions would have achieved the best arrival time results. The ND arc would have been only slightly worse due to the

tendency of the airplane to fly lower than predicted resulting in a slightly lower TAS. In addition, the seemingly lower standard deviation of time error for the nonadjusted non-FMS cases (shown in table 11), was because of a favorable coupling of the time error due to wind and that due to the longer distance flown. Removing the effect of longer distance increased the standard deviation from 8.7 to 15.5 sec, which is more in line with the other cases.

Table 12 presents the arrival time accuracy based on the TSRV FMS predictions for the two VNAV procedures flown (the non-FMS and ND arc did not follow the FMS VNAV path). These data illustrate the arrival time differences between the CTAS and TSRV FMS predictions. The primary factor contributing to these differences between the FMS and CTAS trajectory predictions was the source of wind data. CTAS used wind data from the NOAA MAPS model, whereas the FMS used winds entered manually during the flight, as discussed in the section "Test Procedures." The FMS-entered winds came from hand recording the winds on the previous descent and, in general, were more accurate than the CTAS winds. Figures 33 and 34 present a summary of along-track wind errors for the CTAS and FMS predictions for each of the guidance conditions. Comparison of figure 33(a) with 34(a) clearly shows the lower mean wind error corresponding to the FMS prediction cases. As a result, the mean time error for the FMS predictions was coincidentally the smallest. In addition, the mean time errors for the various guidance conditions are seen to follow the mean wind errors for the CTAS prediction cases (when adjusted to the same distance flown). For the FMS predictions, the variation in wind error was observed to be greater for the FMS TOD guidance cases with a resulting higher variation in arrival time error.

6.3. Sensitivity Analysis

The effects of airplane performance and atmospheric modeling errors on the time profile predictions were examined by using the stand-alone version of the airborne FMS PGA4D trajectory generation program. This analysis was applied to the Phase I idle conditions in an effort to relate the sensitivity analysis to real-world measurements and to identify the contributions of the dominant trajectory prediction error sources. This analysis is restricted to the straight-path idle cases. The straight path is necessary to

isolate navigation (overshoot) errors from the remaining sources. The idle cases are necessary to remove the influence of pilot variations in thrust-drag management.

Two executable versions of the program were created for this analysis. The first version contained the airplane performance model representative of a baseline Boeing 737-100, the same as that used by the CTAS trajectory generation program in the flight tests. The second version contained the performance model of the TSRV airplane as modified in the appendix. A simple straight-line route consisting of a starting point at the PONNY waypoint and ending at the KEANN metering fix (fig. 1) was used for the vertical trajectory generation. Initial and final conditions (altitude, calibrated airspeed, and true track angle) were created to represent each of the idle descent test runs of flights 679 and 680. Two sets of weather data (wind speed, wind direction, and air temperature) were created for each test run. The first set used the weather data recorded by the airplane at pressure altitude steps of 500 ft from top of descent down to the metering fix altitude of 17000 ft. The second set used the CTAS MAPS weather model with wind and temperature values interpolated at the same horizontal location and pressure altitude as was used for the first data set. Four unique combinations of airplane performance and weather models were used to generate trajectories for comparison, as shown in table 13.

Trajectories were generated for each test condition from flights 679 and 680 by using each of the four combinations of performance and weather models. The trajectories generated with the baseline set were used as the references for the trajectory error comparisons. The primary parameter for comparison was time of arrival at the final range of the reference trajectory with TOD assumed to begin at the reference trajectory TOD range. If the test trajectory ended before the reference trajectory final range, the test trajectory final point was extrapolated by assuming constant altitude and ground speed to determine the time of arrival at the reference trajectory end condition. Similarly, if the test trajectory continued past the end of the reference trajectory, the arrival time was computed by linearly interpolating on the range corresponding to the reference trajectory final condition. This method for finding arrival time matched the way the idle descents were flown in Phase I. Time errors were then

computed by subtracting the test trajectory arrival time from the reference trajectory arrival time for each test condition and model combination. A summary of the time error results is given in table 14.

As seen in table 14, the inclusion of both the performance model and weather model revisions in the idle descent trajectory generation resulted in time errors nearly the same as those measured in Phase I, as shown in table 10. The performance model alone accounted for approximately one third of the mean time error with little variation. The weather model accounted for slightly more than two thirds of the total mean time error and nearly all the variation. The constrained procedures would reduce most of the mean error due to performance modeling and a part of the mean error due to the wind model by eliminating the early slow-down at BOD.

6.4. Qualitative Impact of Error Sources

This section summarizes, based on the flight test data analysis, the impact of trajectory prediction error sources. Although not a comprehensive statistical analysis, the discussion indicates the potential impact on trajectory prediction accuracy as well as the flyability and efficiency of CTAS descent advisories. Individual error sources are ranked in terms of their potential time-error impact on CTAS clearance advisories for constrained descents. The rankings are defined as follows based on a 10-min prediction horizon:

Primary	>10 sec impact
Secondary	5–10 sec impact
Minimal	<5 sec impact

The impact on lateral and vertical profile accuracy is also summarized. Where applicable, the discussion is extended to cover other trajectory segments such as ascents, en route cruise, and unconstrained descents.

For active CTAS applications (e.g., time-based clearance advisories for speed, TOD, and routing), trajectory prediction accuracy is primarily affected by errors in winds, tracking, and pilot conformance. In addition to accuracy, another important factor is the flyability and efficiency of the CTAS TOD advisory. This factor is primarily affected by performance modeling as well as atmospheric modeling. The constrained pilot procedure for a CTAS-based clearance,

like a VNAV profile, calls for the pilot to add thrust or drag to correct for altitude profile errors. The magnitude and sense of these corrections directly affect the flyability and fuel efficiency of the profile. The need to add drag on descent is often considered unacceptable for passenger comfort, and for most transport airplanes, drag devices lack effectiveness. The need to add drag or thrust indicates a waste of fuel relative to the optimum profile. Atmospheric errors are of a random nature depending on the atmospheric field, model performance, and route of flight. To ensure flyability in the presence of all errors, the performance models and pilot procedure may need to include buffers. Proper procedures will improve accuracy in the presence of modeling errors, at a cost in efficiency, and will minimize workload.

6.4.1. Radar Track

6.4.1.1. Position. Along-track errors were found to be of **Secondary** impact. The measured along-track error was generally consistent over all Phase II flights with the track position trailing the actual position by 6.3 ± 3.4 sec (Mean ± Standard deviation). Much, if not most of this error may be corrected by a Host track time stamp that is not currently provided to CTAS. If all flights are tracked by radar, the contribution of the mean along-track error tends to cancel when any two trajectories are compared for separation. However, if tracking sources are mixed (e.g., some airplanes tracked by radar, some by automatic dependent surveillance (ADS)), the mean error of the radar-tracked flight would contribute to the conflict prediction error. The mean along-track error would also reveal itself when radar-tracked airplanes are compared with airplanes operating to RTA.

Cross-track errors were found to have a **Minimal** impact both in terms of cross-track position as well as their contribution of error to the prediction of along-track position. (Actual cross-track error, due to pilot navigation, is addressed later in section 6.4.4.)

6.4.1.2. Speed. Ground speed errors were found to have a **Minimal** impact on trajectory segments with speed clearances such as CTAS descent advisories. CTAS descents (as well as ascents and future cruise segments) are predicted by combining the winds along the path with an estimated airspeed based on clearance, flight plan, or file-based user preference. The only impact on accuracy is caused by the influence of

ground speed (and atmospheric model) in estimating the airspeed prior to acceleration to the cleared airspeed.

Ground speed errors would, however, have a **Primary** impact on the prediction accuracy of "open-loop" trajectory segments (i.e., those segments for which speed is inferred from the observed ground speed as opposed to an advisory or clearance airspeed). Although the flight test runs experienced a smaller ground speed error, the measured standard deviation of speed error in level cruise was 13 knots (3 percent for an airplane at 420 knots or about an 18-sec error for a 10-min prediction). During turning maneuvers, the tracker lagged the airplane with substantially greater errors (exceeding 100 knots in many cases). Clearly, the raw tracker data are not good enough during these transients (maneuvers) to support a passive en route conflict probe. Some sort of filtering, or additional data, would be needed to supplement the Host track data during transient maneuvers. One example of a filter, short of an advanced tracking algorithm, would be to simply ignore changes in ground speed during transient periods (e.g., turns) with a lag of 1 to 3 cycles to allow for the positive identification of the transient.

6.4.1.3. Track angle. For many cases, the impact of track-angle errors may be mitigated by path generation algorithms which correlate airplane position with the planned route of flight. For other cases, such as vectoring, open-loop pilot maneuvering (e.g., thunderstorm avoidance), and turns, the impact of track-angle errors may be significant. During vectors, track-angle errors may have a **Primary** impact on accuracy if the track angle is used to project the future path of the airplane. Track errors may have a substantial impact on the predicted path and time to fly depending on navigation geometry. As with ground speed, some sort of filtering or additional data are needed to supplement the Host track data during turn transients, particularly if the data are to be used for monitoring of clearance conformance. For vectors, much of the error may be reduced by providing the ATM automation with an input of the heading clearance to damp out the error in projected heading.

6.4.2. Atmospheric Model

6.4.2.1. Wind component along path. Wind errors were found to have a **Primary** impact on trajectory

segments based on speed clearances such as CTAS descent advisories. For these situations, the modeled wind is added to the clearance airspeed to predict ground speed. If the pilot flies the airspeed precisely, wind model errors directly affect the predicted ground speed. These errors not only affect the time to fly, but they may also have a substantial impact on the TOD location. For constrained CTAS descents, the TOD location error will affect the thrust and/or drag needed to meet the BOD constraint and, therefore, the flyability and efficiency of the CTAS descent profile. For unconstrained descents, wind errors will also introduce errors in the altitude profile as well as TAS errors due to the altitude error.

Wind errors have a **Minimal** impact on open-loop cruise segments that are based on track ground speed. For these segments, the wind model is used to estimate the airspeed at the initial position. The ground speed profile is then predicted based on the airspeed estimate and the winds along the path. If a constant airspeed profile is assumed, then the only variation in ground speed is caused by variations in wind and temperature along the path. During open-loop cruise segments, the ground speed error is primarily caused by the tracker-induced error with an atmospheric influence due to variations in the wind-temperature model error along the path.

6.4.2.2. Wind gradient along path. The main effect of wind gradient error is on the prediction of descent and ascent rate with a **Minimal** impact on time along the path for constrained descents. Sustained gradients observed during the test ranged from 1 to 3 knots/1000 ft altitude with substantially larger gradients occurring during peak jet stream conditions. As noted earlier, a gradient of 1 knot/1000 ft contributes approximately 3.5 percent to the descent rate of a 737. For a 20000-ft descent and a typical descent ratio of 3 n.mi./1000 ft, each knot of gradient error leads to a difference of 2 n.mi. in the optimum TOD. If the segment is flown with vertical constraints (i.e., TOD and BOD), then the error mainly affects the thrust or drag needed to meet the constraints and, therefore, the flyability and efficiency of the descent profile. If the segment is flown without vertical profile constraints, an unmodeled wind gradient leads to an error in the altitude profile which in turn may introduce a small error in the TAS profile for a constant Mach/CAS segment and an error in estimating the transition in airspeed at the BOD.

28

Ascent rates may be more or less sensitive to wind gradient depending on the calm-wind ascent rate, which varies significantly with altitude and weight. An unmodeled wind gradient is expected to develop error in the predicted altitude profile and TOC. These altitude profile errors may lead to significant errors in ground speed caused by errors in the TAS and in wind speed caused by the uncertainty in altitude as well as an error in estimating the TOC transition from climb to cruise airspeed.

6.4.2.3. Temperature. The main impact of temperature (and pressure) is on the prediction of geometric (absolute) altitude rate with a **Minimal** impact on time along the path for constrained descents. For example, each 5°C error in temperature profile leads to approximately an error of 500 ft in the altitude to descend or ascend between FL350 and FL100. Like wind gradient, the main impact of temperature is on the time and distance to descend. For constrained descents, temperature errors primarily affect the thrust or drag required to meet the constraints. Although temperature errors also affect airspeed estimation during constant Mach/CAS segments (approximately a 1-percent error in TAS for each 5°C error in temperature), the relatively small errors observed during the flight test had a negligible effect on the accuracy of the descent predictions. If the segment is flown without vertical profile constraints, a temperature error may contribute to an error in the altitude profile which in turn may introduce a small error in the TAS profile for a constant Mach/CAS segment as well as an error in estimating the transition in airspeed at the BOD. For ascents, temperature not only affects the geometric altitude, it also affects the climb thrust of the airplane, both of which contribute to errors in predicting the altitude profile, TOC, and ground speed profile.

6.4.3. Airplane Performance Modeling

Errors in the performance model affect trajectory prediction accuracy in a similar fashion to wind gradient. For constrained descents, the impact on time is **Minimal** with the main influence on the flyability and efficiency of the profile. Although the net thrust (and weight) has a direct effect on the time to accelerate or decelerate, these transitions tend to be short and have little effect on the trajectory prediction. For unconstrained descents, performance modeling errors may contribute to errors in the altitude profile which in turn

may introduce a small error in the TAS profile for a constant Mach/CAS segment and an error in estimating the transition in airspeed at the BOD. The Phase I sensitivity analysis presented earlier indicated that the 5-percent error in the CTAS performance model for the TSRV led to a time error of 5 sec over a descent of 18000 ft. Earlier analysis of weight errors indicated that descent rate error varies with speed and is relatively insensitive to weight over a large portion of the speed envelope centered about the speed for maximum lift-to-drag ratio (ref. 6).

For ascents, performance model errors have a **Primary** impact on the accuracy of time and distance to climb with significant sensitivity to weight and speed profile. In addition, performance modeling errors may affect the accuracy of determining advisory limits such as the high-speed boundary or service ceiling in cruise. For future applications such as trajectory negotiation, precision between ATM and user (airborne or ground based) performance models might be important in order to accurately probe for conflicts as well as minimize deviations from user preferences.

6.4.4. Pilot Conformance

6.4.4.1. Navigation. Navigation errors, depending on airplane equipage and knowledge of pilot intent, may have a **Primary** impact on trajectory prediction accuracy. As seen for the non-FMS cases, turn errors may contribute a significant error in predicted distance flown. Although the non-FMS cases studied in this test emphasized the uncertainty in the pilot's turn overshoot, the lack of error for the LNAV cases underscores the importance of turn model geometry which may have a significant effect on the predicted distance flown for typical turns associated with the extended terminal area and vectoring. In addition to the distance flown, turn overshoot and lateral cross-track errors associated with conventional airway navigation may result in cross-track errors of up to several miles even within legal navigational limits defined by instrument flight rules.

6.4.4.2. Speed. The sensitivity of trajectory prediction accuracy to speed conformance is significant. A speed conformance error affects a closed-loop trajectory segment in the same way that a ground speed (track) estimate error affects an open-loop segment. Although speed conformance was good during these flight tests,

the TSRV speed-tracking performances (both manual pilot and FMS/autopilot) were not representative of speed conformance expected of airline pilots and commercial FMS equipment. Operational procedures must highlight the need for adherence to the predicted speed schedule in order to achieve good arrival time results.

7. Recommendations

This paper presents a sample of en route trajectory prediction error sources under real-world operational conditions. Although the data provide a good "order-of-magnitude" basis, the data are not a statistically significant set. The recommendation is that a comprehensive trajectory accuracy sensitivity study be performed to provide a method for the analysis of the conflict-probe accuracy under operational conditions. Conflict prediction accuracy is derived directly from the relative trajectory prediction accuracy for an airplane pair. Trajectory prediction accuracy depends on the airplane type, atmospheric prediction accuracy, trajectory segments and orientation, and time horizon. A comprehensive sensitivity study would require the development of several sets of statistically significant error source data.

The first and most significant error source is atmospheric prediction, which has a complex effect on trajectory prediction accuracy. A comprehensive analysis of atmospheric prediction accuracy, as it pertains to trajectory prediction, would help determine the sensitivity and overall expected performance of conflict-probe automation tools under operational conditions. Such a study should be conducted over an extended period of time (e.g., 1 year) to measure the frequency of significant errors due to seasonal variations in weather phenomena. The study should also cover a moderate-size airspace (e.g., an en route ARTCC) to capture the positional and trajectory orientation effects and during the normal hours of flight operations to capture temporal effects such as variations in sensor data availability. Previous evaluations have focused on the gross accuracy averaged over time and position (ref. 17). Because the performance of conflict-probe tools varies with time and trajectory characteristics, the study must be focused on trajectory applications (i.e., provide a realistic correlation between the atmosphere and trajectories). Such a study would also be useful for (1) determining cost beneficial methods for improving atmospheric prediction accuracy where it is

needed most for trajectory prediction and (2) creation of a data set to support the development of tools to predict the accuracy of atmospheric forecasts at the time of the forecast to provide an efficient bound for conflict-probe error buffers.

The second error source that should be studied further is airplane tracking. Although the steady state accuracy of the FAA Host tracker may be adequate, the large track velocity errors associated with transients (maneuvers) are unacceptable for effective conflict prediction. These maneuvers may not be common during en route cruise, but they do occur frequently in the extended terminal area. Methods for improving track velocity accuracy or mitigating the impact of such errors on trajectory prediction tools are needed. Aside from ADS, two additional solutions exist: the use of advanced track filters and the use of logic to inhibit calculations based on Host track data during transient periods.

The third error source relates to the modeling of airplane performance. Although errors in CTAS performance models do not significantly affect time profile accuracy in descent, model errors do affect the flyability and efficiency of DA-based clearances for non-FMS airplanes and have a small effect on the accuracy of the altitude profile. Performance modeling errors, including weight estimation, are expected to have a much greater impact on climb profile predictions in terms of both time and distance to climb. Generally, performance varies not only as a function of type but also between individual airframes of identical type (because of age and modification). Developing a database that indicates the performance variation over the fleet of airplanes operating in the national airspace system would be useful. This database should use input of airplane operators and manufacturers.

The fourth source of errors, pilot conformance, may be useful to determine the accuracy to which speed and course clearances are conformed under operational conditions. Such a study would complement the data within this report (pilot conformance errors were minimized to isolate the other error sources). More importantly, it is critical to understand when, and under what conditions, CTAS does not have accurate knowledge of the intended course, speed, and TOD. The present flight tests evaluated trajectory predictions under the assumption that CTAS

had accurate knowledge of the appropriate clearances. The validity of this assumption should be evaluated by a study of actual track data to determine how often and why the CTAS heuristics and controller inputs would fail to reasonably represent the intended clearance. The data gleaned from such a study would provide insight that would lead to improvements in the CTAS routing heuristics as well as reductions in the need for controller inputs.

Finally, there is clearly the need for additional work on operational procedures for constrained descents which minimize the trajectory errors. In particular, the procedures should emphasize the need to maintain the CTAS-expected speed schedule throughout the descent in order to minimize time errors. Studies which document the differences in current descent procedures between different airplane types and different operators of the same airplane type would be useful in defining new common procedures. Field tests using the actual airplane operators and air traffic controllers, such as those conducted in reference 22, are useful for final validation and user acceptance of the new procedures.

8. Concluding Remarks

The Transport Systems Research Vehicle (TSRV) Boeing 737 based at the Langley Research Center flew 57 arrival trajectories that included cruise and descent segments; at the same time, descent clearance advisories from the Center-TRACON Automation System (CTAS) were followed. These descents were conducted at Denver for two flight experiments (Phase I in October 1992 and Phase II in September 1994). The actual trajectories (recorded onboard the TSRV) were compared with predictions calculated by the CTAS trajectory synthesis algorithms and the TSRV Flight Management System (FMS).

The CTAS Descent Advisor was found to provide a reasonable prediction of metering fix arrival times during these tests. Overall arrival time errors (Mean + Standard deviation) were measured to be approximately 24 sec during Phase I and 15 sec during Phase II. These results, although not statistically significant, were obtained under real-world operational conditions and are representative of the level of performance which should be expected from active CTAS descent clearance advisories.

The major source of error during these tests was found to be the predicted winds aloft used by CTAS. Overall along-track mean wind errors of 10 to 15 knots with standard deviations of about 15 knots were experienced during the cruise segments of both Phases I and II. Mean wind error reduced to between 5 and 10 knots during descent; however, the standard deviation remained at 10 knots or more. The sensitivity analysis of Phase I idle descents revealed that about two thirds of the mean time error and nearly all the variation in time error were due to wind errors. Analysis of Phase II runs also revealed wind errors to be the overriding factor in the arrival time errors measured during that test as well.

Airplane position and velocity estimates provided to CTAS by the Air Traffic Control (ATC) Host radar tracker were found to be a relatively insignificant error source during these tests. Position errors were predominantly along track, with the tracker lagging the actual airplane position by an average of 6.3 sec with a standard deviation of 3.4 sec throughout Phase II. If all airplane positions are provided by the same radar tracking system, the mean along-track error tends to cancel when two trajectories are compared by CTAS for conflict probing. The cross-track component of radar tracking error was found to be relatively small, with an overall error of approximately 0.22 n.mi. standard deviation measured during Phase II. Ground speed errors during the stabilized initial condition locations for the test runs were also minimal, with a mean plus standard deviation error of less than 10 knots. Measurements of radar tracking performance at other flight conditions revealed significant ground speed errors when the airplane was turning. Ground speed errors of 100 knots or more (Mean + Standard deviation) recorded during turns rendered the radar tracking unusable as a source for airplane ground speed. These ground speed errors were found to persist for 1 to 3 min following a turn.

Airplane performance modeling errors within CTAS were found to not significantly affect arrival time errors when the constrained descent procedures were used during these tests. The TSRV airplane performance differed from the CTAS Boeing 737-100 model data, in terms of lower net thrust minus drag (TMD), by approximately 5 percent over the descent. The principal effect of these modeling errors was on the calculated versus desired top of descent (TOD) for

an efficient idle descent. Although the impact of these modeling errors on the time profile for descents was small, they are expected to have a significant impact on the predictions of ascent segments.

The most significant effect related to the flight guidance used by the TSRV was observed to be the lateral path errors recorded when conventional VOR (very high frequency omnidirectional radio range) guidance was used during the non-FMS cases of Phase II. The Phase II runs involved a 60° turn during descent. Cross-track errors of 24000 ft (Mean plus Standard deviation) occurred following the turn during these cases, which contributed to an average 1.3 n.mi. longer range flown. This translated directly into approximately 13 sec of mean arrival time error for the non-FMS test cases. The use of FMS lateral navigation (LNAV) eliminated this error.

Vertical trajectory errors, resulting from wind and airplane performance modeling errors, were also dependent on the method of flight guidance. Flight procedures which utilized the FMS-generated path for vertical guidance exhibited the largest vertical errors during the initial portion of the descent, whereas procedures using CTAS guidance (TOD and speed schedule) tended to build up errors during descent with the maximum occurring closer to the bottom of descent. The altitude errors recorded during these tests peaked at about 2000 ft (Mean plus Standard deviation) for both the non-FMS and FMS reference conditions, with the airplane being below predicted altitude for the non-FMS reference and above predicted altitude for the FMS reference conditions. The contribution of these altitude errors to the overall arrival time was determined to be insignificant. Overall, the constrained pilot procedures assisted by LNAV and VNAV (vertical navigation) guidance served to mitigate the impact of modeling errors on the accuracy of the altitude profile prediction.

Appendix

TSRV Performance Model Update

The stabilized cruise and descent conditions flown in Phase I were used to refine the performance model of the airplane to reflect the actual performance measured during the test. Data tables were then generated by this revised performance model. The following sections describe the methods used in updating the airplane performance model and present the resulting modifications made to the thrust and drag models.

A.1. Drag

The first step in updating the airplane drag model was to compute the error in drag coefficient based on flight-extracted drag. The TSRV airplane was not instrumented to accurately extract drag information during unstable and maneuvering flight conditions. Calibrated angle of attack, sideslip, and longitudinal and lateral accelerations were not available in the recorded data. The benign cruise and descent trajectories, however, allowed the use of classical performance equations for computations of approximate airplane drag. This technique was deemed adequate for the purposes of this experiment.

The standard point mass equations of motion in a vertical plane were used to extract drag from the measured flight data. These equations are

$$\dot{V}_a = \frac{g(T - D)}{W} - g\gamma - \dot{V}_w \qquad (A1)$$

$$\dot{h} = V_a\gamma \qquad (A2)$$

Combining equations (A1) and (A2), and solving for drag give

$$D = T - W\left(\frac{\dot{V}_a + \dot{V}_w}{g} + \frac{\dot{h}}{V_a}\right) \qquad (A3)$$

Because the altitude and altitude rate measurement were based on pressure altitudes, the following correc-

tion was applied to correct for nonstandard temperatures and obtain true altitude rate:

$$\dot{h} = \dot{h}_p \frac{T_k}{T_{k,s}} \qquad (A4)$$

Drag coefficient was then computed as

$$C_D = \frac{D}{qS_{\text{ref}}} \qquad (A5)$$

where

$$q = 1481\delta_{\text{am}}M^2 \qquad (A6)$$

Drag coefficient error is then computed as

$$\Delta C_D = C_D - C_{D,m} \qquad (A7)$$

where $C_{D,m}$ is the baseline model drag coefficient computed from lift coefficient and Mach number.

Application of these equations to the flight data was accomplished by first defining criteria for identifying stable flight segments for analysis. The following criteria were used based on the available recorded data:

1. Normal acceleration between 31.0 and 33.0 ft/sec/sec

2. Roll attitude less than 5°

3. Criteria 1 and 2 valid for at least 10 sec

The stable flight segments consisted of a minimum of 10 sec and maximum of 30 sec while the criteria were valid. The parameters required for equations (A3), (A4), and (A5) were averaged over the segment to provide a single value of drag coefficient error for the segment. This technique was applied to the 13 trajectories flown with the idle thrust descent procedure.

Figure A1 presents drag coefficient error versus Mach number. The data reveal a fair amount of scatter in the data; however, a constant offset of approximately 0.003 in C_D (30 drag counts) is evident. The baseline Boeing 737-100 drag model was therefore

33

modified by adding a constant 0.003 to $C_{D,m}$ for the revised TSRV drag model.

A.2. Idle Thrust

Update of the idle thrust model required a careful review of the baseline TSRV thrust model. The analysis conducted in reference 24 provided the basis of the current TSRV engine model. As described in that report, idle thrust is a function of Mach number with an adjustment if the engine is operating at the minimum fuel flow limit. With this technique, a baseline idle thrust model was created for the TSRV airplane by using the manufacturer's performance data for the Boeing 737-100 airplane with Pratt and Whitney JT8D-7 engines. A function of engine pressure ratio (EPR) versus Mach number was generated which produced the idle thrust values presented in the manufacturer's data for idle fuel flows above the minimum limit (540 lb/hr). The generalized fuel flow model was then extended to include EPR values in the idle range. The resulting model provided a good match to the idle thrust and fuel values provided in the manual using the generalized fuel flow and thrust versus EPR functions.

The process of updating the TSRV idle thrust model involved modifying this baseline idle EPR versus Mach relationship and determining an appropriate value for minimum fuel flow. The five idle descent runs of flight 679, which encompassed the flight envelope of the airplane utilized for this experiment, were analyzed for this purpose. Figure A2 shows the measured EPR at idle for all runs versus Mach number for both engines. As predicted by the engine model, a definite minimum EPR boundary is evident. A shift of 0.045 in the EPR from the baseline engine model resulted in a good match between the flight and model EPR limit.

EPR values above the limit shown in figure A2 occur when the engine is operating at the minimum fuel flow limit. The original minimum fuel flow of 540 lb/hr was adjusted until a reasonable match to the average measured minimum fuel flow and correspond-

ing EPR value was achieved. Figure A3 presents an example of minimum fuel flow for one of the flight 679 runs with the original and revised minimum fuel flow illustrated.

A final check on the validity of the idle thrust model was done by comparing the predicted model values of idle thrust with the computed values based on measured EPRs for all the idle thrust descent runs. Figure A4 presents the composite of the mean and standard deviation of thrust error at discrete altitudes during the descents. The original model had mean errors of between 200 and 500 lb with maximum standard deviations of approximately 250 lb. The revised model reduces the mean errors to less than 100 lb with standard deviations of 200 lb or less. The largest values of standard deviation are a direct result of idle surge bleed operation in the altitude region of 20000 to 30000 ft. This unavoidable situation is discussed in greater detail in reference 24.

A.3. Descent Performance Model

In order to determine the overall performance modeling error for descent calculations, the combination of idle thrust and drag errors must be considered. The stabilized descent points from the idle descent test runs were further analyzed to determine the error in the original model of thrust minus drag (TMD) compared with the measured flight results. Actual thrust was approximated by using the measured EPR and state conditions. Drag was computed by using the techniques described in the previous drag error analysis. Model values of thrust and drag came from the original models based on the state conditions and flight idle throttle setting.

The TMD modeling errors were computed as a percentage of the baseline model values and plotted versus altitude in figure A5. As seen in the figure, the actual TMD varied from 2 percent greater (more negative) at 17000 ft to about 10 percent greater than the model TMD at 35000 ft. This compares with the constant drag error of approximately 11 percent.
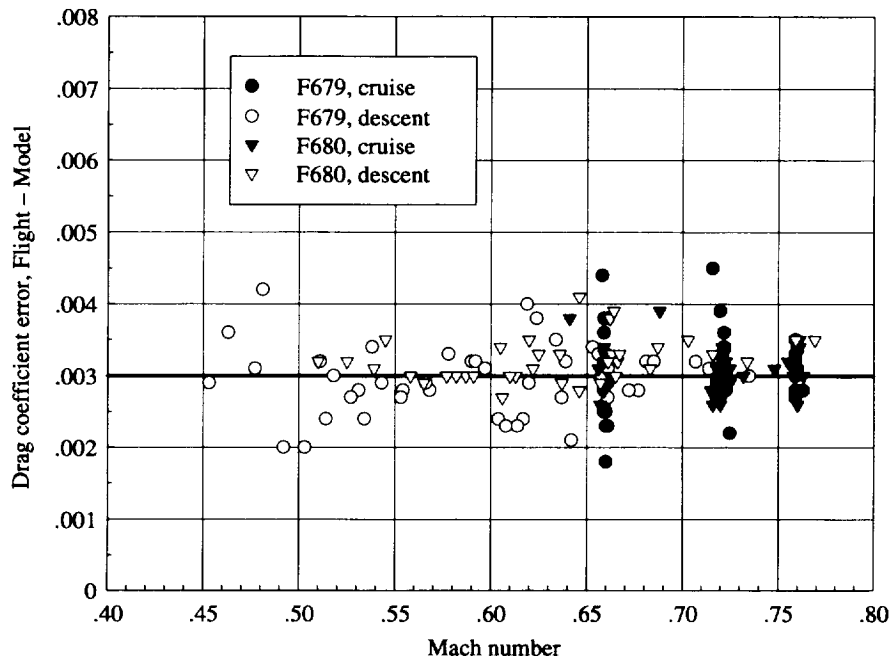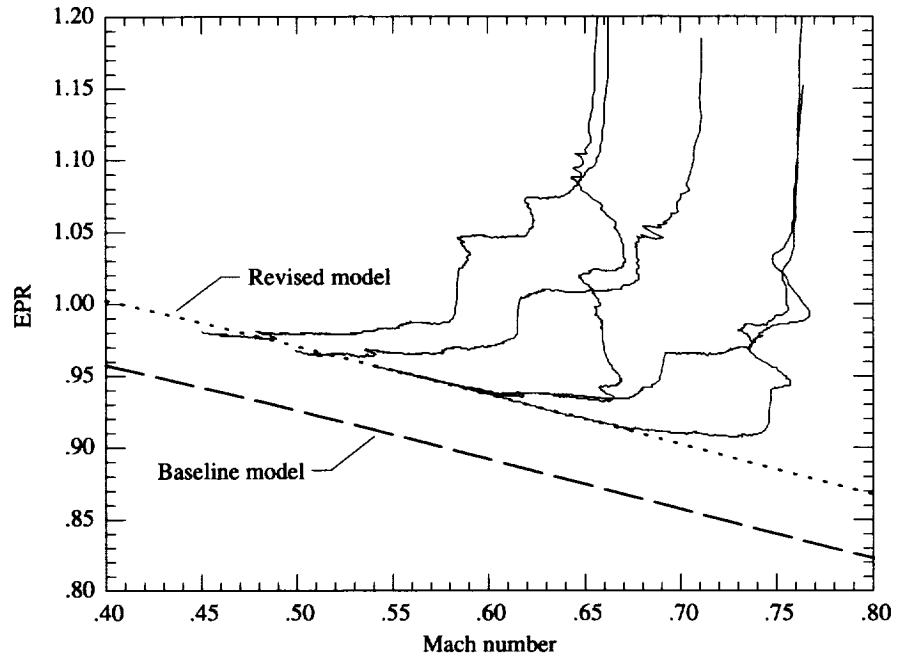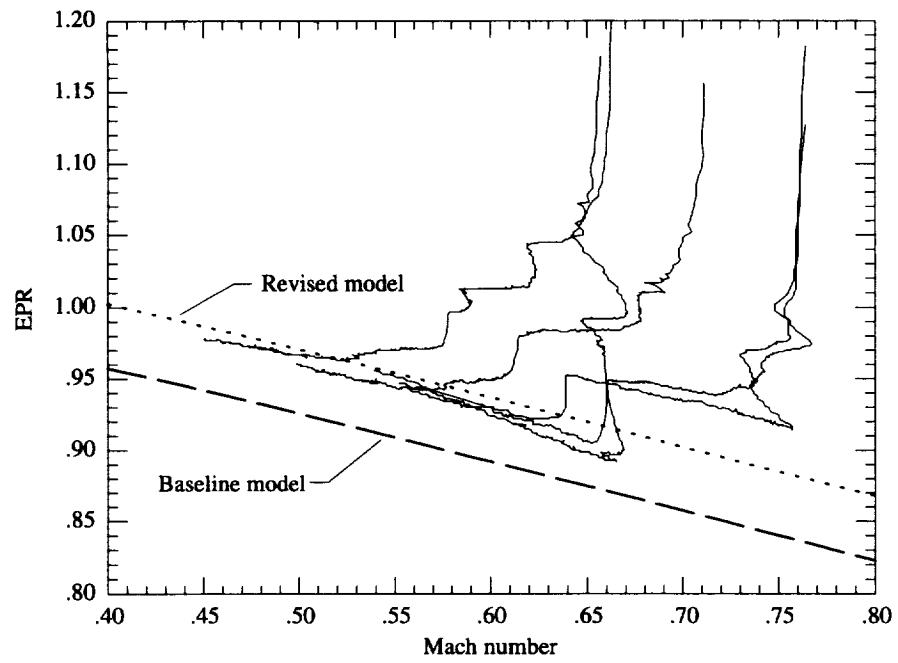
34

Figure A1. Drag coefficient error from idle descent test runs of Phase I.

(a) Left engine.

(b) Right engine.

Figure A2. Measured EPR at idle for descents of flight 679 with baseline and revised minimum EPR models shown.
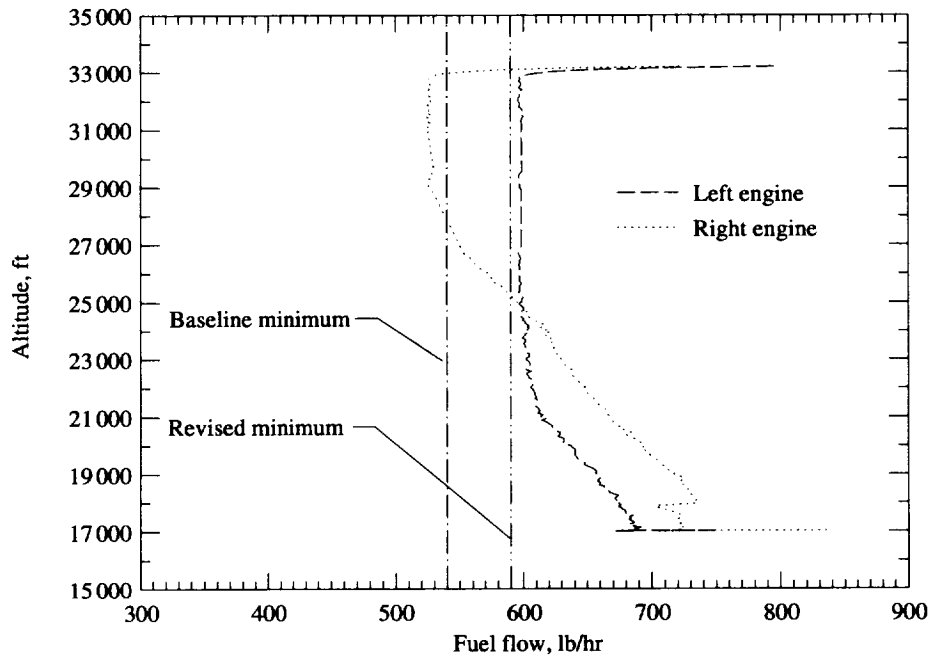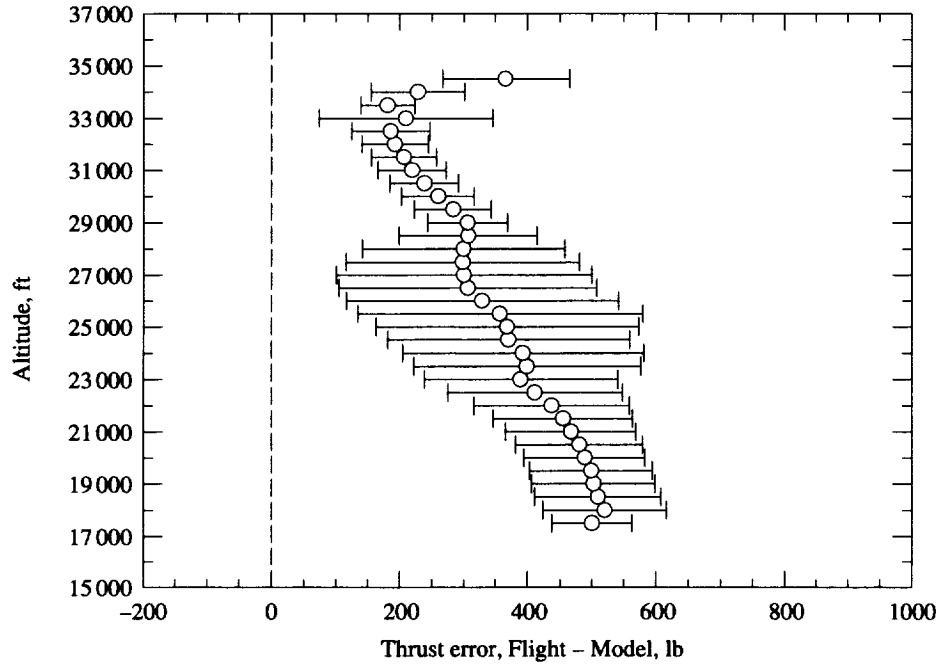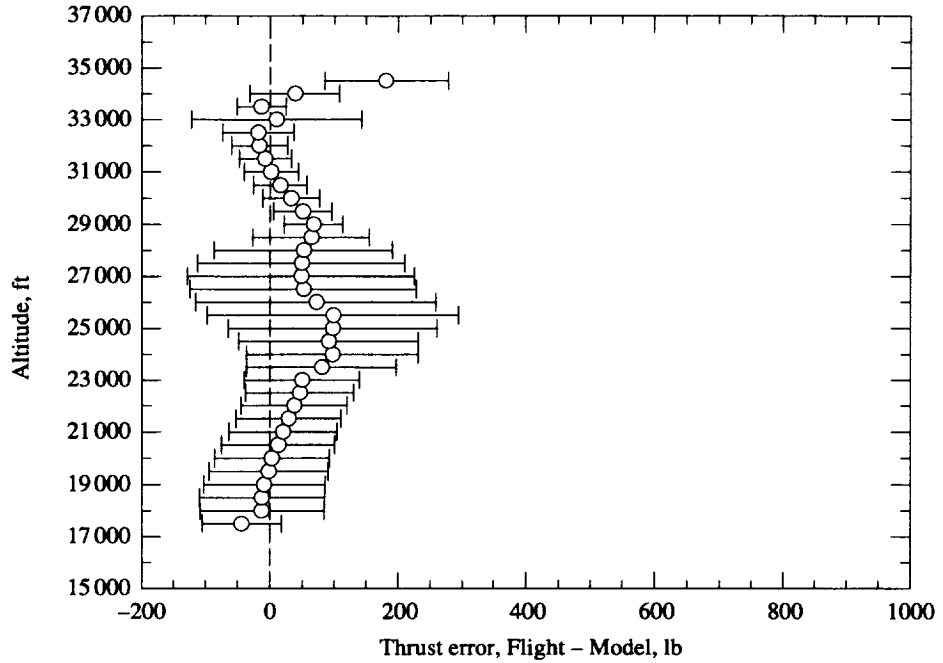
Figure A3. Minimum fuel flow flight 679, run 3.

(a) Baseline engine model.

(b) Revised engine model.

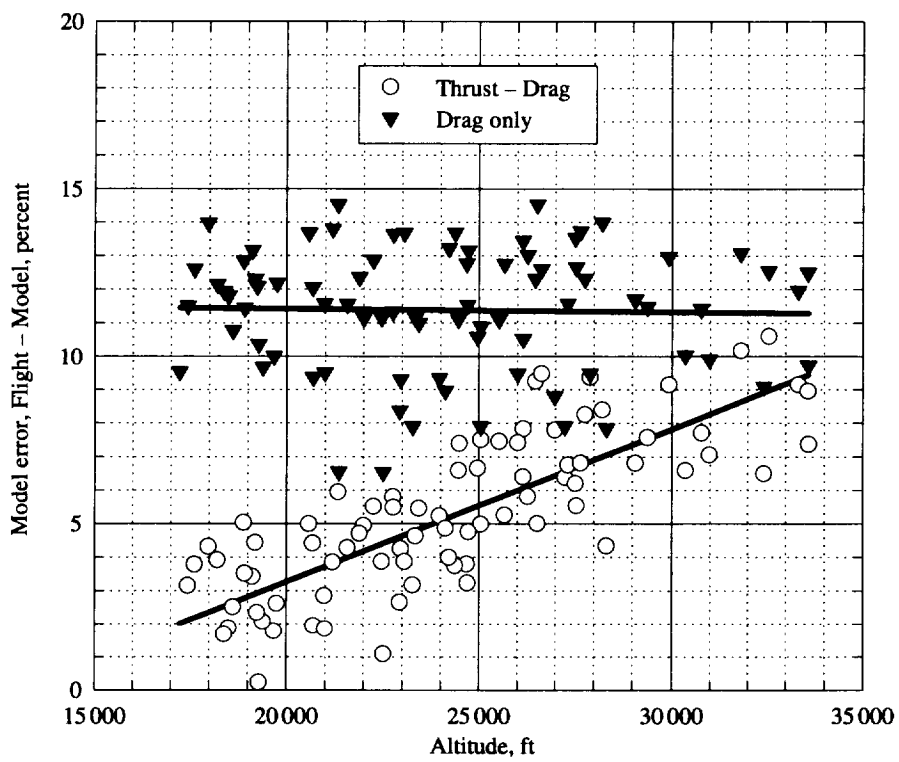Figure A4. Composite idle thrust error for all idle descent test runs.

Figure A5. Descent performance modeling errors in baseline TSRV model.

References

1. Erzberger, Heinz; Davis, Thomas J.; and Green, Steven: Design of Center-TRACON Automation System. *Machine Intelligence in Air Traffic Management*, Andre Benoit, ed., AGARD CP-538, Oct. 1993, pp. 11-1–11-12.

2. Williams, David H.; and Green, Steven M.: *Airborne Four-Dimensional Flight Management in a Time-Based Air Traffic Control Environment*. NASA TM-4249, 1991.

3. Den Braven, William: *Design and Evaluation of an Advanced Air-Ground Data-Link System for Air Traffic Control*. NASA TM-103899, 1992.

4. Williams, David H.; and Green, Steven M.: *Piloted Simulation of an Air-Ground Profile Negotiation Process in a Time-Based Air Traffic Control Environment*. NASA TM-107748, 1993.

5. Green, Steven M.; Den Braven, William; and Williams, David H.: *Development and Evaluation of a Profile Negotiation Process for Integrating Aircraft and Air Traffic Control Automation*. NASA TM-4360, 1993.

6. Green, Steven M.; Davis, Thomas J.; and Erzberger, Heinz: A Piloted Simulator Evaluation of a Ground-Based 4D Descent Advisor Algorithm. *AIAA Guidance, Navigation and Control Conference—Technical Papers*, Volume 2, AIAA, Aug. 1987, pp. 1173–1180. (Available as AIAA-87-2522.)

7. Davis, Thomas J.; and Green, Steven M.: *Piloted Simulation of a Ground-Based Time-Control Concept for Air Traffic Control*. NASA TM-101085, 1989.

8. Hunter, George; Weidner, Tara; Couluris, George; Sorensen, John; and Bortins, Richard: CTAS Error Sensitivity, Fuel Efficiency, and Throughput Benefits Analysis. 96150-02 (Subcontract under FAA Contract DTAFA01-94-Y-01046 to Crown Commun., Inc.), Seagull Technol., Inc., July 1996.

9. Couluris, G. J.; Weidner, T.; and Sorensen, J. A.: Initial Air Traffic Management (ATM) Enhancement Potential Benefits Analysis. 96151-01 (Subcontract under FAA Contract DTFA01-96-Y-01009 to Crown Commun., Inc.), Seagull Technol., Inc., Sept. 1996.

10. Erzberger, Heinz: Design Principles and Algorithms for Automated Air Traffic Management. *Knowledge-Based Functions in Aerospace Systems*, AGARD-LS-200, 1995.

11. *Final Report of RTCA Task Force 3—Free Flight Implementation*. RTCA, Inc., 1995. (Reprinted Feb. 1996.)

12. Jardin, M. R.; and Erzberger, H.: Atmospheric Data Acquisition and Interpolation for Enhanced Trajectory-Prediction Accuracy in the Center-TRACON Automation System. AIAA-96-0271, Jan. 1996.

13. Slattery, Rhonda; and Green, Steve: *Conflict-Free Trajectory Planning for Air Traffic Control Automation*. NASA TM-108790, 1994.

14. Slattery, Rhonda A.; and Zhao, Yiyuan: En-Route Descent Trajectory Synthesis for Air Traffic Control Automation. *Proceedings of the American Control Conference*, June 1996, pp. 3430–3434.

15. Green, Steven M.; Goka, Tsuyoshi; and Williams, David H.: Enabling User Preferences Through Data Exchange. AIAA-97-3682, 1997.

16. Benjamin, Stanley G.; Bleck, Rainer; Grell, Georg; Pan, Zaitao; Smith, Tracy Lorraine; Brown, John M.; Ramer, James E.; Miller, Patricia A.; and Brundage; Kevin A.: Aviation Forecasts From the Hybrid-B Version of MAPS—Effects of New Vertical Coordinate and Improved Model Physics. *Fifth Conference on Aviation Weather Systems*, American Meterol. Soc., Aug. 1993, pp. J-5–J-9.

17. Benjamin, Stanley G.; Brundage, Kevin J.; Miller, Patricia A.; Smith, Tracy Lorraine; Grell, Georg A.; Kim, Dongsoo; Brown, John M.; and Schlatter, Thomas W.: The Rapid Update Cycle at NMC. *Tenth Conference on Numerical Weather Prediction*, American Meterol. Soc., July 1994, pp. 566–568.

18. Staff of NASA Langley Research Center and Boeing Commercial Airplane Co.: *Terminal Configured Vehicle Program—Test Facilities Guide*. NASA SP-435, 1980.

19. Knox, Charles E.: *Description of the Primary Flight Display and Flight Guidance System Logic in the NASA B-737 Transport Systems Research Vehicle*. NASA TM-102710, 1990.

20. Erzberger, Heinz; and Nedell, William: *Design of Automated System for Management of Arrival Traffic*. NASA TM-102201, 1989.

21. Computer Program Functional Specifications—Multiple Radar Data Processing. Model A4e1.3, NAS-MD-320, FAA, Aug. 1995.

22. Cashion, Patricia; Feary, M.; Smith, N.; Goka, T.; Graham, H.; and Palmer, E.: Development and Initial Field Evaluation of Flight Deck Procedures for Flying CTAS Descent Clearances. *Proceedings of the Eighth International Symposium on Aviation Psychology*, Volume 1, Richard S. Jensen and Lori A. Rakovan, eds., Assoc. of Aviation Psychologists, 1995, pp. 438–443.

23. Jardin, M. R.; and Green, S. M.: Atmospheric Data Error Analysis for the 1994 CTAS Descent Advisor Preliminary Field Test. NASA/TM-1998-112228, 1998.

24. Williams, D. H.: Impact of Mismodeled Idle Engine Performance on Calculation and Tracking of Optimal 4-D Descent Trajectories. *Fifth American Control Conference*, Volume 2, IEEE, 1986, pp. 681–686.

41

Table 1. Test Conditions for Phase I

Test condition	Cruise speed	Descent Mach/CAS	Descent strategy	Description
1i	Mach 0.72	0.72/280	Idle	Nominal, typical company profile
2i	Mach 0.76	0.76/330	Idle	Fast, earliest arrival time
3i	220 KCAS	/220	Idle	Slow, latest arrival time
4i	Mach 0.76	0.76/280	Idle	Fast cruise, long descent at nominal CAS
5i	220 KCAS	*MC/280	Idle	Slow cruise, long descent at constant Mach
6i	Mach 0.72	0.76/310	Idle	Fast descent, Mach acceleration descent
7i	Mach 0.72	/240	Idle	Slow descent, long TOD deceleration
1cf	Mach 0.72	0.72/280	Constrained	Condition 1 flown from FFD
2cf	Mach 0.76	0.76/330	Constrained	Condition 2 flown from FFD
3cf	220 KCAS	/220	Constrained	Condition 3 flown from FFD
1cr	Mach 0.72	0.72/280	Constrained	Condition 1 flown from RFD
2cr	Mach 0.76	0.76/330	Constrained	Condition 2 flown from RFD
3cr	220 KCAS	/220	Constrained	Condition 3 flown from RFD

*MC is Mach at cruise altitude at 220 KCAS.

Table 2. Test Conditions for Phase II

Test condition	Speed schedule	Automation level pilot procedure	Lateral guidance	Vertical guidance	Flight deck
1a	0.72/0.72/280	Conventional non-FMS	VOR/DME	Airspeed with CTAS TOD	FFD
2a	0.76/0.76/240				
3a	0.76/0.76/320				
1b	0.72/0.72/280	Conventional FMS	LNAV	FMS with VNAV TOD	RFD
2b	0.76/0.76/240				
3b	0.76/0.76/320				
1c	0.72/0.72/280	FMS with CTAS TOD	LNAV	FMS with CTAS TOD	RFD
2c	0.76/0.76/240				
3c	0.76/0.76/320				
1d	0.72/0.72/280	Range-altitude arc	LNAV	Range-altitude arc with CTAS TOD	RFD
2d	0.76/0.76/240				
3d	0.76/0.76/320				

Table 3. Phase I Test Runs

Flight	Date (UTC)	Run	Test condition (table 1)	Flight deck	Metering fix	Arrival time, UTC	Comments
R678	10/21/92	1	1i	FFD	KEANN	20:09:48	Day flight with good weather
		2	2i	RFD	KEANN	20:50:04	
		3	3i	RFD	KEANN	21:26:10	
R679	10/23/92	1	7i	RFD	KEANN	4:38:40	Night flight with strong jet stream winds
							Run 1 excluded from analysis
		2	5i	RFD	KEANN	5:14:49	
		3	6i	RFD	KEANN	5:50:24	
		4	4i	RFD	KEANN	6:23:50	
		5	3i	RFD	KEANN	6:56:05	
R680	10/24/92	1	5i	RFD	KEANN	2:50:32	Night flight with strong jet stream winds and pronounced wind gradient
		2	1i	RFD	KEANN	3:25:36	
		3	6i	RFD	KEANN	4:04:26	
		4	4i	RFD	KEANN	4:38:55	
		5	7i	RFD	KEANN	5:09:46	
R681A	10/26/92	1	1c	RFD	KEANN	18:22:44	Day flight with good weather
		2	2c	RFD	KEANN	18:57:11	
R681B	10/26/92	3	3c	RFD	KEANN	20:54:57	Day flight with good weather
		4	1c	FFD	KEANN	21:31:19	
		5	2c	FFD	KEANN	22:09:08	
		6	3c	FFD	KEANN	22:43:26	
R682A	10/27/92	1	1c	RFD	KEANN	18:27:13	Day flight with good weather
		2	2c	RFD	KEANN	19:01:36	
		3	3c	FFD	KEANN	19:34:16	Run 3 excluded from analysis
		4	2c	FFD	KEANN	20:05:54	Run 4 excluded from analysis
R682B	10/27/92	5	3c	RFD	KEANN	22:08:40	Day flight with good weather
		6	1c	FFD	KEANN	22:46:35	
		7	2c	RFD	KEANN	23:37:36	

Table 4. Phase II Test Runs

Flight	Date (UTC)	Run	Test condition (table 2)	Flight deck	Metering fix	Arrival time, UTC	Comments
R728	9/16/94	1	1b	RFD	DRAKO	*n/a	Day flight with good weather
							Run 1 aborted
		2	1b	RFD	DRAKO	18:16:21	
		3	1c	RFD	DRAKO	18:56:23	
		4			KEANN	n/a	Run 4 weather data only
R729A	9/17/94	1	2a	FFD	DRAKO	n/a	Day flight with good weather
							Run 1 aborted
		2	2a	FFD	DRAKO	17:47:03	
		3	3a	FFD	DRAKO	18:19:43	
		4	1a	FFD	DRAKO	18:53:26	
		5	1d	RFD	DRAKO	19:30:11	
R729B	9/17/94	6	2b	RFD	DRAKO	22:12:54	Day flight with good weather
		7	2c	RFD	DRAKO	22:49:04	
		8	3d	RFD	DRAKO	n/a	Run 8 aborted
		9	3d	RFD	DRAKO	23:43:18	
	9/18/94	10	3a	FFD	DRAKO	0:14:31	
R730A	9/19/94	1	3b	RFD	DRAKO	17:27:30	Day flight with convective buildups
		2	2a	FFD	DRAKO	18:02:00	
		3	2d	RFD	DRAKO	18:37:54	
		4	3c	RFD	DRAKO	19:13:14	
		5	2d	RFD	DRAKO	19:48:26	
R730B	9/19/94	6			KEANN	n/a	Day flight with convective buildups
							Run 6 weather data only
		7	3d	RFD	DRAKO	n/a	Run 7 aborted
		8	1d	RFD	DRAKO	22:50:40	
R731	9/20/94	1			KEANN	n/a	Day flight with good weather
							Run 1 weather data only
	9/21/94	2	1b	RFD	DRAKO	0:04:50	
		3	1c	RFD	DRAKO	n/a	Run 3 aborted
		4	1c	RFD	DRAKO	1:08:35	
		5	3d	RFD	DRAKO	1:41:33	
R732	9/21/94	1	3b	RFD	DRAKO	17:27:25	Day flight with strong frontal passage
		2	3c	RFD	DRAKO	18:03:20	
		3	2b	RFD	DRAKO	18:44:31	
		4	2c	RFD	DRAKO	n/a	Run 4 aborted
R733	9/22/94	1			KEANN	n/a	Day flight with good weather and strong winds aloft
							Run 1 weather data only
		2	2c	RFD	DRAKO	18:27:36	
		3	1a	FFD	DRAKO	19:01:43	
		4	2b	RFD	DRAKO	19:36:41	Flown without autopilot
		5	2d	RFD	DRAKO	20:11:12	Accelerate to 300 knots in descent

*n/a means not any.

44

Table 5. Radar Tracking Errors

(a) Radar tracking errors at CTAS initial conditions for unaccelerated flight

Error	Phase I		Phase II	
	Mean	Std. dev.	Mean	Std. dev.
Ground speed, knots	−1.6	6.5	5.0	4.3
Track angle, deg	3.0	5.0	0.14	2.57
Position, n.mi.	0.65	0.34	0.98	0.42
Along-track				
Distance, n.mi.	0.62	0.35	0.94	0.42
Time, sec	5.9	3.1	7.2	3.2
Cross track, n.mi.	0.10	0.14	0.18	0.19

(b) Radar tracking errors at metering fix crossing conditions for deceleration segments

Error	Phase I		Phase II	
	Mean	Std. dev.	Mean	Std. dev.
Ground speed, knots	−32.2	24.6	−38.5	24.2
Track angle, deg	2.9	3.4	2.4	4.1
Position, n.mi.	0.44	0.24	0.67	0.42
Along-track				
Distance, n.mi.	0.38	0.27	0.63	0.29
Time, sec	4.3	3.0	6.9	3.1
Cross track, n.mi.	0.05	0.18	0.15	0.10

Table 6. Radar Track Position Error Statistics for Phase II Flights

Flight	Elapsed flight time, hr:min:sec	Along-track error				Cross-track error	
		Mean, n.mi.	Std. dev., n.mi.	Mean, sec	Std. dev, sec	Mean, n.mi.	Std. dev., n.mi.
728	2:14:00	0.684	0.396	5.9	3.4	−0.024	0.199
729a/b	5:05:36	0.777	0.398	6.8	3.5	0.008	0.248
730a/b	3:28:00	0.688	0.399	6.1	3.5	0.006	0.277
731	2:19:36	0.731	0.390	6.3	3.2	−0.044	0.207
732	2:07:24	0.719	0.384	6.3	3.3	−0.037	0.197
733	1:34:36	0.703	0.382	6.2	3.4	−0.028	0.207
Total	16:49:12	0.717	0.392	6.3	3.4	−0.020	0.223

Table 7. Radar Track Ground Speed and Track Angle Errors for Phase II Flight Segments

Segment	Ground speed error, knots		Track angle error, deg	
	Mean	Std. dev.	Mean	Std. dev.
Level flight	2.3	12.3	0.1	4.6
Altitude change	−2.3	12.9	0.7	5.1
Turn	37.0	58.9	4.9	27.8
Postturn	56.4	55.8	5.0	12.9

Table 8. Mean and Standard Deviation Errors in Pilot Adherence to CTAS Descent Speed Schedule

Speed	Phase I				Phase II			
	FFD		RFD		FFD		RFD	
	Mean	Std. dev.	Mean	Std. dev.	Mean	Std. dev.	Mean	Std. dev.
Cruise Mach	0.005	0.009	0.001	0.003	0.010	0.007	0.001	0.004
Descent Mach	0.008	0.007	0.001	0.009	0.009	0.008	0.004	0.008
Descent CAS, knots	−0.9	3.4	−0.2	3.1	1.5	5.5	0.3	4.8

46

Table 9. Top of Descent Errors From Phase II

Procedure	TOD error, n.mi.	
	Mean	Std. dev.
Non-FMS	1.2	1.0
FMS TOD	2.5	2.8
CTAS TOD	1.0	0.9
ND arc	0.5	0.4
All runs	1.4	1.7
All procedures using CTAS TOD*	0.9	0.8

*Includes non-FMS, CTAS TOD, and ND arc.

Table 10. Arrival Time Errors (Actual – Predicted) at Metering Fix
for Phase I

Procedure	Arrival time error, sec	
	Mean	Std. dev.
Idle descent	16.6	9.9
RFD constrained	9.9	6.4
FFD constrained	16.4	14.8
All runs	14.7	9.6

Table 11. Arrival Time Errors (Actual – CTAS predicted)
at Metering Fix for Phase II

Procedure	Arrival time error, sec	
	Mean	Std. dev.
Non-FMS	1.9	8.7
FMS TOD	–4.6	13.9
CTAS TOD	–9.9	10.2
ND arc	2.3	13.8
All runs	–2.7	12.3

Table 12. Arrival Time Errors (Actual – FMS predicted)
at Metering Fix for Phase II

Procedure	Arrival time error, sec	
	Mean	Std. dev.
FMS TOD	2.0	11.3
CTAS TOD	2.8	4.4

Table 13. Combinations of Airplane Performance and Weather Models Used in Sensitivity Analysis
of Phase I Idle Descents

Set name	Performance model	Weather model
Baseline	Boeing 737-100	CTAS MAPS
Revised performance	TSRV	CTAS MAPS
Revised weather	Boeing 737-100	Flight measured
Revised both	TSRV	Flight measured

Table 14. Arrival Time Error Resulting From Modeling
Errors in Phase I Idle Descents

Model parameter	Time error, sec	
	Mean	Std. dev.
Performance	5.0	1.5
Weather	12.1	8.8
Both	16.8	9.6
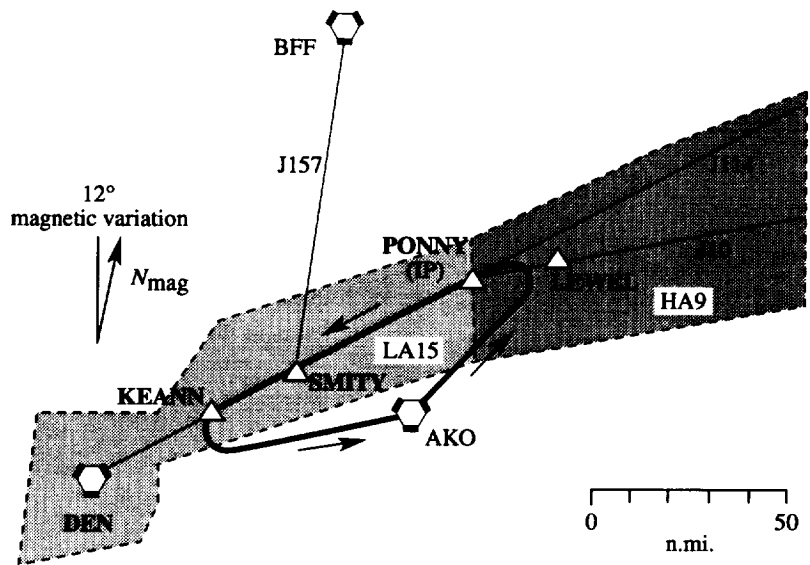
Figure 1. Flight test area for Phase I.
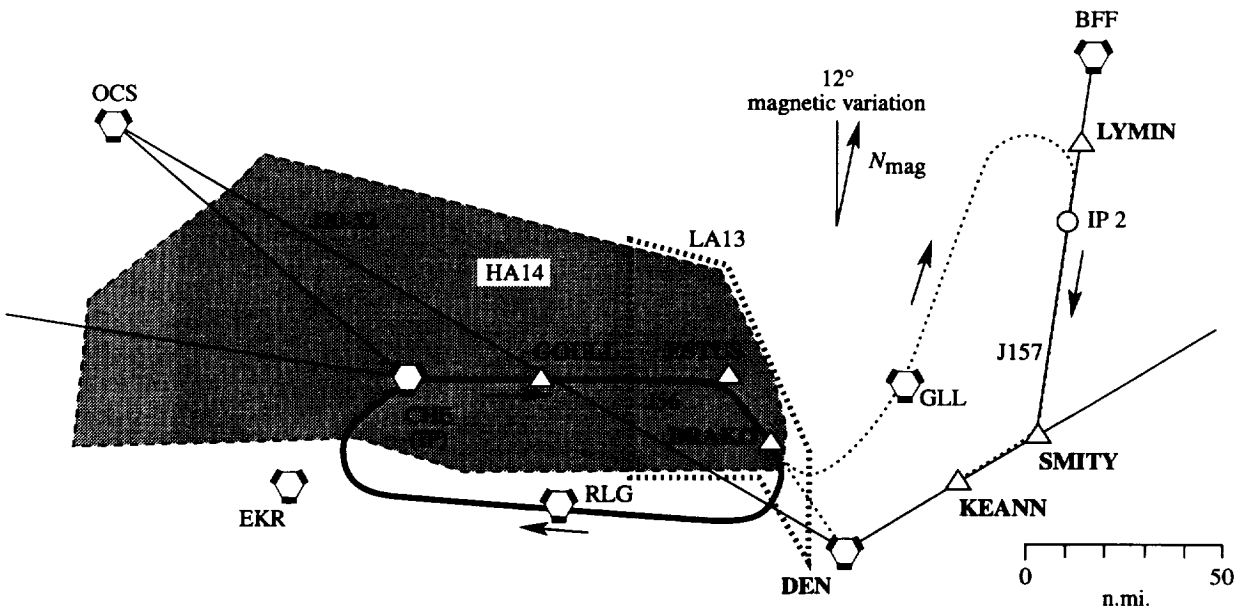
Figure 2. Flight test area for Phase II.

L-89-12405

Figure 3. TSRV Boeing 737-100 test airplane.
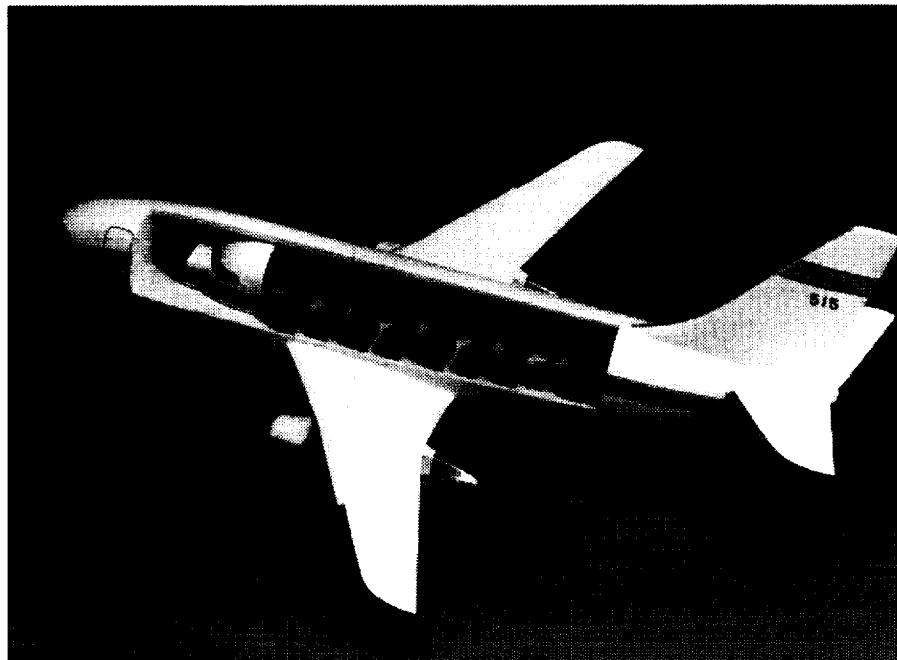
L-80-2580

Figure 4. Research flight deck (RFD) location in TSRV airplane.
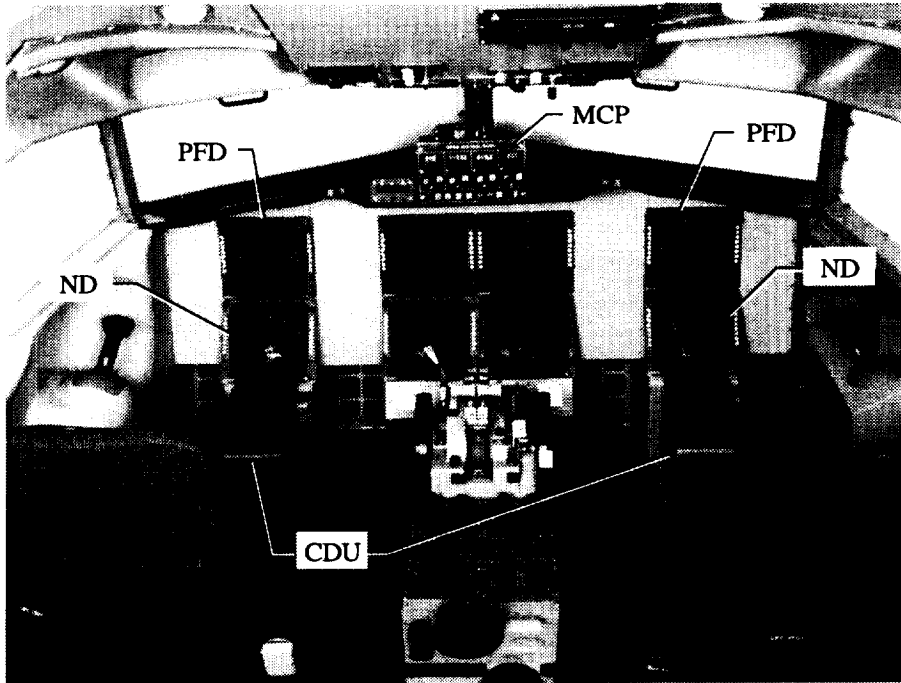
L-90-13735

Figure 5. TSRV research flight deck.
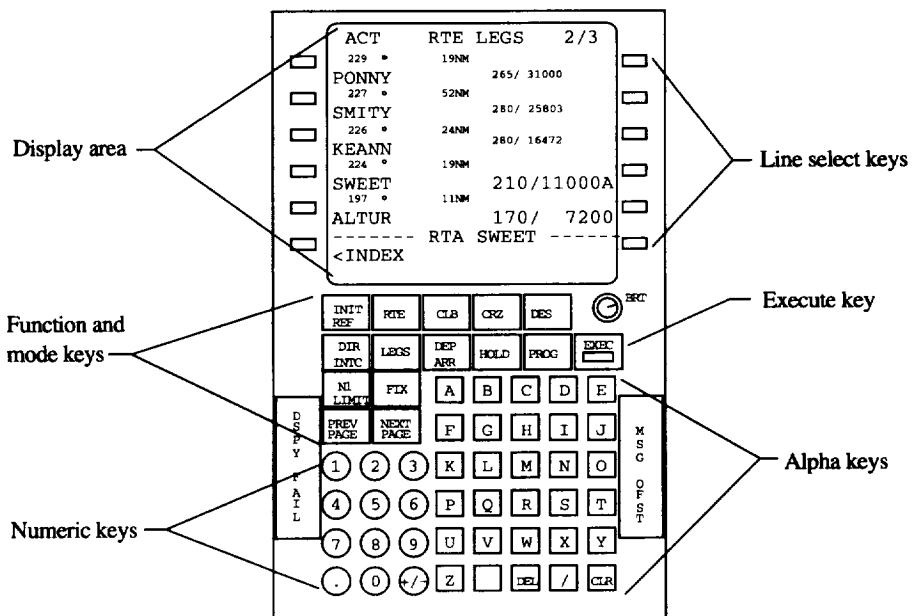
Figure 6. TSRV control display unit (CDU).
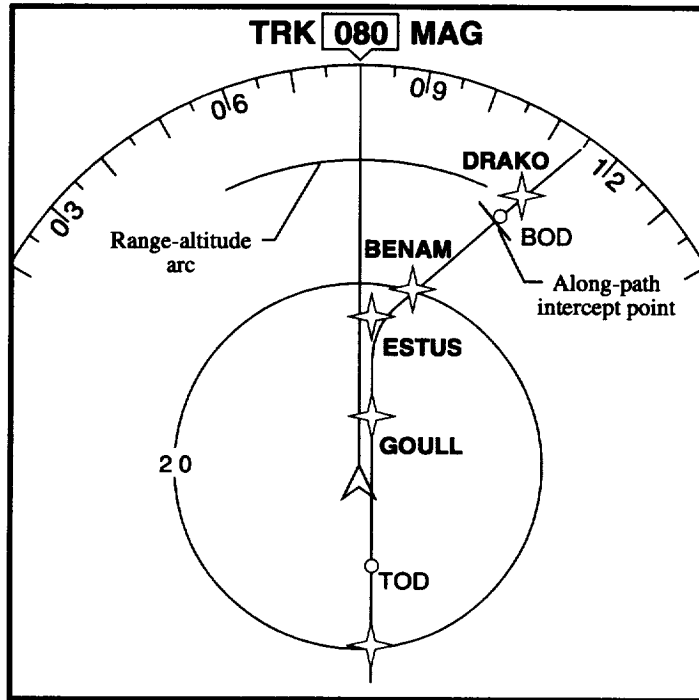
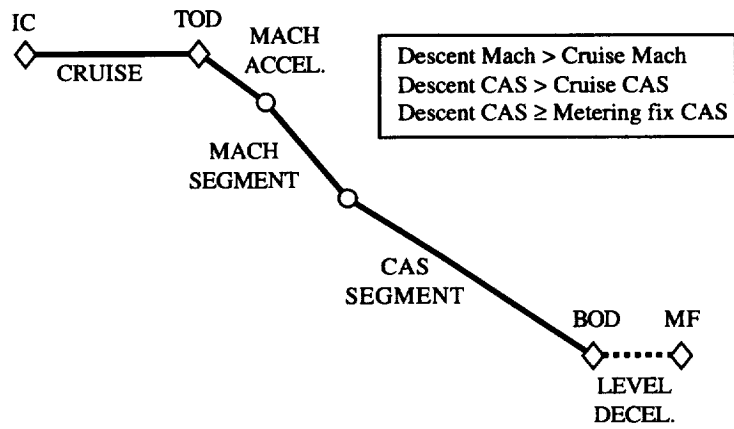Figure 7. TSRV navigation map display showing range-altitude arc and intercept point.
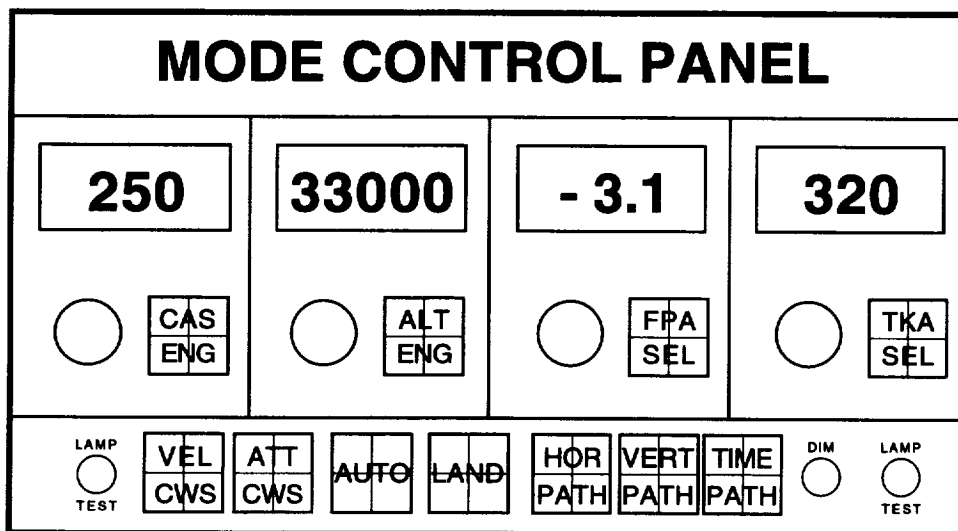
Figure 8. TSRV mode control panel (MCP).

TSRV

VHF "test"
communications

Normal ATC VHF
(pilot ↔ controller)
communications

Denver ARTCC

Traffic
Management
Coordinator

DA Test
Engineer

Controller

Traffic Management Unit

Radar Sector
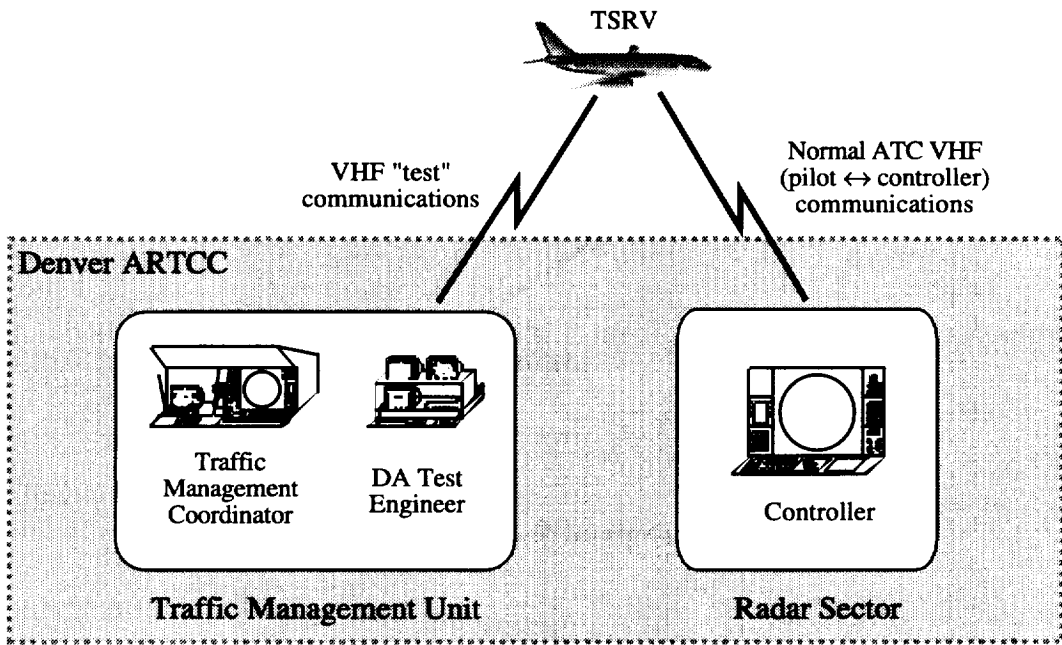
Figure 9. Experimental setup at Denver Center.

(a) Slow descent profile.

IC TOD

CRUISE LEVEL DECEL.

Descent CAS < Cruise CAS
Descent CAS ≥ Metering fix CAS

CAS SEGMENT

BOD MF

LEVEL DECEL.
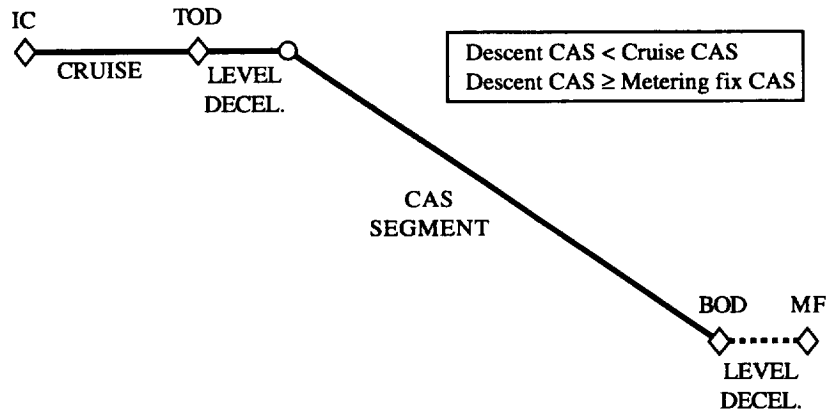
(a) Slow descent profile.

(b) Nominal descent profile.

IC TOD

CRUISE

Descent Mach = Cruise Mach
Descent CAS > Cruise CAS
Descent CAS ≥ Metering fix CAS

MACH SEGMENT

CAS SEGMENT

BOD MF

LEVEL DECEL.
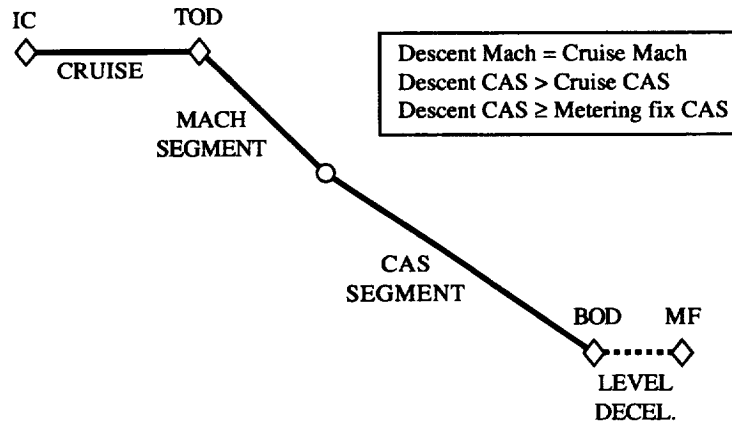
(b) Nominal descent profile.

(c) Fast descent profile.

IC TOD MACH ACCEL.

CRUISE

Descent Mach > Cruise Mach
Descent CAS > Cruise CAS
Descent CAS ≥ Metering fix CAS

MACH SEGMENT

CAS SEGMENT

BOD MF

LEVEL DECEL.

(c) Fast descent profile.

Figure 10. Vertical profile procedures as function of speed.

RFD Procedure: VNAV Using FMS TOD

3. 10 n.mi. from TOD:

- Disengage autothrottle.
- Select CDU DESCENT page.

4. At FMS TOD:

- Throttle to idle.
- Set MCP CAS to descent CAS.

DME FMS TOD

5. Descent Control Procedure:

- Maintain VERT PATH speed using throttle and/or speed brake.

2. Following CTAS Clearance:

- Verify crossing conditions at DRAKO on LEGS page.
- Enter descent speed on DESCENT page.
- Engage VERT PATH.
- Set MCP altitude to 17000 ft.
- Enter CTAS DME distance as circle around DEN VOR on FIX page.

6. Bottom of Descent:

- Enter Altimeter setting prior to 19000 ft.
- Set MCP CAS to 250.
- Select VCSS prior to 18000 ft.
- Smoothly capture crossing conditions at DRAKO.

1. Prior To CTAS Clearance:

- Level at cruise altitude, on path, at test condition cruise Mach.
- AUTO, ALT, HOR PATH, CAS ENG.

BOD ○———○ **DRAKO**
17000/250 KCAS

(a) Test conditions 1b and 3b.

RFD Procedure: VNAV Using FMS TOD

3. 10 n.mi. from TOD:

- Disengage autothrottle.
- Select CDU DESCENT page.

4. At FMS TOD:

- Throttle to idle.
- Set MCP CAS to descent CAS (240).

DME FMS TOD

5. Descent Control Procedure:

- Maintain VERT PATH speed using throttle and/or speed brake.

2. Following CTAS Clearance:

- Verify crossing conditions at DRAKO on LEGS page.
- Enter descent speed on DESCENT page.
- Engage VERT PATH.
- Set MCP altitude to 17000 ft.
- Enter CTAS DME distance as circle around DEN VOR on FIX page.

6. Bottom of Descent:

- Enter Altimeter setting prior to 19000 ft.

1. Prior To CTAS Clearance:

- Level at cruise altitude, on path, at test condition cruise Mach.
- AUTO, ALT, HOR PATH, CAS ENG.

○ **DRAKO**
17000/240 KCAS

(b) Test condition 2b.

Figure 11. Test cards for Phase II descent using conventional FMS.

RFD Procedure: VNAV Using CTAS TOD

Conditions 1c and 3c.
.72/280 and .76/320
Early descent.

3. 10 n.mi. from DME arc:
- Engage FPA mode.
- Set MCP altitude to 17000 ft.
- Disengage autothrottle.
- Select CDU DESCENT page.

4. At DME arc:
- Set FPA to -1.5 deg.
- Throttle to maintain descent Mach.
- Set MCP CAS to descent CAS.

DME   FMS TOD

5. Descent Control Procedure:
- Adjust throttle to maintain descent speeds.
- Engage VERT PATH at FMC TOD. –
  Reset FPA to -1.5 deg.
- Throttle to idle at VERT PATH capture.
- Maintain VERT PATH speed using throttle and/or speed brake.

2. Following CTAS Clearance:
- Verify crossing conditions at DRAKO on LEGS page.
- Enter descent speed on DESCENT page.
- Enter CTAS DME distance as circle around DEN VOR on FIX page.

6. Bottom of Descent:
- Enter Altimeter setting prior to 19000 ft.
- Set MCP CAS to 250.
- Select VCSS prior to 18000 ft.
- Smoothly capture crossing conditions at DRAKO.

1. Prior To CTAS Clearance:
- Level at cruise altitude, on path, at test condition cruise Mach.
- AUTO, ALT, HOR PATH, CAS ENG.

BOD   DRAKO 17000/250 KCAS

(a) Test conditions 1c and 3c; early descent.

RFD Procedure: VNAV Using CTAS TOD

Conditions 1c and 3c.
.72/280 and .76/320
Late descent.

3. 10 n.mi. from DME arc:
- Engage FPA mode.
- Set MCP altitude to 17000 ft.
- Disengage autothrottle.
- Select CDU DESCENT page.

4. At DME arc:
- Throttle to idle.
- Set FPA to -4 deg (-6 for Mach .76).
- Select VERT PATH (should ARM).
- Set MCP CAS to descent CAS.

FMS DME
TOD

5. Descent Control Procedure:
- Establish FPA closing on vertical path.
- Maintain VERT PATH speed using speed brake.
- Retract speed brake when vertical path is captured.

2. Following CTAS Clearance:
- Verify crossing conditions at DRAKO on LEGS page.
- Enter descent speed on DESCENT page.
- Enter CTAS DME distance as circle around DEN VOR on FIX page.

6. Bottom of Descent:
- Enter Altimeter setting prior to 19000 ft.
- Set MCP CAS to 250.
- Select VCSS prior to 18000 ft.
- Smoothly capture crossing conditions at DRAKO.

1. Prior To CTAS Clearance:
- Level at cruise altitude, on path, at test condition cruise Mach.
- AUTO, ALT, HOR PATH, CAS ENG.

BOD   DRAKO 17000/250 KCAS

(b) Test conditions 1c and 3c; late descent.

Figure 12. Test cards for Phase II descent using FMS with CTAS top of descent.

RFD Procedure: VNAV Using CTAS TOD

3. 10 n.mi. from DME arc:
- Engage FPA mode.
- Set MCP altitude to 17000 ft.
- Disengage autothrottle.
- Select CDU DESCENT page.

4. At DME arc:
- Throttle to idle.
- Set MCP CAS to descent CAS (240).
- Maintain Altitude until within 5 knots of descent CAS
- Set FPA to -1.5 deg when at descent CAS.

DME   FMS TOD

5. Descent Control Procedure:
- Adjust throttle to maintain descent speeds.
- Engage VERT PATH when past FMC TOD and converging on vertical path. -- Reset FPA to -1.5 deg.
- Throttle to idle.
- Maintain VERT PATH speed using throttle and/or speed brake.

2. Following CTAS Clearance:
- Verify crossing conditions at DRAKO on LEGS page.
- Enter descent speed on DESCENT page.
- Enter CTAS DME distance as circle around DEN VOR on FIX page.

6. Bottom of Descent:
- Enter Altimeter setting Prior to 19000 ft.

1. Prior To CTAS Clearance:
- Level at cruise altitude, on path, at test condition cruise Mach.
- AUTO, ALT, HOR PATH, CAS ENG.

DRAKO
17000/240 KCAS

(c) Test conditions 2c; early descent.

RFD Procedure: VNAV Using CTAS TOD

3. 10 n.mi. from DME arc:
- Engage FPA mode.
- Set MCP altitude to 17000 ft.
- Disengage autothrottle.
- Select CDU DESCENT page.

4. At DME arc:
- Throttle to idle.
- Set MCP CAS to descent CAS.
- Maintain Altitude until within 5 knots of descent CAS
- Set FPA to -3 deg when at descent CAS.

FMS DME
TOD

5. Descent Control Procedure:
- Select VERT PATH.
- Establish FPA closure on vertical path.
- Maintain VERT PATH speed using speed brake.
- Retract speed brake when vertical path is captured.

2. Following CTAS Clearance:
- Verify crossing conditions at DRAKO on LEGS page.
- Enter descent speed on DESCENT page.
- Enter CTAS DME distance as circle around DEN VOR on FIX page.

6. Bottom of Descent:
- Enter Altimeter setting Prior to 19000 ft.

1. Prior To CTAS Clearance:
- Level at cruise altitude, on path, at test condition cruise Mach.
- AUTO, ALT, HOR PATH, CAS ENG.

DRAKO
17000/240 KCAS

(d) Test conditions 2c; late descent.

Figure 12. Concluded.

RFD Procedure: Altitude-Range Arc

Conditions 1d and 3d.
.72/280 and .76/320
Early descent.

3. 10 n.mi. from DME arc:
- Engage FPA mode.
- Set MCP altitude to 17000 ft.
- Disengage autothrottle.
- Select CDU DESCENT page.

4. At DME arc:
- Set FPA to -4.0 deg (-6.0 for Mach .76).
- Throttle to idle.
- Set MCP CAS to descent CAS.

DME / FMS TOD

5. Descent Control Procedure:
- Adjust FPA to maintain descent Mach at idle thrust.
- When CAS reaches descent CAS, Adjust FPA so that Alt/Range Arc crosses BOD.
- Maintain descent CAS using throttle and/or speed brake.

2. Following CTAS Clearance:
- Verify crossing conditions at DRAKO on LEGS page.
- Enter descent speed on DESCENT page.
- Enter CTAS DME distance as circle around DEN VOR on FIX page.

6. Bottom of Descent:
- Enter Altimeter setting prior to 19000 ft.
- Set MCP CAS to 250.
- Select VCSS prior to 18000 ft.
- Smoothly capture crossing conditions at DRAKO.

1. Prior To CTAS Clearance:
- Level at cruise altitude, on path, at test condition cruise Mach.
- AUTO, ALT, HOR PATH, CAS ENG.

BOD O————O DRAKO
17000/250 KCAS

(a) Test conditions 1d and 3d; early descent.

RFD Procedure: Altitude-Range Arc

Conditions 1d and 3d.
.72/280 and .76/320
Late descent.

3. 10 n.mi. from DME arc:
- Engage FPA mode.
- Set MCP altitude to 17000 ft.
- Disengage autothrottle.
- Select CDU DESCENT page.

4. At DME arc:
- Set FPA to -4 deg (-6 for Mach .76).
- Throttle to idle.
- Set MCP CAS set to descent CAS.

FMS TOD   DME

5. Descent Control Procedure:
- Adjust FPA to maintain descent Mach at idle thrust.
- When CAS reaches descent CAS, Adjust FPA so that Alt/Range Arc crosses BOD.
- Maintain descent CAS using speed brake and/or throttle.

2. Following CTAS Clearance:
- Verify crossing conditions at DRAKO on LEGS page.
- Enter descent speed on DESCENT page.
- Enter CTAS DME distance as circle around DEN VOR on FIX page.

6. Bottom of Descent:
- Enter Altimeter setting prior to 19000 ft.
- Set MCP CAS to 250.
- Select VCSS prior to 18000 ft.
- Smoothly capture crossing conditions at DRAKO.

1. Prior To CTAS Clearance:
- Level at cruise altitude, on path, at test condition cruise Mach.
- AUTO, ALT, HOR PATH, CAS ENG.

BOD O————O DRAKO
17000/250 KCAS

(b) Test conditions 1d and 3d; late descent.

Figure 13. Test cards for Phase II descent using range-altitude arc.

RFD Procedure: Altitude-Range Arc

3. 10 n.mi. from DME arc:
- Engage FPA mode.
- Set MCP altitude to 17000 ft.
- Disengage autothrottle.
- Select CDU DESCENT page.

4. At DME arc:
- Throttle to idle.
- Set MCP CAS to descent CAS.
- Maintain altitude until within 5 knots of descent CAS.

DME   FMS TOD

5. Descent Control Procedure:
- Adjust FPA so that Alt/Range Arc crosses DRAKO.
- Maintain descent CAS using throttle and/or speed brake.

2. Following CTAS Clearance:
- Verify crossing conditions at DRAKO on LEGS page.
- Enter descent speed on DESCENT page.
- Enter CTAS DME distance as circle around DEN VOR on FIX page.

6. Bottom of Descent:
- Enter Altimeter setting Prior to 19000 ft.

1. Prior To CTAS Clearance:
- Level at cruise altitude, on path, at test condition cruise Mach.
- AUTO, ALT, HOR PATH, CAS ENG.

DRAKO
17000/240 KCAS

(c) Test conditions 2d; early descent.

RFD Procedure: Altitude-Range Arc

3. 10 n.mi. from DME arc:
- Engage FPA mode.
- Set MCP altitude to 17000 ft.
- Disengage autothrottle.
- Select CDU DESCENT page.

4. At DME arc:
- Throttle to idle.
- Set MCP CAS to descent CAS.
- Maintain altitude until within 5 knots of descent CAS.

FMS TOD   DME

5. Descent Control Procedure:
- Adjust FPA so that Alt/Range Arc crosses DRAKO.
- Maintain descent CAS using speed brake and/or throttle.

2. Following CTAS Clearance:
- Verify crossing conditions at DRAKO on LEGS page.
- Enter descent speed on DESCENT page.
- Enter CTAS DME distance as circle around DEN VOR on FIX page.

6. Bottom of Descent:
- Enter Altimeter setting Prior to 19000 ft.

1. Prior To CTAS Clearance:
- Level at cruise altitude, on path, at test condition cruise Mach.
- AUTO, ALT, HOR PATH, CAS ENG.

DRAKO
17000/240 KCAS

(d) Test conditions 2d; late descent.

Figure 13. Concluded.

(a) Air temperature measurements.
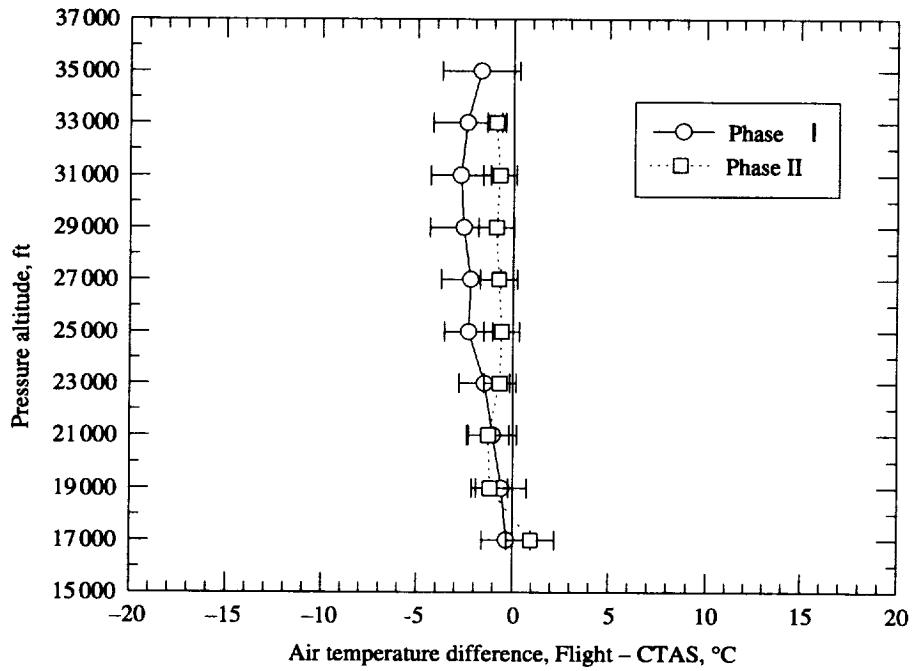
(b) Air temperature modeling errors.

Figure 14. Air temperature measurements and modeling errors.

60
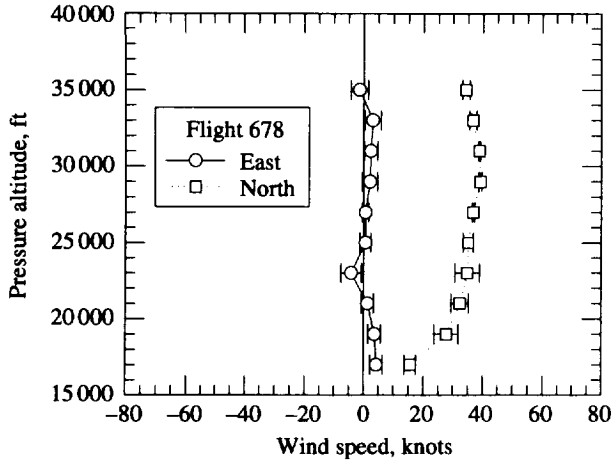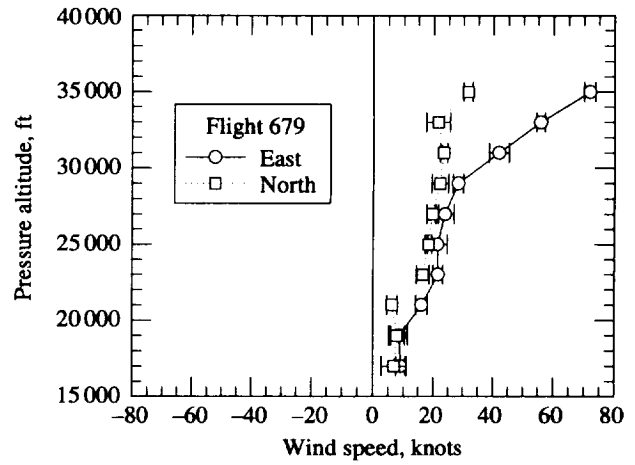
(a) Flight 678.
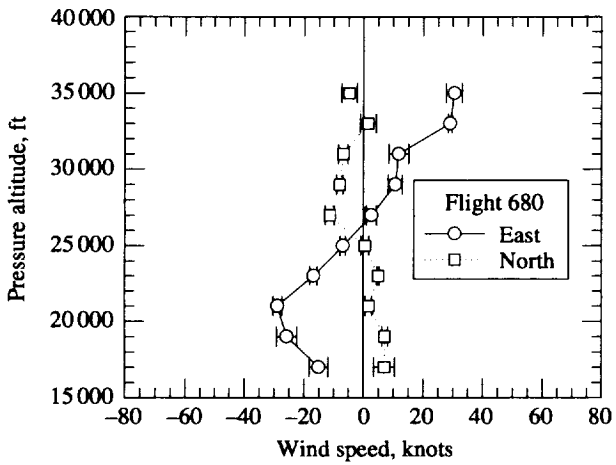
(b) Flight 679.
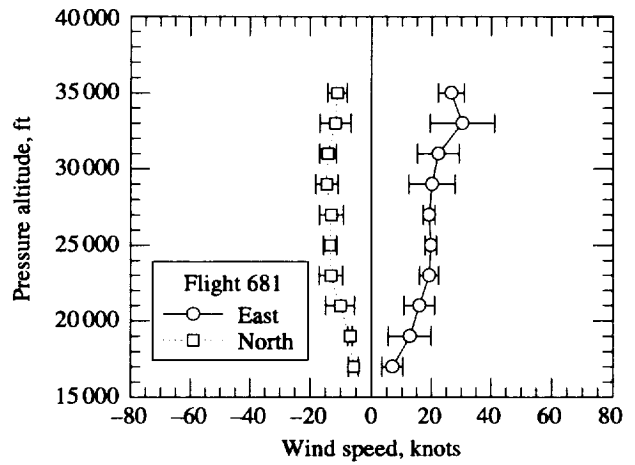
(c) Flight 680.
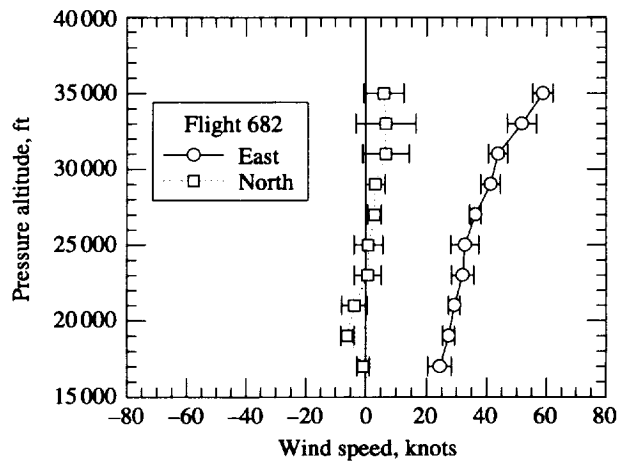
(d) Flight 681.

(e) Flight 682.

Figure 15. Measured winds from Phase I test.

61
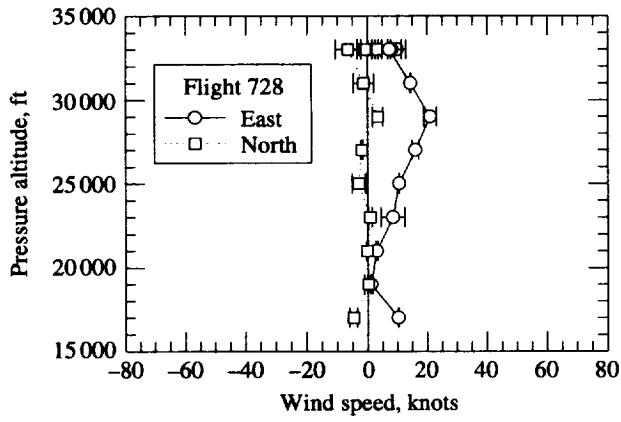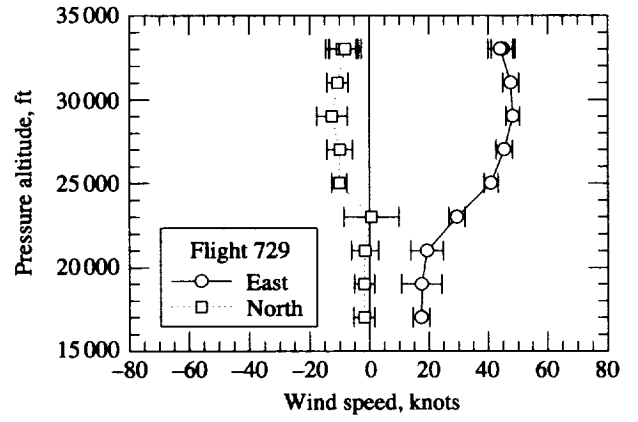
(a) Flight 728.
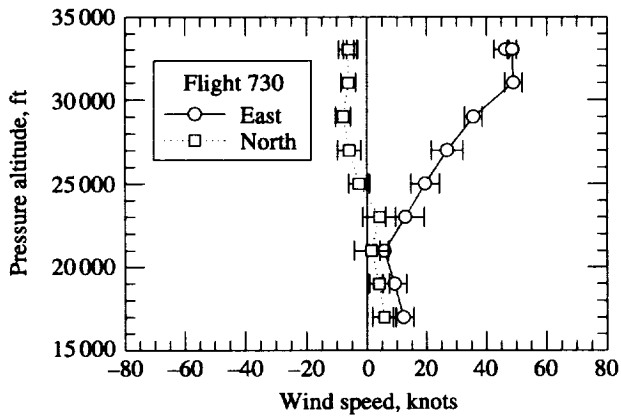
(b) Flight 729.
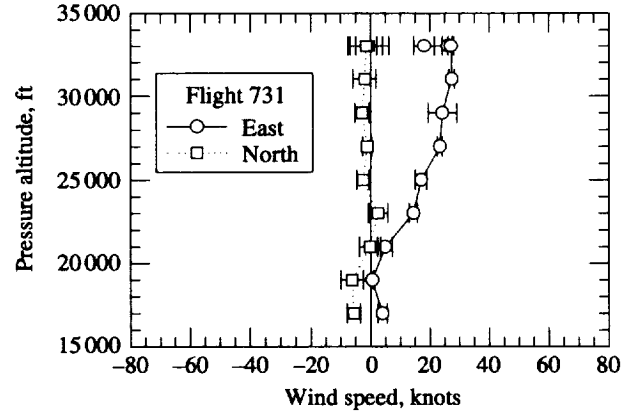
(c) Flight 730.
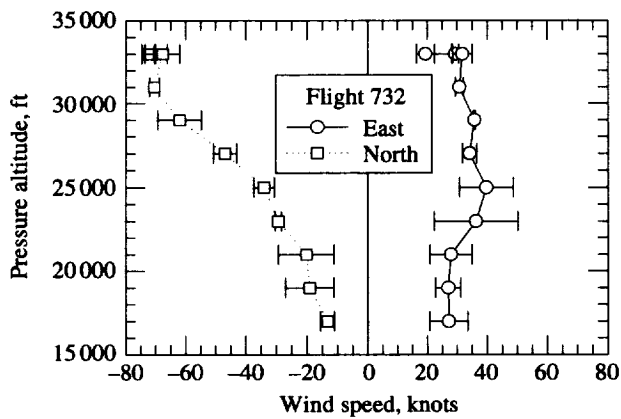
(d) Flight 731.
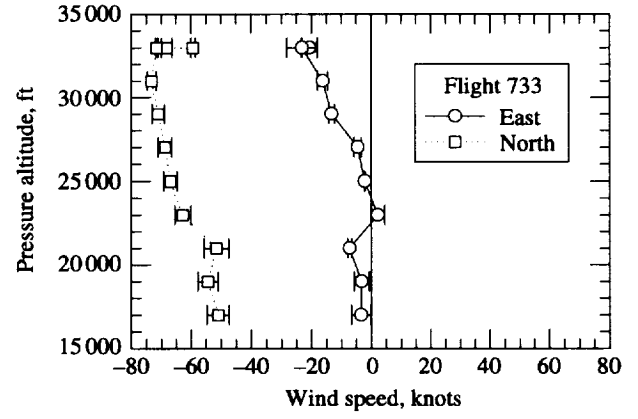
(e) Flight 732.

(f) Flight 733.

Figure 16. Measured winds from Phase II test.
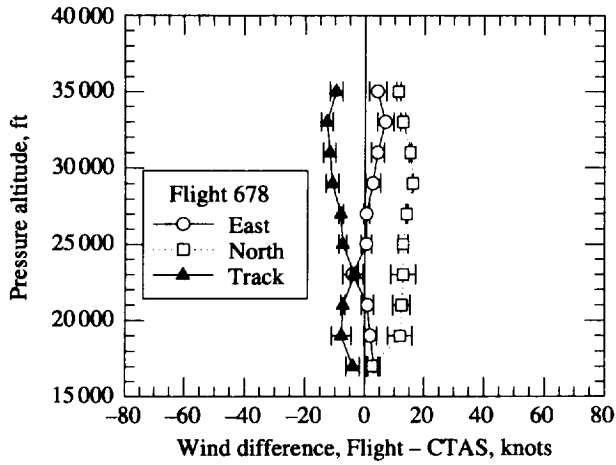
(a) Flight 678.
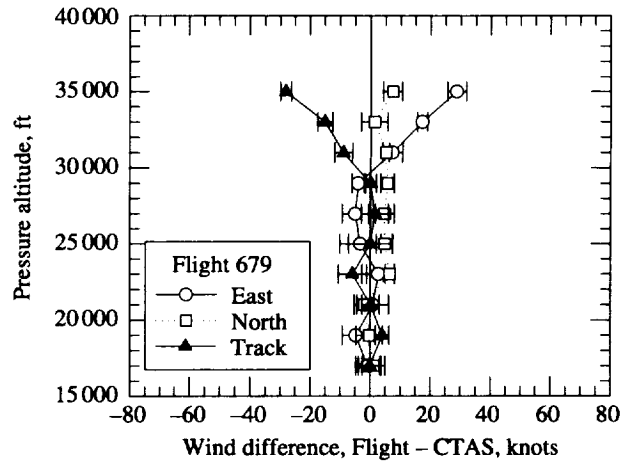
(b) Flight 679.
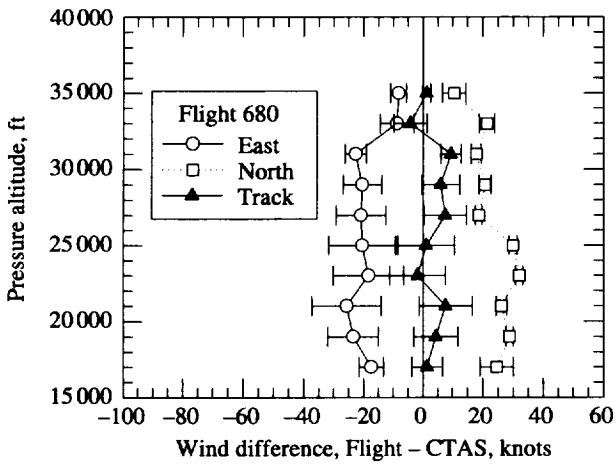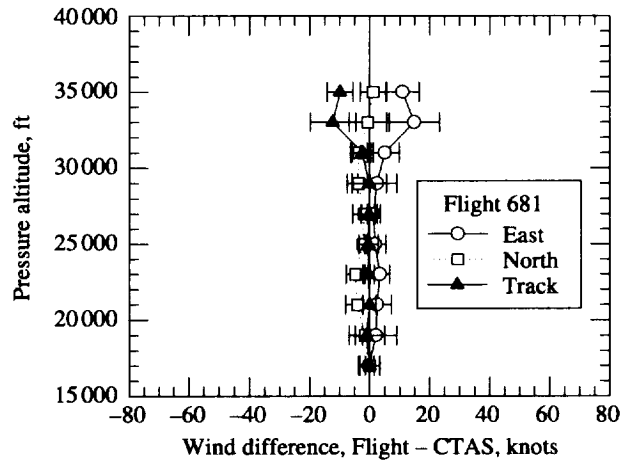
(c) Flight 680.
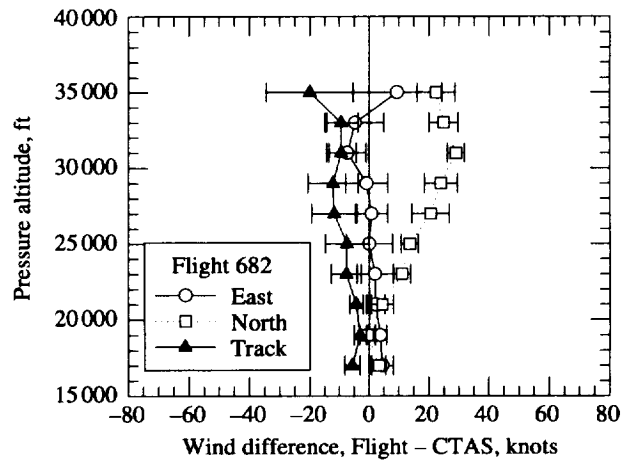
(d) Flight 681.

(e) Flight 682.

Figure 17. CTAS wind model errors from Phase I.

63
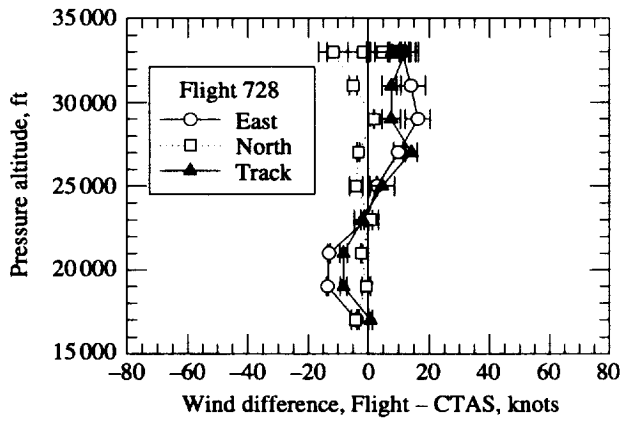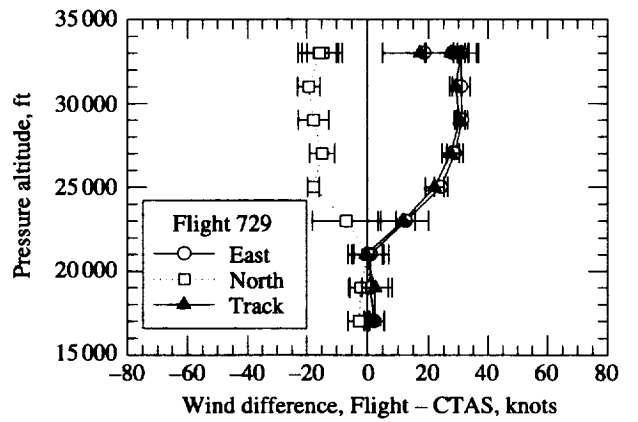
(a) Flight 728.
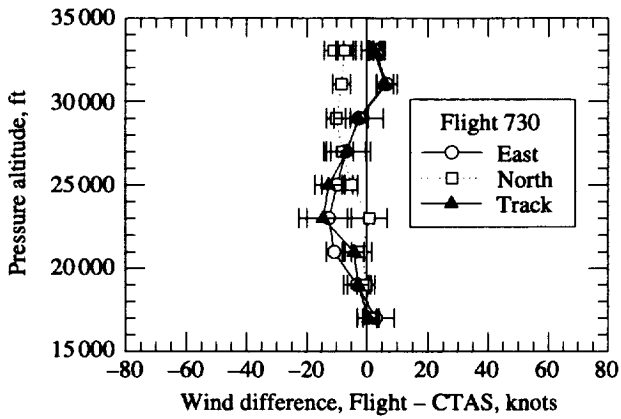
(b) Flight 729.
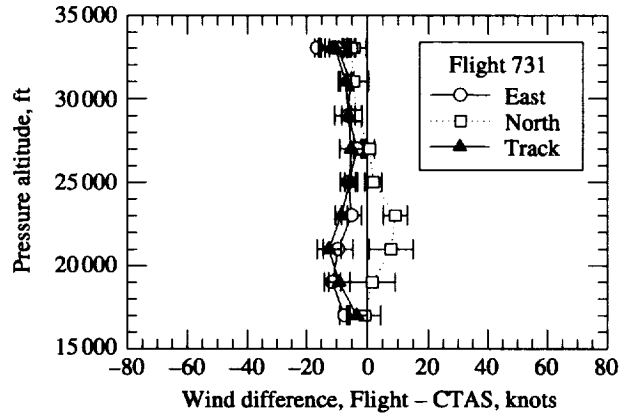
(c) Flight 730.
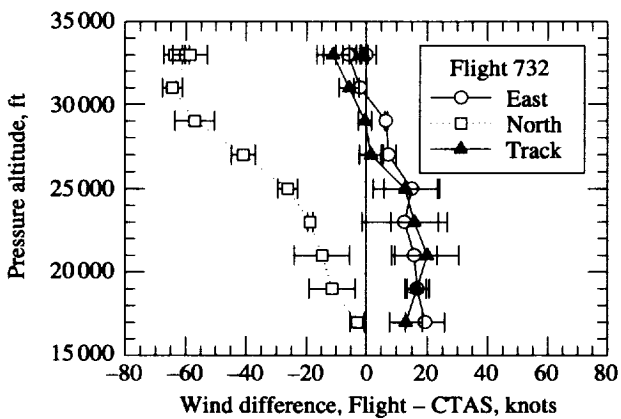
(d) Flight 731.
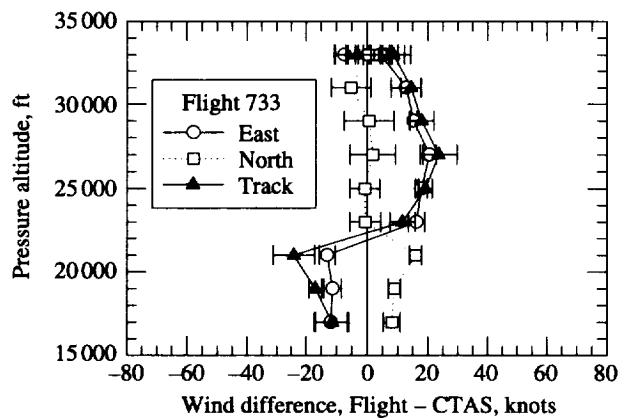
(e) Flight 732.

(f) Flight 733.

Figure 18. CTAS wind model errors from Phase II test.

64
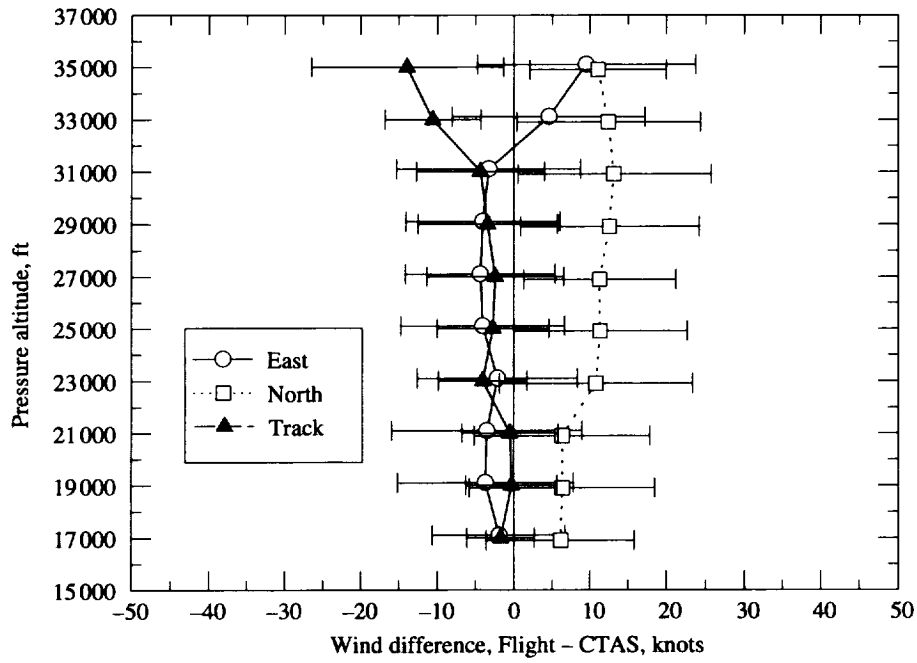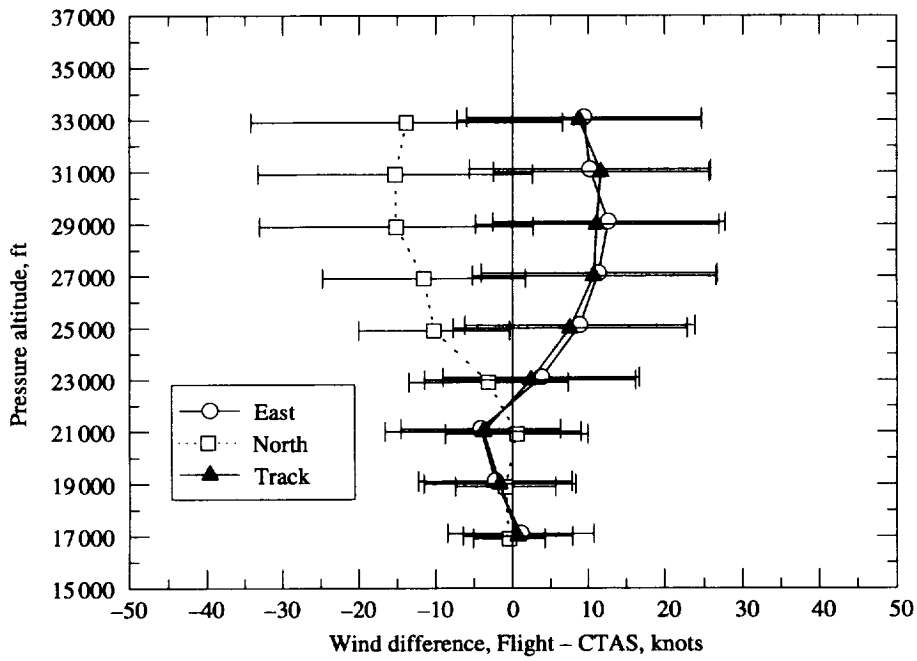
(a) Phase I test.

(b) Phase II test.

Figure 19. Composite CTAS wind model errors.
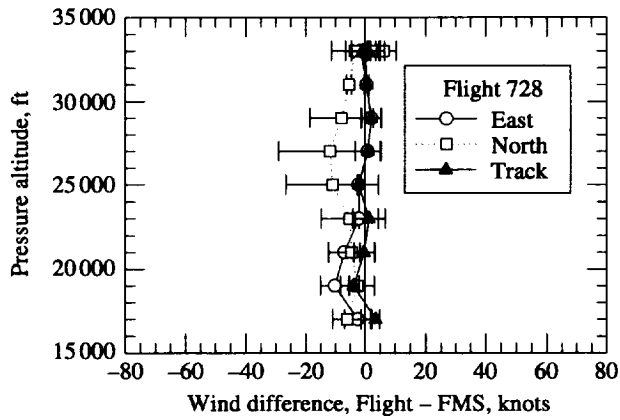
(a) Flight 728.
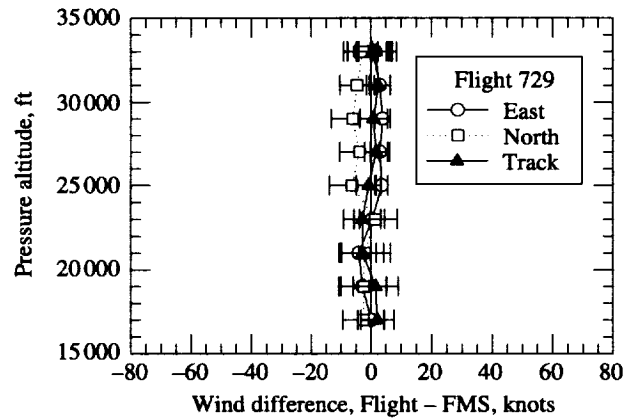
(b) Flight 729.
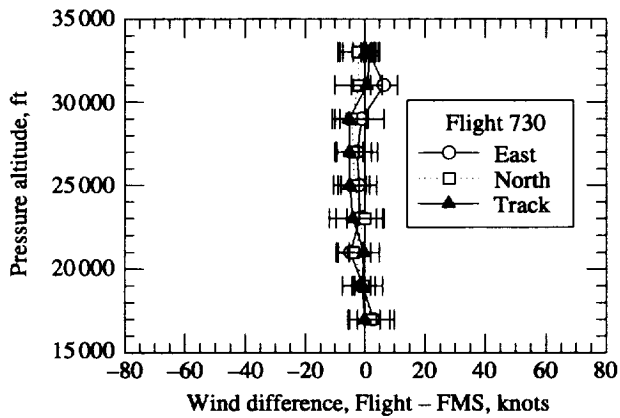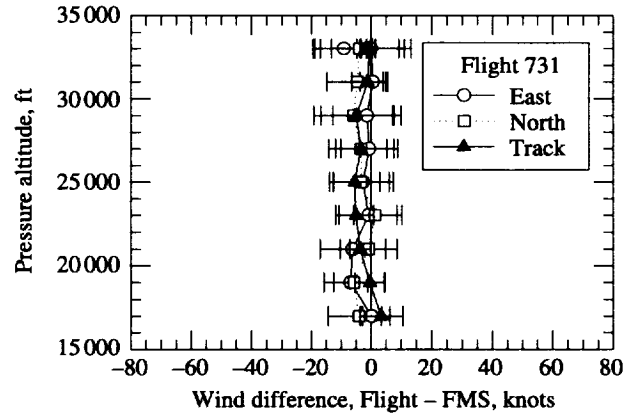
(c) Flight 730.
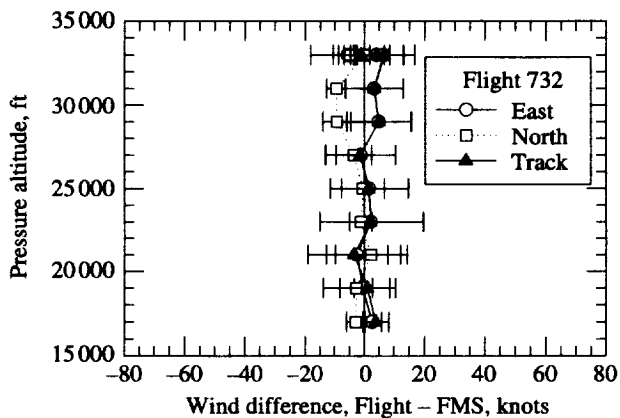
(d) Flight 731.
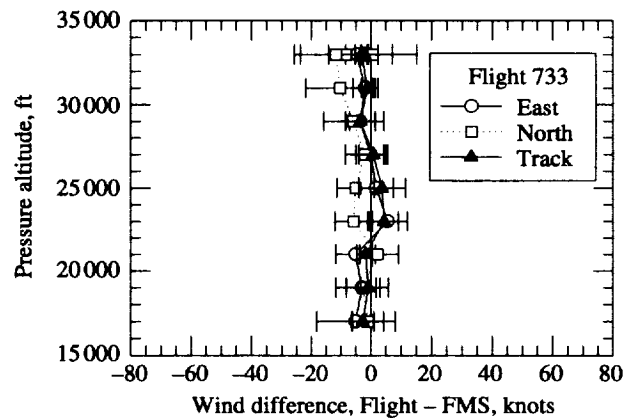
(e) Flight 732.

(f) Flight 733.

Figure 20. FMS wind model errors from Phase II.

66
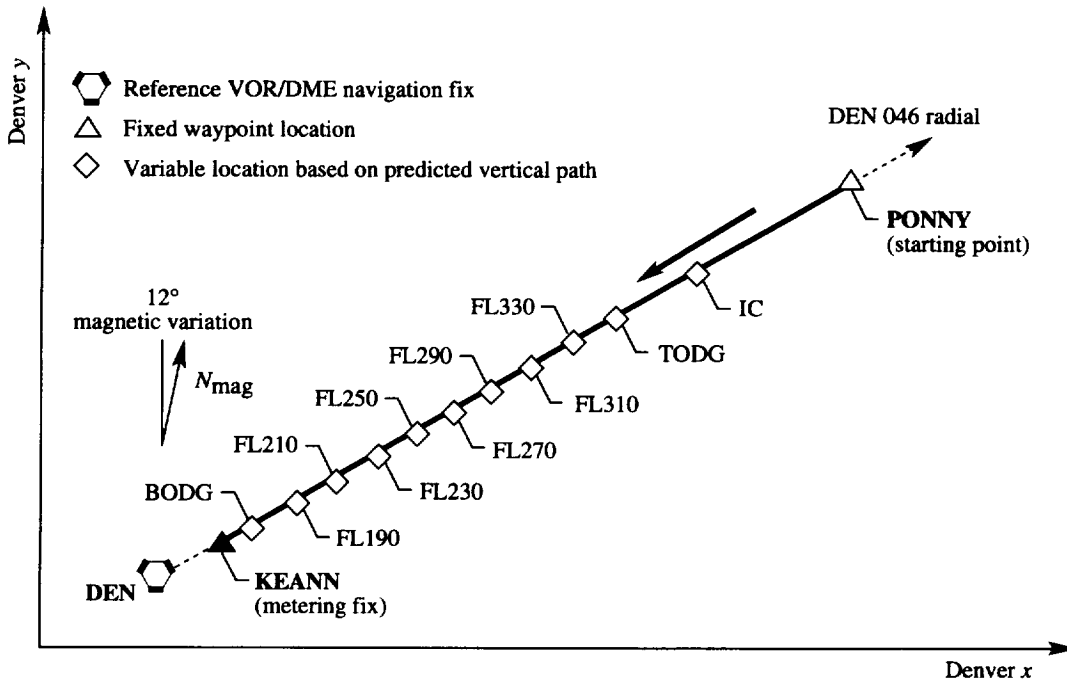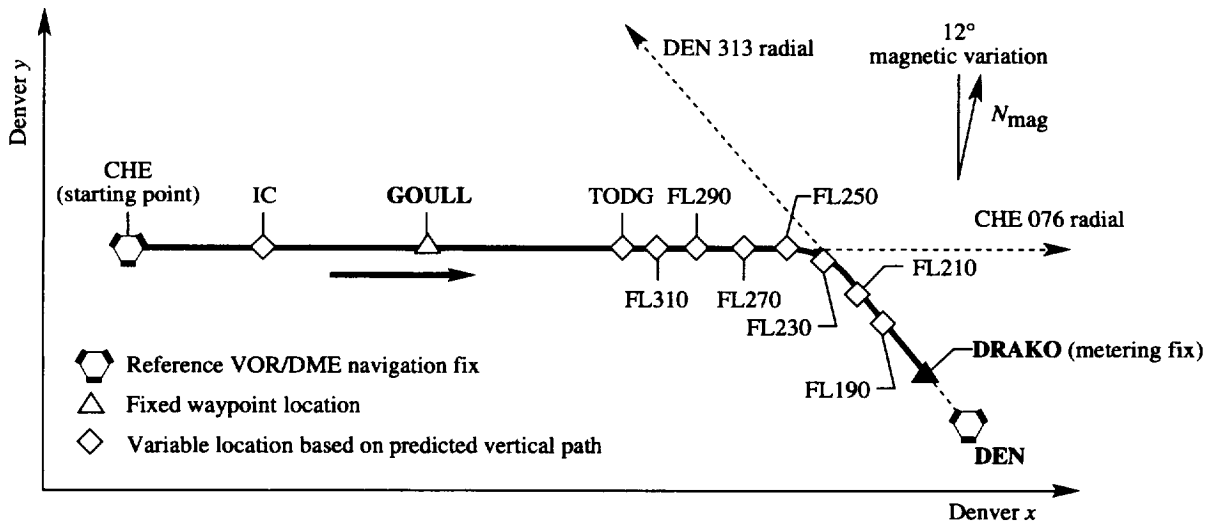
(a) Phase I.

(b) Phase II.

Figure 21. Analysis gates for trajectory comparisons.
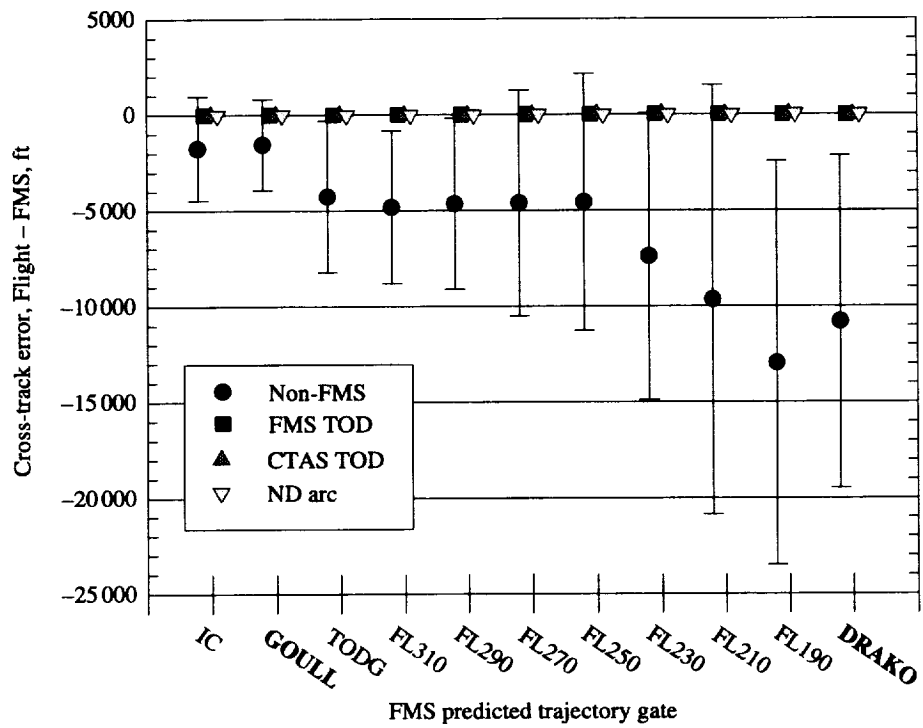
Figure 22. Cross-track error relative to FMS path.
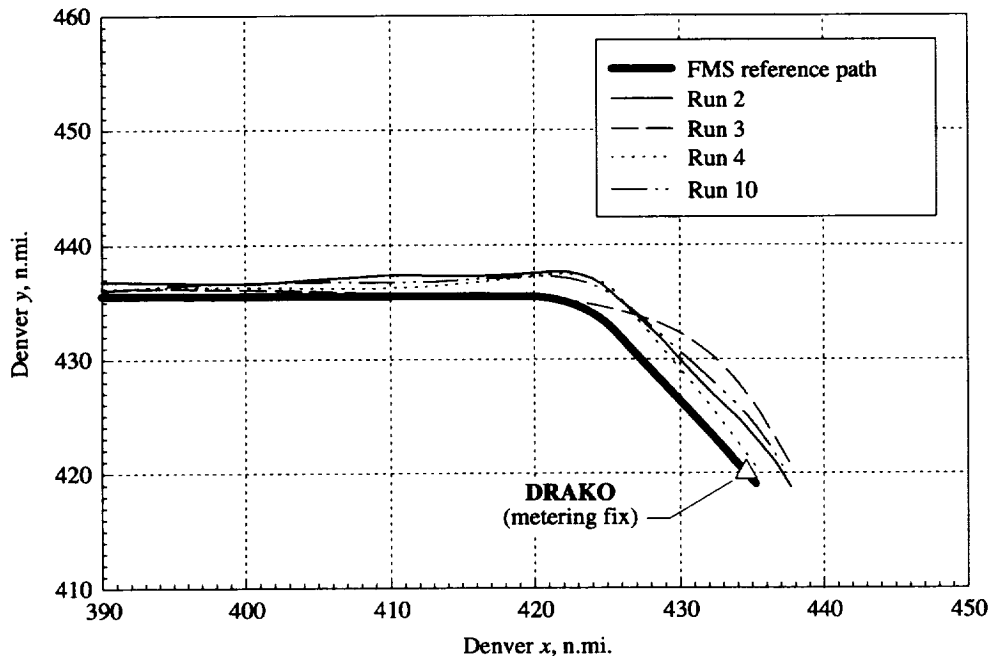
Figure 23. Lateral paths flown during flight 729 using VOR guidance.
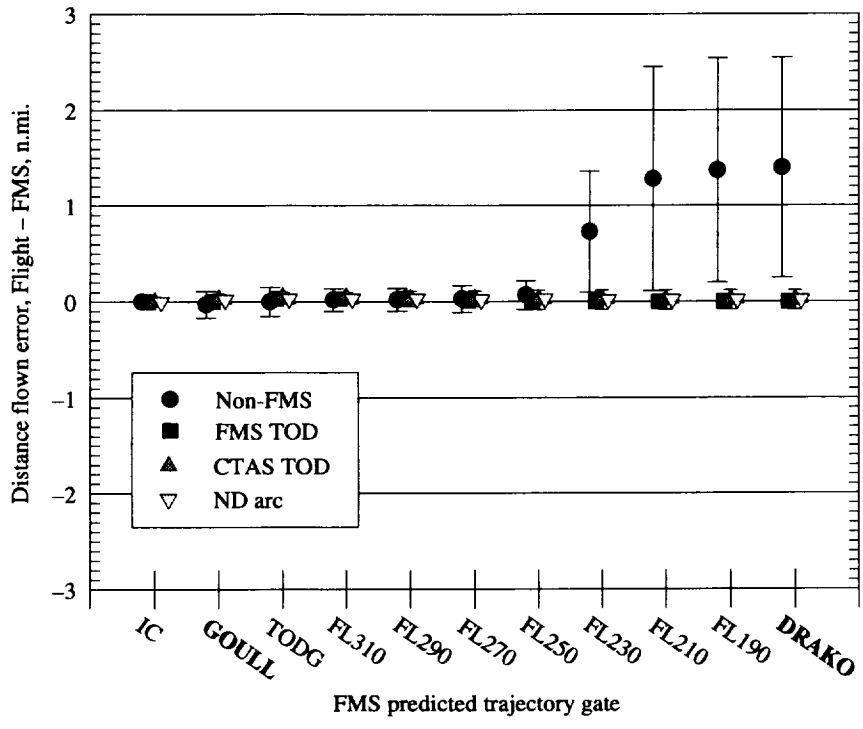
Figure 24. Distance flown error relative to FMS path.
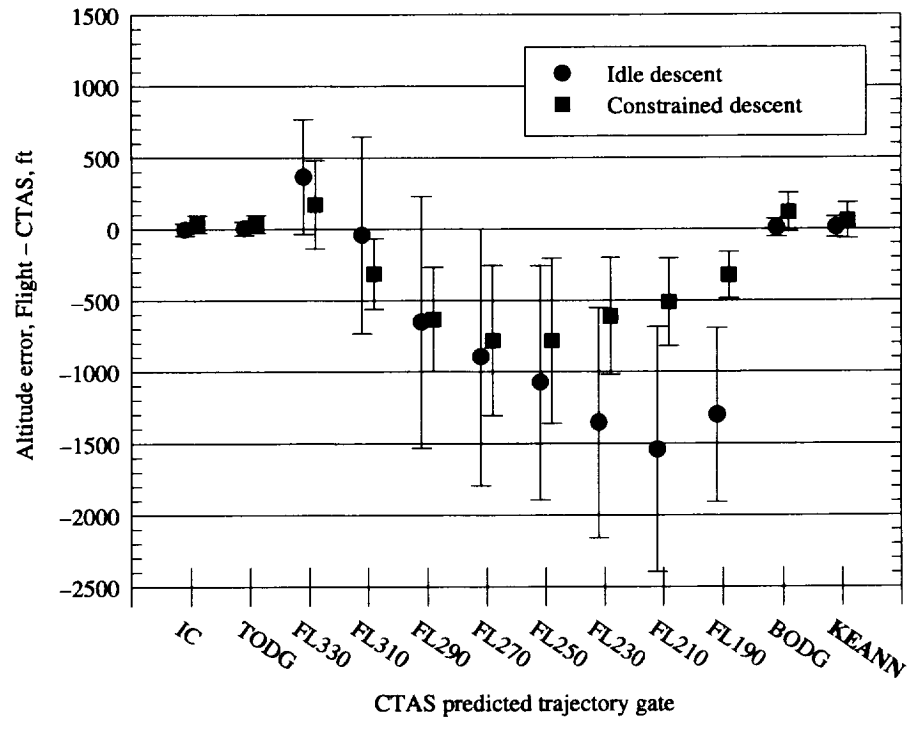
Figure 25. Altitude error summary from Phase I.
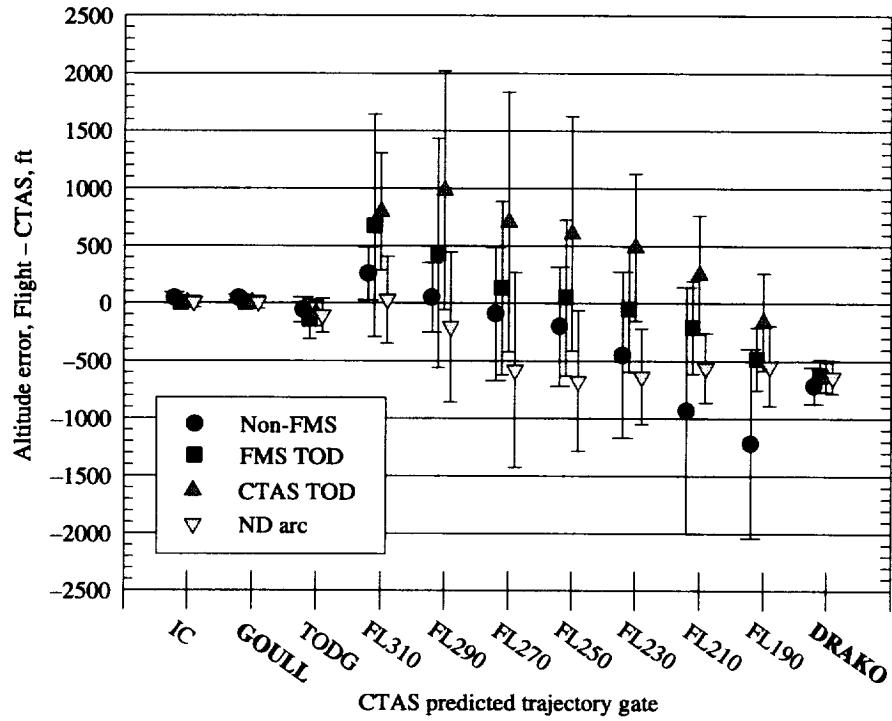
Figure 26. Altitude error relative to CTAS path from Phase II flight test.
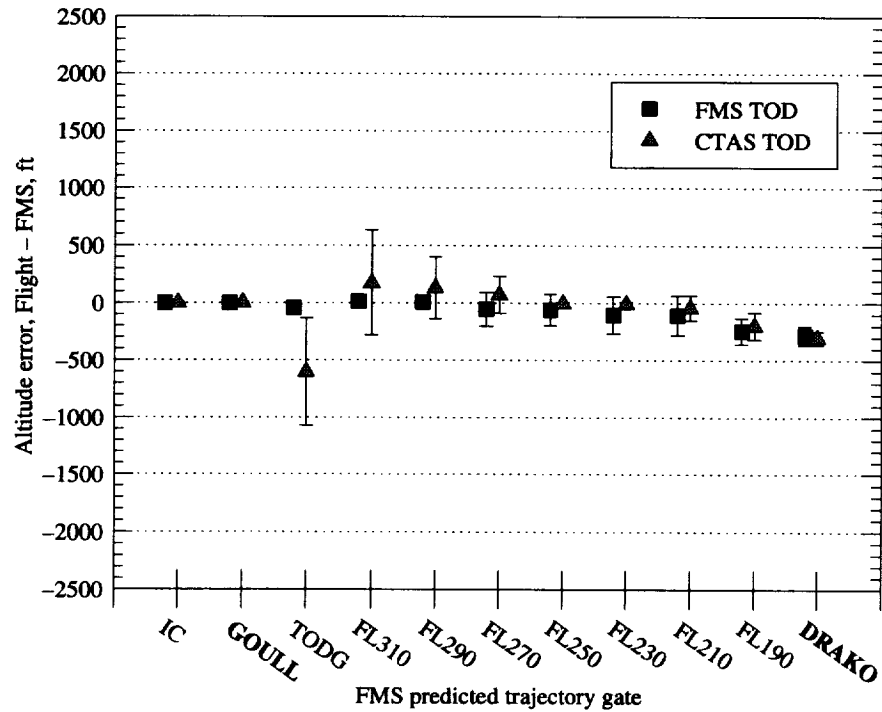
Figure 27. Altitude error relative to FMS path from Phase II.
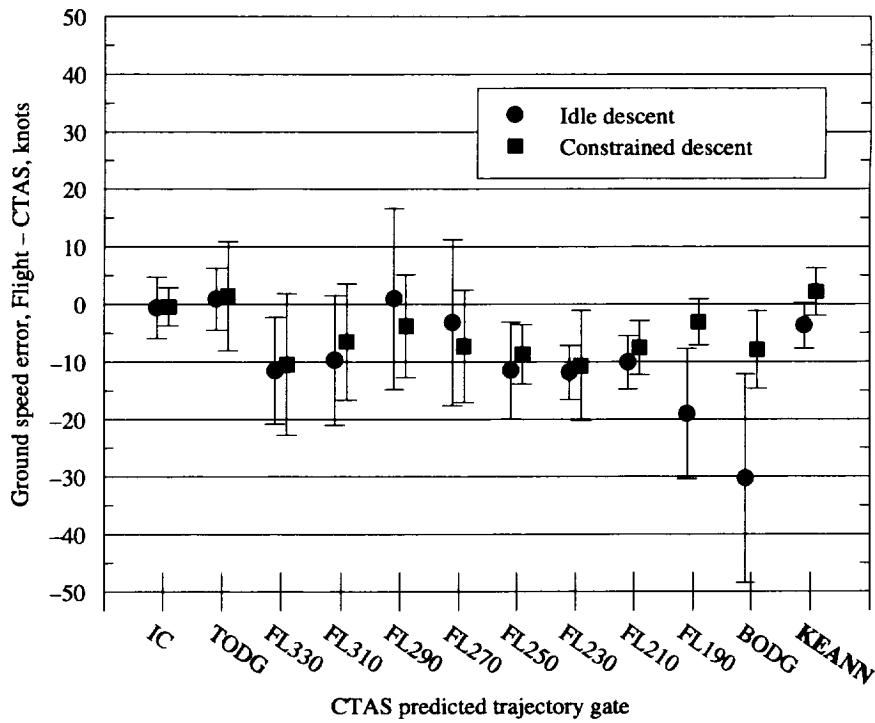
(a) Ground speed errors.
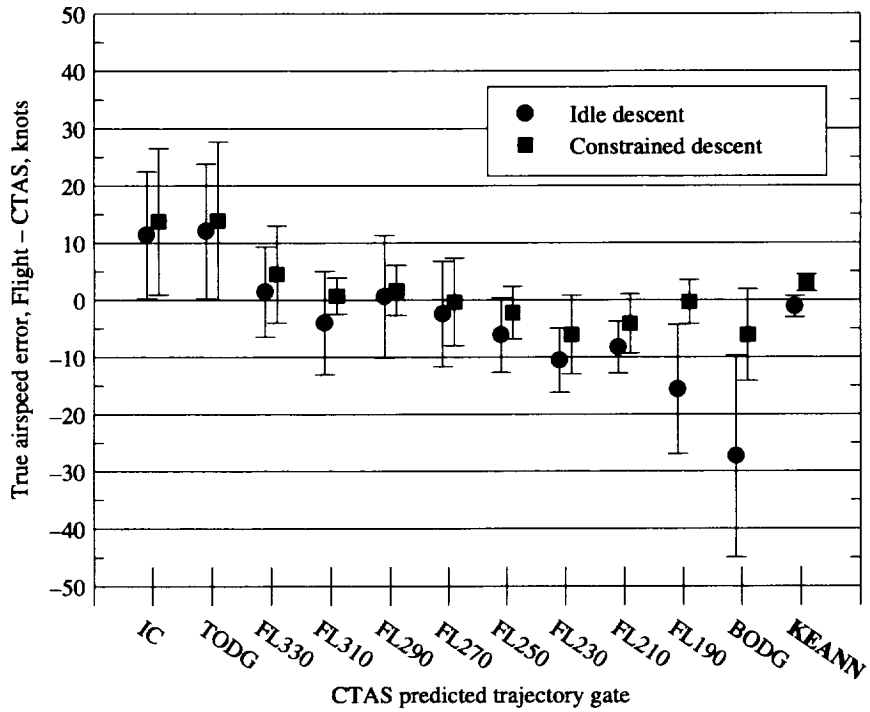
(b) True airspeed errors.

Figure 28. CTAS speed errors from Phase I.

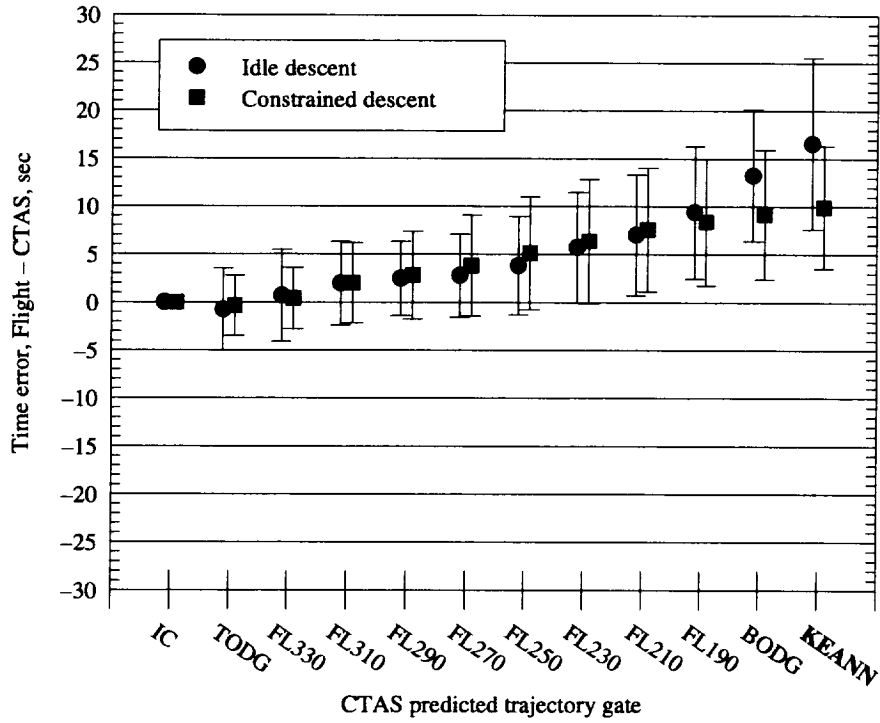71
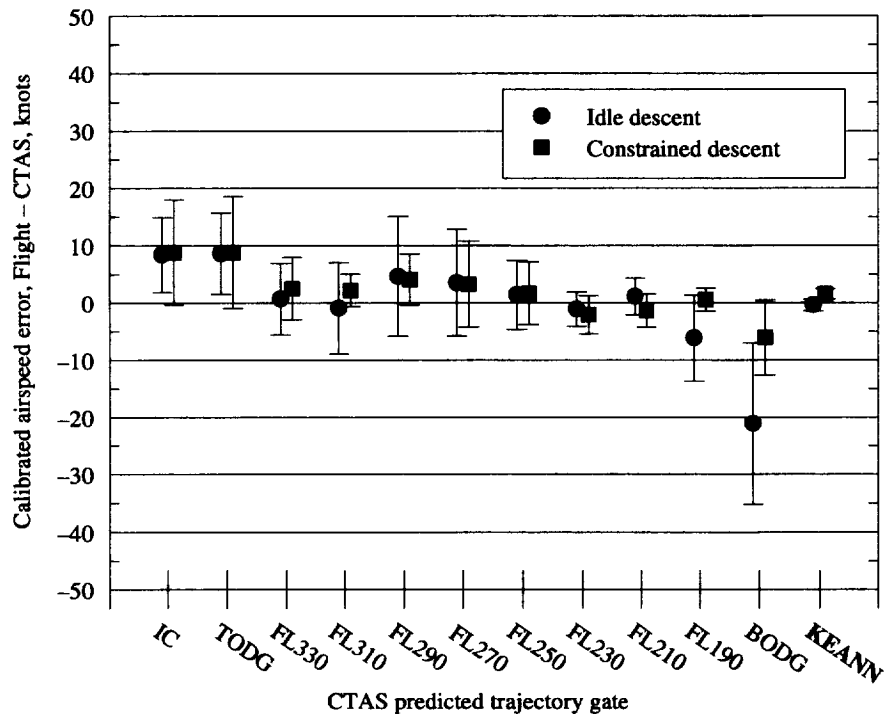
(c) Calibrated airspeed errors.

Figure 28. Concluded.
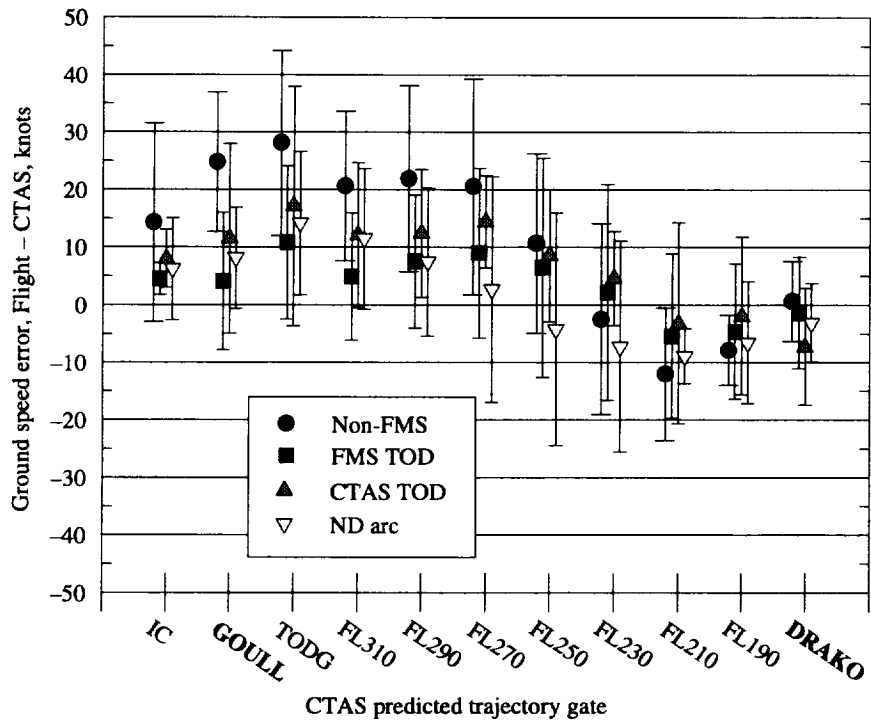
(a) Ground speed errors.
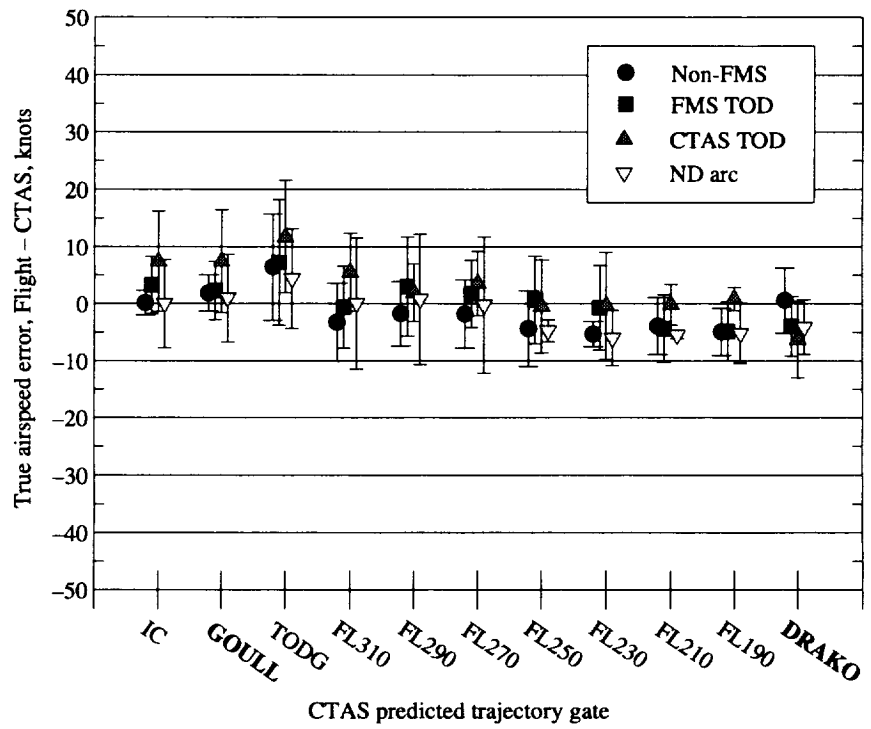
(b) True airspeed errors.

Figure 29. CTAS speed errors from Phase II.
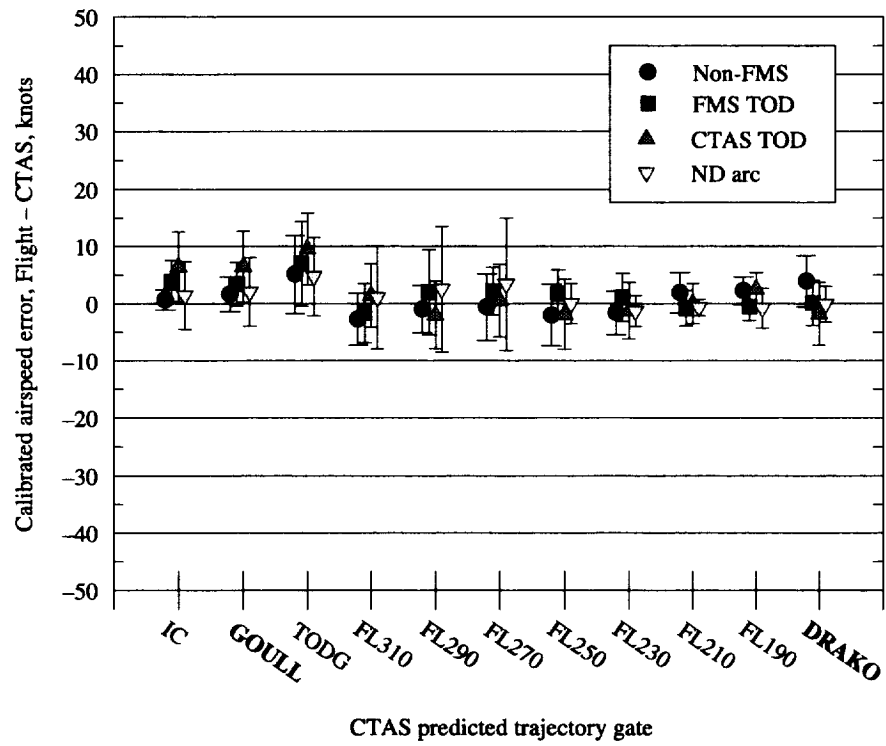
(c) Calibrated airspeed errors.

Figure 29. Concluded.
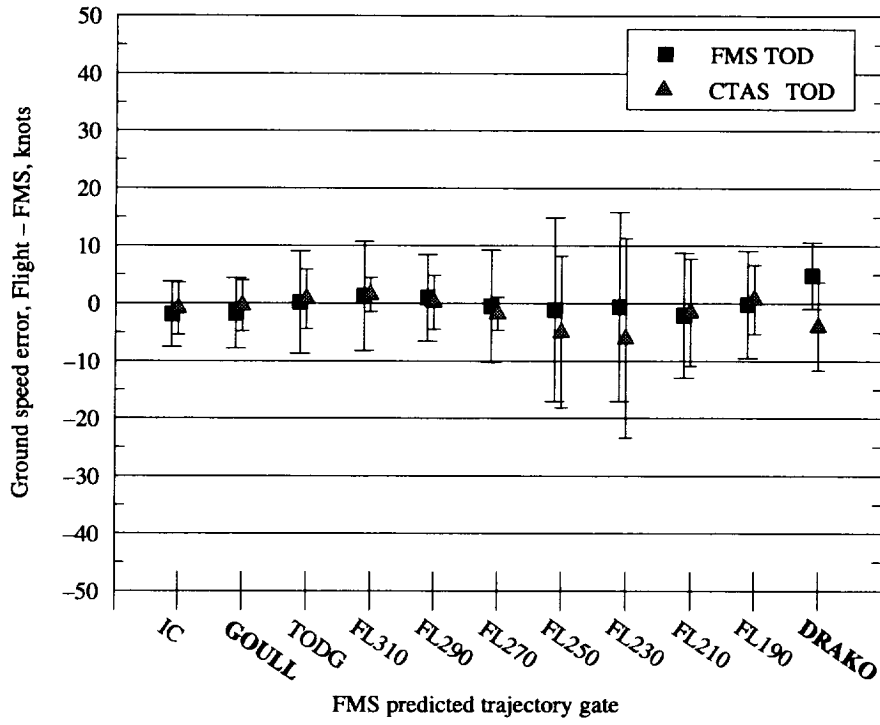
(a) Ground speed errors.
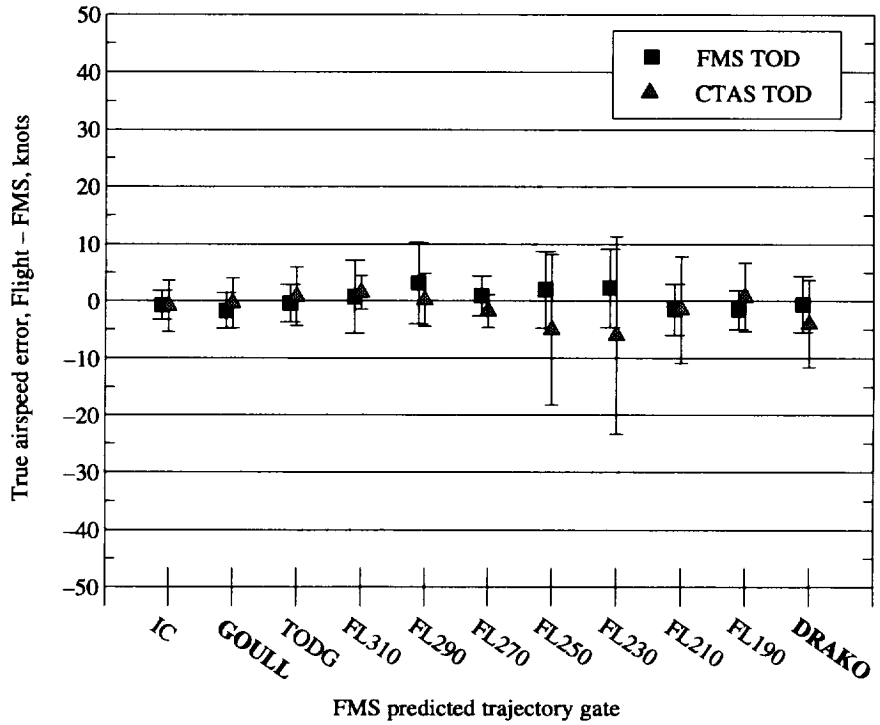
(b) True airspeed errors.

Figure 30. FMS speed errors from Phase II.

75
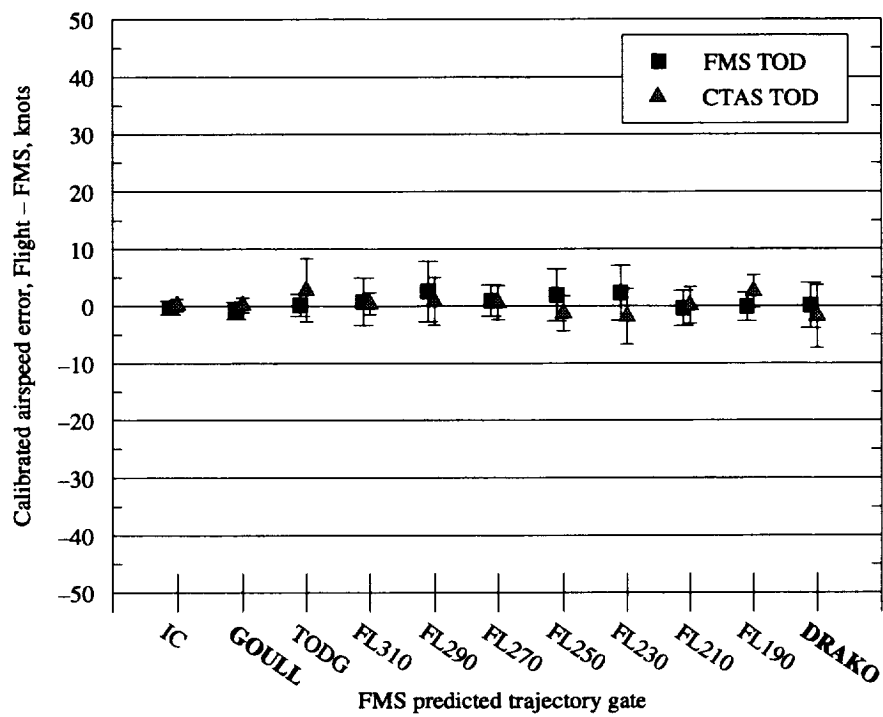
(c) Calibrated airspeed errors.

Figure 30. Concluded.
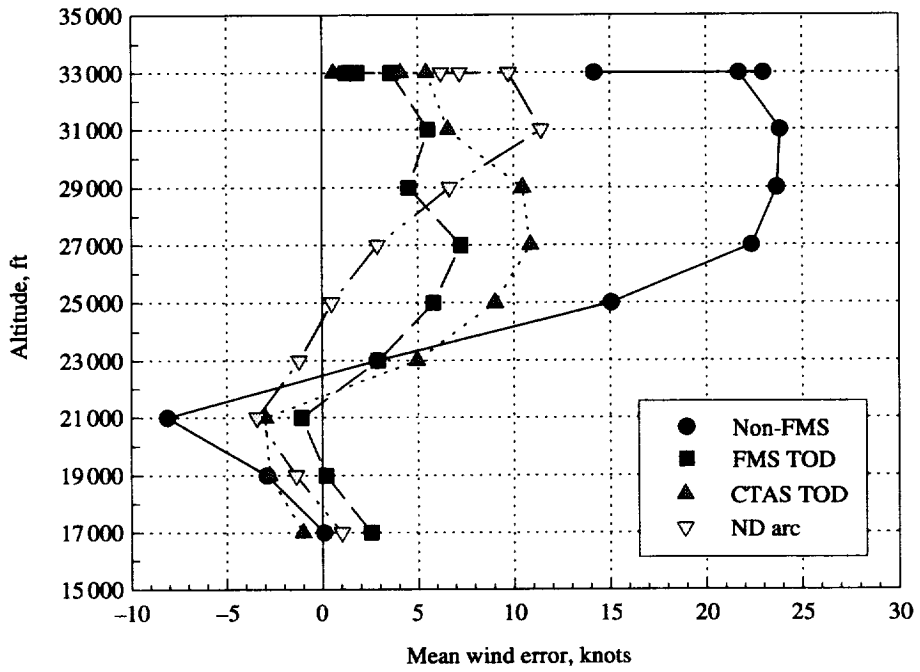
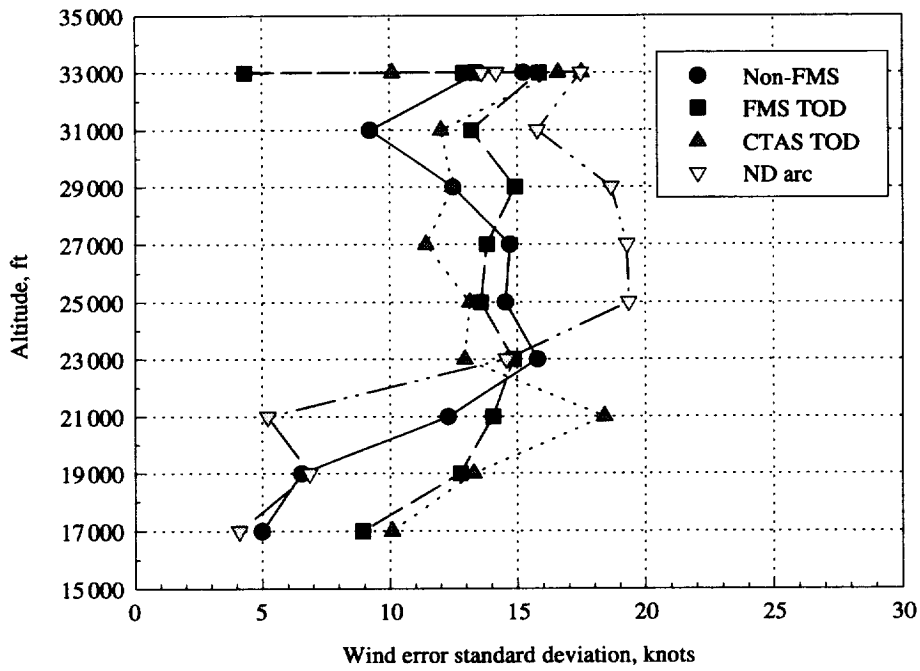Figure 31. Time error relative to CTAS path from Phase I.
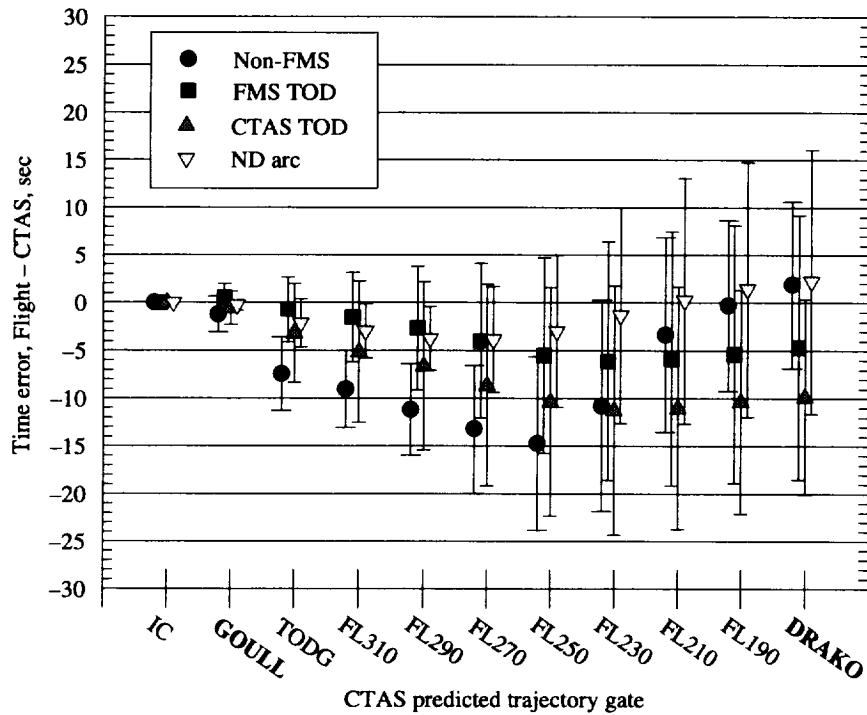
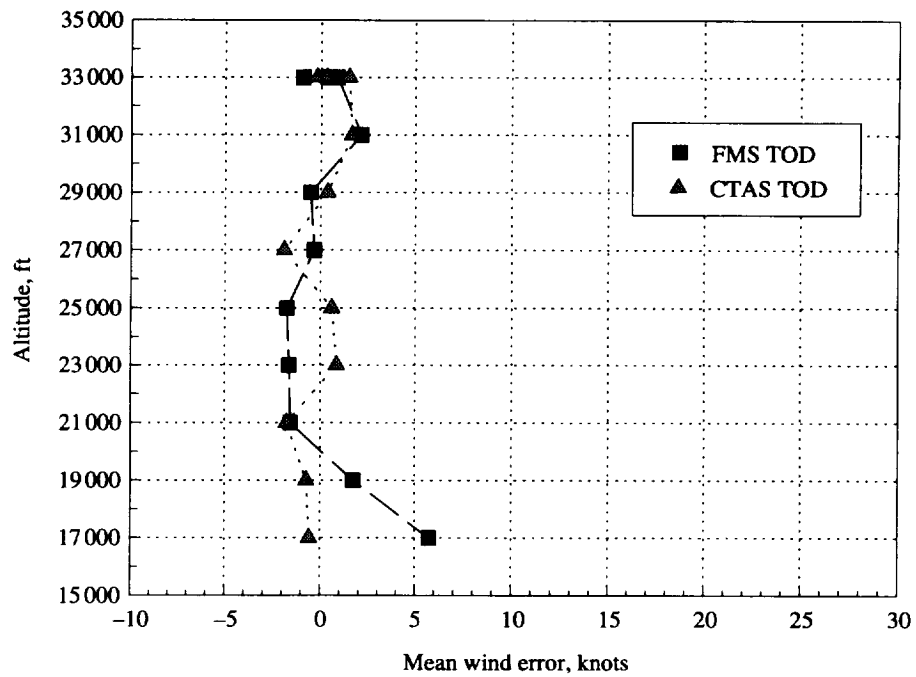Figure 32. Time error relative to CTAS path from Phase II.

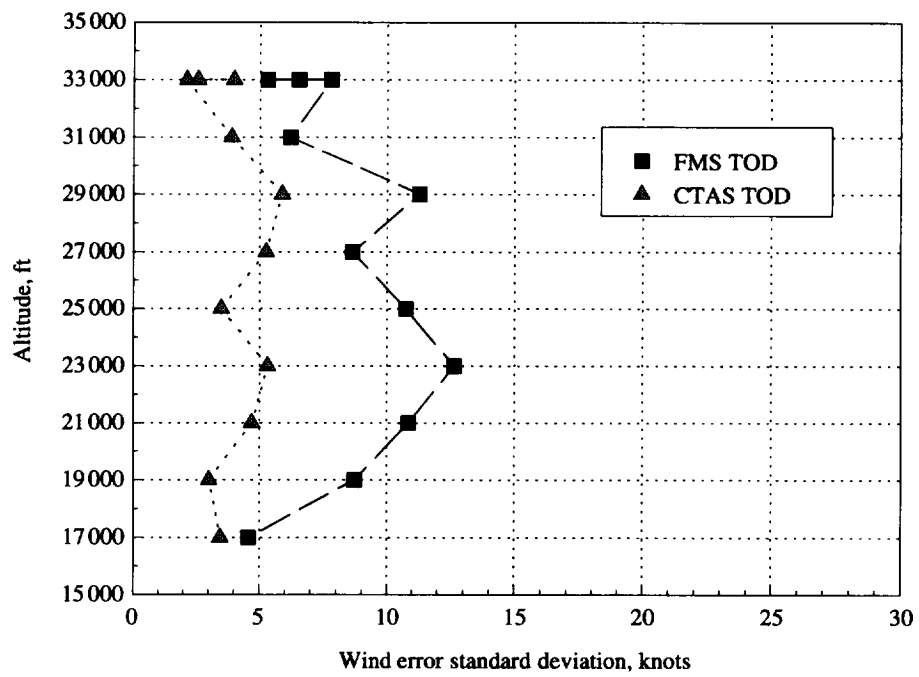(a) Mean along-track wind error component.

(b) Standard deviation in along-track wind error.

Figure 33. CTAS along-track wind errors fro Phase II.

(a) Mean along-track wind error component.

(b) Standard deviation in along-track wind error.

Figure 34. FMS along-track wind errors for Phase II.

REPORT DOCUMENTATION PAGE

Public reporting burden for this collection of information is estimated to average 1 hour per response, including the time for reviewing instructions, searching existing data sources, gathering and maintaining the data needed, and completing and reviewing the collection of information. Send comments regarding this burden estimate or any other aspect of this collection of information, including suggestions for reducing this burden, to Washington Headquarters Services, Directorate for Information Operations and Reports, 1215 Jefferson Davis Highway, Suite 1204, Arlington, VA 22202-4302, and to the Office of Management and Budget, Paperwork Reduction Project (0704-0188), Washington, DC 20503.

1. AGENCY USE ONLY (Leave blank)	2. REPORT DATE July 1998	3. REPORT TYPE AND DATES COVERED Technical Publication

4. TITLE AND SUBTITLE Flight Evaluation of Center-TRACON Automation System Trajectory Prediction Process	5. FUNDING NUMBERS WU 538-04-11-16
6. AUTHOR(S) David H. Williams and Steven M. Green	

7. PERFORMING ORGANIZATION NAME(S) AND ADDRESS(ES) NASA Langley Research Center Hampton, VA 23681-2199	8. PERFORMING ORGANIZATION REPORT NUMBER L-17644

9. SPONSORING/MONITORING AGENCY NAME(S) AND ADDRESS(ES) National Aeronautics and Space Administration Washington, DC 20546-0001	10. SPONSORING/MONITORING AGENCY REPORT NUMBER NASA/TP-1998-208439

11. SUPPLEMENTARY NOTES

David H. Williams: Langley Research Center, Hampton, VA; Steven M. Green: Ames Research Center, Moffett Field, CA

12a. DISTRIBUTION/AVAILABILITY STATEMENT Unclassified–Unlimited Subject Category 04 Distribution: Standard Availability: NASA CASI (301) 621-0390	12b. DISTRIBUTION CODE

13. ABSTRACT (Maximum 200 words)

Two flight experiments (Phase I in October 1992 and Phase II in September 1994) were conducted to evaluate the accuracy of the Center-TRACON Automation System (CTAS) trajectory prediction process. The Transport Systems Research Vehicle (TSRV) Boeing 737 based at Langley Research Center flew 57 arrival trajectories that included cruise and descent segments; at the same time, descent clearance advisories from CTAS were followed. Actual trajectories of the airplane were compared with the trajectories predicted by the CTAS trajectory synthesis algorithms and airplane Flight Management System (FMS). Trajectory prediction accuracy was evaluated over several levels of cockpit automation that ranged from a conventional cockpit to performance-based FMS vertical navigation (VNAV). Error sources and their magnitudes were identified and measured from the flight data. The major source of error during these tests was found to be the predicted winds aloft used by CTAS. The most significant effect related to flight guidance was the cross-track and turn-overshoot errors associated with conventional VOR guidance. FMS lateral navigation (LNAV) guidance significantly reduced both the cross-track and turn-overshoot error. Pilot procedures and VNAV guidance were found to significantly reduce the vertical profile errors associated with atmospheric and airplane performance model errors.

14. SUBJECT TERMS CTAS; FMS; Trajectory prediction; Flight management; Air traffic control	15. NUMBER OF PAGES 88
	16. PRICE CODE A05

17. SECURITY CLASSIFICATION OF REPORT Unclassified	18. SECURITY CLASSIFICATION OF THIS PAGE Unclassified	19. SECURITY CLASSIFICATION OF ABSTRACT Unclassified	20. LIMITATION OF ABSTRACT

NSN 7540-01-280-5500